ISSN 1814-9758

UKRAINICA BIOORGANICA ACTA

2021, Vol. 16, N 1

Scientific journal • Established in 2004

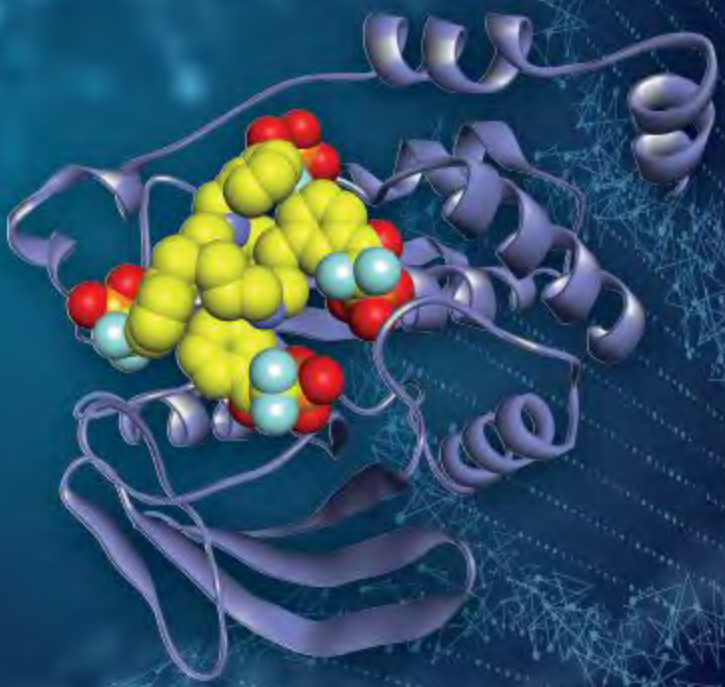

National Academy of Sciences of Ukraine

V.P. KUKHAR INSTITUTE OF BIOORGANIC CHEMISTRY AND PETROCHEMISTRY
INSTITUTE OF MOLECULAR BIOLOGY AND GENETICS

UKRAINICA BIOORGANICA ACTA

Vol. 16, N 1, 2021

Scientific journal *Established in 2004* *Issued twice a year*

Founders/Publishers: Institute of Molecular Biology and Genetics of the NAS of Ukraine
V.P. Kukhar Institute of Bioorganic Chemistry and Petrochemistry of the NAS of Ukraine

Editorial address: V.P. Kukhar Institute of Bioorganic Chemistry and Petrochemistry of the NAS of Ukraine,
1 Murmanska St.,
Kyiv, Ukraine, 02094

Tel.: +38044-5585388;
E-mail: uba@bioorganica.org.ua
www.bioorganica.org.ua

The state registration certificate for print media: series KV No 24164-14004 PR, 01.10.2019

Editors: N.V. Lyutenko, L.V. Pletnova ***Page layout:*** V.V. Shvadchak, E.V. Vilchynska

Signed for printing 21.06.2021. Format 210 x 297. Coated paper 115 g/m².
Fonts: Times New Roman. Publishing sheets: 5.1. Edition 100 copies. Order 458.
Original layout design: E.V. Vilchynska, Enamine Ltd.
Print: LLC "SPE "Interservice", Kyiv, Boryspilska St. 9, tel.: +38044 3628307. Lic. DK 3534, 24.07.2009

NATIONAL ACADEMY OF SCIENCES OF UKRAINE
V.P. KUKHAR INSTITUTE OF BIOORGANIC CHEMISTRY AND PETROCHEMISTRY
INSTITUTE OF MOLECULAR BIOLOGY AND GENETICS

UKRAINICA BIOORGANICA ACTA

Volume 16, N 1, June, 2021 **Kyiv**

hpps://doi.org/10.15407/bioorganica2021.01

C O N T E N T S

Research articles

З М І С Т

Експериментальні роботи

ISSN 1814-9758. Ukr. Bioorg. Acta, 2021, Vol. 16, N 1
UDC 544.122.3 : 547.466.22 : 546.742
DOI: hpps://doi.org/10.15407/bioorganica2021.01.003

Ukrainica Bioorganica Acta
www.bioorganica.org.ua

UBA

RESEARCH ARTICLE

Aldol addition-cyclization reaction cascade on a platform of chiral Ni(II) complex of glycine schiff base

Yupiao Zou[1], Zizhen Yin[1], Haibo Mei[1], Hiroyuki Konno[2], Hiroki Moriwaki[3], Vadim A. Soloshonok[4,5]* and Jianlin Han[1]*

[1] *College of Chemical Engineering, Nanjing Forestry University, 159 Lonpan Road, Nanjing, 210037, China*
[2] *Department of Biochemical Engineering, Graduate School of Science and Technology, Yamagata University, Yonezawa, Yamagata 992-8510, Japan*
[3] *Hamari Chemicals Ltd., 1-19-40, Nankokita, Suminoe-ku, Osaka, 559-0034, Japan*
[4] *Department of Organic Chemistry I, Faculty of Chemistry, University of the Basque Country UPV/EHU, Paseo Manuel Lardizábal 3, 20018 San Sebastián, Spain*
[5] *IKERBASQUE, Basque Foundation for Science, Maria Diaz de Haro 3, 48013 Bilbao, Spain*

Abstract: Using platform of a new type of chiral Ni(II) complex of glycine Schiff base we designed addition-cyclization reaction cascade to explore aspects of kinetic/thermodynamic formation of the corresponding (*S*)(2*S*,3*S*)/(*S*)(2*S*,3*R*) diastereomers. It was found that the final lactone products reflect the thermodynamic stereocontrol due to much greater rates of the reversible aldol addition vs. subsequent cyclization step. The observed 4/1 (*S*)(2*S*,3*S*)/(*S*)(2*S*,3*R*) diastereoselectivity in the reactions of new type of (*S*)-Ni(II) complexes constitute an improvement over the previously reported 1.7/1 ratio.

Keywords: asymmetric synthesis; aldol additions; tailor-made amino acids; Ni(II) complexes; Schiff bases; cascade/domino/tandem reaction.

Introduction

Tailor-made amino acids (AAs) [1] are in high demand in modern pharmaceutical industry. Along with fluorine [2], AAs' residues can be found in a growing number of marketed drugs and medicinal formulations [3]. The growing acceptance of peptides and modified peptides as drugs [4], strongly suggest that the pivotal role of tailor-made AAs in the design of pharmaceuticals will continue to increase [5]. Asymmetric synthesis of AAs is a mature science offering a plethora of various approaches [6]. Over the last decade, preparation of tailor-made AAs via Ni(II) complex intermediates (Scheme 1) has emerged as the most frequently used, methodologically dominant approach [7-8].

In this approach, chiral tridentate ligands 1 can be directly used in the reactions with racemic α- and β-AAs offering highly efficient deracemization, as well as (*S*)-to-(*R*) interconversion protocols [9-10]. In a more general version, chiral ligands **1** are transformed to Ni(II) complexes of glycine Schiff bases **2** by the reaction with glycine and source of Ni(II) ions. Compounds **2** are widely used as chiral nucleophilic glycine equivalents in the alkyl halide alkylations [11], Michael [12], Mannich [13], aldol [14] addition reactions, as well as various multi-step transformations [15]. Products **3** can be conveniently disassembled to release target AAs **4** along with the recovery and reuse of chiral ligands **1**. The overall process is economically and operationally attractive for large-scale asymmetric synthesis of tailor-made AAs [16]. Among the above-mentioned major pathways for homologation of the glycine moiety in complexes **2**, aldol addition, due to its inherent reversibility, is the most challenging approach (Scheme 2) [7b]. In this methodological work, using a new

Received: 10.05.2021
Revised: 24.05.2021
Accepted: 27.05.2021
Published online: 30.06.2021

* Corresponding author. Tel.: +34-94-301-5177;
e-mail: vadym.soloshonok@ehu.es (V. A. Soloshonok);
hanjl@njfu.edu.cn (J. Han)
ORCID: 0000-0003-0681-4526 (V. A. Soloshonok);
0000-0002-3817-0764 (J. Han)

type of chiral ligands, we designed an aldol-cyclization reaction cascade in attempt to investigate the effect of the formation of irreversible final products on the overall stereochemical outcome of this reaction sequence. The results reported here expand our knowledge of Ni(II) complexes aldol reactivity and highlight noticeably greater stereocontrolling properties of new type of chiral tridentate ligands.

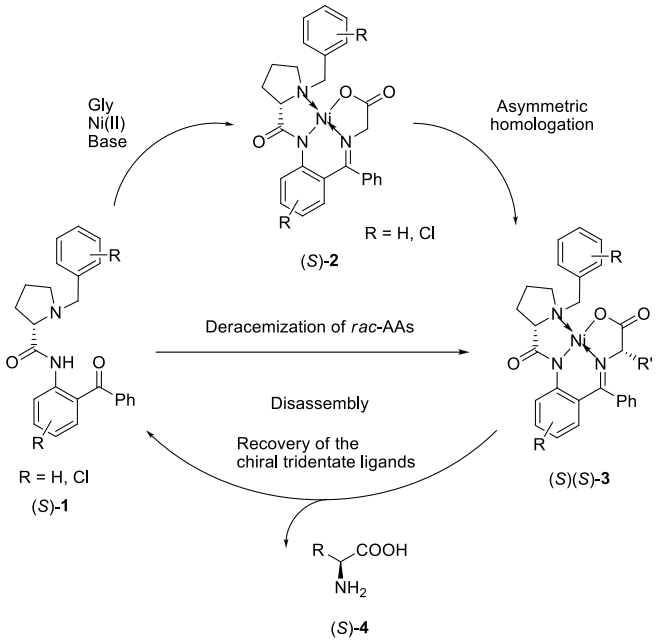

Scheme 1. Asymmetric synthesis of tailor-made amino acids via homologation of chiral glycine (*S*)-**1** Schiff base.

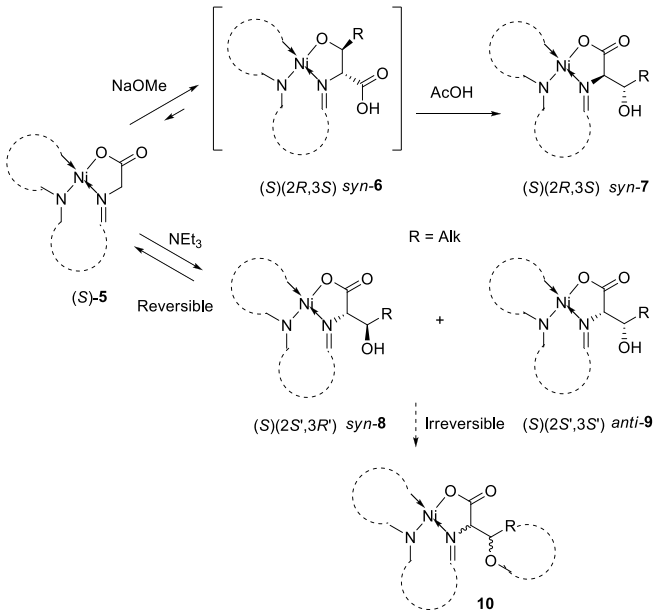

Scheme 2. General aspects of aldol addition reactions of Ni(II) complexes **5**; formation of reversible *syn*-**8** and *anti*-**9**, followed by cyclization to afford irreversible products **10**.

From the standpoint of mechanism and stereochemical outcome, aldol addition reactions of Ni(II) complexes of glycine Schiff bases have two distinct patterns (Scheme 2) depending on the reaction conditions. The first type of reactivity is observed in the presence of strong bases, such as alkoxides [17] or DBU [18]. In this case the reactions

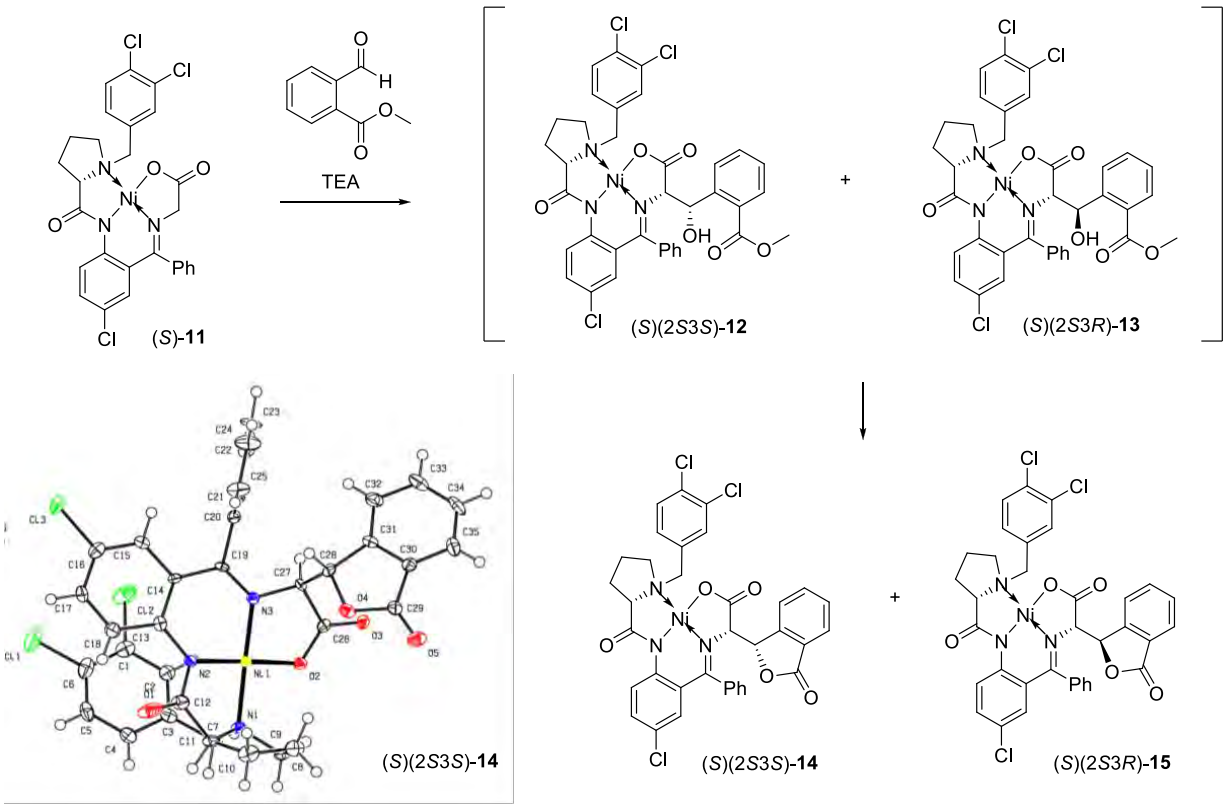

Scheme 3. Aldol addition-cyclization reaction cascade; major (*S*)(2*S*,3*S*)-**14** and minor (*S*)(2*S*,3*R*)-**15** products and crystallographic structure of major diastereomer (*S*)(2*S*,3*S*)-**14**.

proceed with very high diastereoselectivity (> 90% de) and are virtually irreversible due to the *in situ* formation of hydroxy group-coordinated species **6**. Upon acidification of the reaction mixture, during work-up procedure, compounds **6** rearrange to a normal, carboxy group-coordinated complexes **7**. In the second option, under weakly basic conditions, such as catalyzed by triethylamine, aldol addition reactions are distinctively reversible with the equilibrium strongly favoring the starting compounds [19].

Consequently, the reactions usually require over 10-fold of the corresponding aldehyde to achieve a meaningful conversion of starting Ni(II) complexes **5**. Furthermore, under these reaction conditions the thermodynamically controlled diastereoselectivity (*syn*-**8** and *anti*-**9**) is quite low, ranging from 0 to 35% de. Considering these challenging inherent synthetic limitations, we were interested to know whether or not the stereochemical outcome can be improved when the aldol addition is followed by a transformation of reversible products *syn*-**8** and *anti*-**9** to irreversible derivatives **10**.

Results and Discussion

We posited that such process can be realized in addition-cyclization reaction cascade with in situ esterification of the key hydroxy group critical for the reverse aldol addition. As presented in Scheme 2, we selected methyl 2-formyl-benzoate, possessing well-positioned aldehyde and ester functionalities for the desired addition-cyclization cascade. As for the starting glycine Schiff base Ni(II) complex, we selected recently developed compound (*S*)-**11**, derived from strategically chloro-substituted ligand [20]. Complex (*S*)-**11** has never been used in the aldol additions but showed superior stereocontrolling properties in the alkyl halide alkylation [21] and deracemization of unprotected α- [22] and β-AAs [10].

After a series of preliminary experiments, we established that 6 equivalents of triethylamine, as a base, and 2 equivalents of methyl 2-formylbenzoate can be suitably used as the starting point in the investigation. As presented in Table 1, screening the reaction solvents, such as dichloromethane (entry1), acetone (entry 2), acetonitrile (entry 3) and methanol (entry 4) at ambient temperature gave more or less similar results in term of diastereoselectivity affording (*S*)(2*S*,3*S*)-complex **14** as the major reaction product. Diastereomers (*S*)(2*S*,3*S*)-**14** and (*S*)(2*S*,3*R*)-**15** were separated by column chromatography and fully characterized. Absolute configuration of major (*S*)(2*S*,3*S*)-**14** was established by single crystal X-ray analysis (Scheme 3 and SI). Absolute configuration of minor product (*S*)(2*S*,3*R*)-**15** was inferred based on its optical rotation ($[\alpha]^D$ = +1811.8), suggesting the (2*S*) stereochemistry and the (3*R*) by the deduction. No products with the (2*R*) absolute configuration, showing negative sign [19] of optical rotation, were found in the reaction mixture.

Considering entries 1-4, we concluded that the reaction solvent has virtually no effect on the diastereoselectivity of this aldol additions providing products (*S*)(2*S*,3*S*)-**14** and

Table 1. Optimization of reaction conditions[a].

Entry	Temp (°C)	Solvent	Ester (equiv)	Yield (%)	Dr[c]
1	rt	CH_2Cl_2	2.0	21	32:68
2	rt	aceton	2.0	16	28:72
3	rt	MeCN	2.0	12	34:66
4	rt	MeOH	2.0	53	37:63
5	-20	MeOH	2.0	66	64:36
6	0	MeOH	2.0	76	54:46
7	40	MeOH	2.0	58	25:75
8	60	MeOH	2.0	50	22:78
9	80	MeOH	2.0	45	19:81
10	40	MeOH	3.0	77	13:87
11	40	MeOH	5.0	93	20:80
12	40	MeOH	10.0	93	26:74
13[d]	40	MeOH	5.0	89	21:79
14[d]	40	MeOH	2.0	79	22:78

[a] Reaction conditions: *S*-CBPB **11** (0.1 mmol), methyl 2-formyl-benzoate, triethylamine (6 eq.), solvent (2.5 mL), 12 h;
[b] Isolated yield;
[c] Dr was determined by ^{1}H NMR;
[d] Ethyl 2-formylbenzoate was used.

(*S*)(2*S*,3*R*)-**15** in ratios between 28:72 and 37:63. By contrast, the chemical yields ranged much more prominently depending the reaction solvent (entry 3 vs. 4), suggesting methanol as an optimal choice (entry 4). Thus using menthol as a solvent, we explored the effect of the reaction temperature on the diastereoselectivity. Quite unexpectedly, the reaction of glycine Schiff base Ni(II) complex (*S*)-**2** with methyl 2-formylbenzoate conducted at -20 °C gave rise to the reverse diastereomeric preferences affording (*S*)(2*S*,3*R*)-**15** as a major product (entry 5). The same trend of the diastereoselectivity was still observed in the reaction conducted at 0 °C, albeit the preference for diastereomer (*S*)(2*S*,3*R*)-**15** was significantly reduced (entry 6). In sharp contrast the aldol addition performed at elevated temperature (40 °C, entry 7). Further increase of the reaction temperature to 60 °C (entry 8) and 80 °C (entry 9) led to gradual increase in (2*S*,3*S*) diastereoselectivity recording the diastereomeric ratios of 22:78 and 19:81, respectively. On the other hand, the chemical yield followed the opposite trend gradually decreasing from 76% (entry 6) to 45% (entry 9).

Based on these results, we concluded that the optimal temperature for these aldol reactions should be 40 °C (entry 7). It should be noted that the reactions were quite sluggish and the starting materials were never fully converted to products (*S*)(2*S*,3*S*)-**14** and (*S*)(2*S*,3*R*)-**15** within the standard 12 hours of the reaction time. Accordingly, we conducted series of reactions using greater than 2 equivalents excess of methyl 2-formylbenzoate. As presented in entries 10-12 the increase in the aldehyde stoichiometry allowed for noticeable improvement of the chemical yield to a respected 93% (entries 11, 12), suggesting 5 equivalents of the aldehyde as the optimal condition. Similar results were observed with application of

ethyl 2-formylbenzoate in the place of methyl 2-formylbenzoate (entries 13, 14).

Conclusions

In conclusion, in this methodological work we explored the triethylamine-catalyzed addition-cyclization reaction cascade between a new type of chiral Ni(II) complex of glycine Schiff and methyl/ethyl 2-formylbenzoates. The results obtained point to the thermodynamically controlled diastereoselectivity due to the much greater reaction rates of the reversible aldol additions vs. irreversible cyclizations. Nevertheless, the observed temperature-dependent oscillation of the stereochemical preferences, giving preference for (2*S*,3*R*) at low and (2*S*,3*S*) at elevated temperatures, was quite unexpected. Furthermore, the achieved 4/1 level of diastereoselectivity with over 90% chemical yields suggest synthetic potential of these reactions clearly deserving more comprehensive and focused investigation.

Experimental section

All the commercial reagents including solvents were used directly without further purification. All the experiments were monitored by thin layer chromatography (TLC) with UV light. The TLC employed 0.25 mm silica gel coated on glass plates. Column chromatography was performed with silica gel 60 (300-400 mesh). NMR spectra were recorded on Bruker 600 MHz spectrometers. Mass spectra (MS) were measured on Shimadzu LCMS-2020 with an etrospray ionization (ESI) probe operating in positive mode. Values of optical rotation were measured on Automatic Polarimeter SGW-531.

*General procedures for the reaction between methyl 2-formylbenzoate and (S)-**11***

Into a 10 mL vial were taken (*S*)-**11** (0.1 mmol), methyl 2-formylbenzoate (5 equiv), triethylamine (6 equiv), methanol (2.5 mL). The mixture was stirred at 40 °C for 12 h. Then the reaction was concentrated in vacuo. The residue was purified by column chromatography using DCM/EtOAc (1:1, v/v) as eluent to afford the desired product.

Compound (*S*)(2*S*3*S*)-**14**: red solid, mp 168-169 °C; $[\alpha]_D^{25}$ +2514.4 (c 0.09, MeOH). ^{1}H NMR (600 MHz, $CDCl_3$) δ 8.99 (d, *J* 2.04 Hz, 1H), 8.14 (d, *J* 9.24 Hz, 1H), 7.88-7.86 (m, 1H), 7.80-7.79 (m, 1H), 7.77-7.74 (m, 1H), 7.72-7.69 (m, 1H), 7.60-7.57 (m, 1H), 7.54-7.48 (m, 2H), 7.45-7.43 (m, 1H), 7.41 (d, *J* 8.16 Hz, 1H), 7.19-7.17 (m, 1H), 7.10-7.08 (m, 1H), 6.73 (d, *J* 2.58 Hz, 1H), 6.40-6.39 (m, 1H), 5.29 (s, 1H), 4.51 (d, *J* 1.74 Hz, 1H), 4.27 (d, *J* 12.66 Hz, 1H), 4.19-4.11 (m, 1H), 3.61-3.58 (m, 1H), 3.41-3.38 (m, 1H), 3.21 (d, *J* 12.72 Hz, 1H), 2.94-2.88 (m, 1H), 2.68-2.60 (m, 1H), 2.31-2.27 (m, 1H), 2.12-2.06 (m, 1H). ^{13}C{^{1}H} NMR (150 MHz, $CDCl_3$) δ 180.5, 172.3, 171.4, 169.3, 145.2, 141.5, 135.2, 134.3, 133.8, 133.4, 133.2, 133.1, 132.9, 132.1, 131.0, 130.7, 130.1, 129.9, 129.8, 127.4, 127.1, 127.0, 125.9, 125.7, 125.5, 124.7, 121.6, 81.6, 72.8, 71.7, 63.0, 58.9, 31.3, 29.9, 23.2. MS (ESI) *m/z* Calcd. for $C_{35}H_{27}Cl_3N_3NiO_5^+$ $[M+H]^+$ 732.0. Found 732.0.

Compound (*S*)(2*S*3*R*)-**15**: red solid, mp 142-144 °C; $[\alpha]_D^{25}$ +1811.8 (c 0.06, MeOH). ^{1}H NMR (600 MHz, $CDCl_3$) δ 9.00 (d, *J* 2.04 Hz, 1H), 8.18 (d, *J* 9.36 Hz, 1H), 7.82-7.80 (m, 1H), 7.75-7.73 (m, 1H), 7.50-7.42 (m, 4H), 7.32 (d, *J* 8.22 Hz, 1H), 7.27-7.25 (m, 1H), 7.15-7.12 (m, 1H), 7.07-7.05 (m, 1H), 6.92-6.91 (m, 1H), 6.41 (d, *J* 2.58 Hz, 1H), 6.06 (d, *J* 3.84 Hz, 1H), 6.00-5.98 (m, 1H), 4.50 (d, *J* 3.9 Hz, 1H), 4.29 (d, *J* 12.6 Hz, 1H), 4.11-4.05 (m, 1H), 3.58-3.56 (m, 1H), 3.40-3.37 (m, 1H), 3.18-3.14 (m, 2H), 2.73-2.66 (m, 1H), 2.29-2.22 (m, 1H), 2.16-2.11 (m, 1H). ^{13}C{^{1}H} NMR (150 MHz, $CDCl_3$) δ 179.8, 175.4, 172.4, 168.6, 144.9, 141.7, 135.2, 134.5, 133.6, 133.4, 133.3, 132.9, 132.8, 132.3, 131.1, 130.2, 129.8, 129.7, 129.6, 129.2, 128.8, 127.2, 127.1, 125.9, 125.8, 125.4, 123.5, 123.4, 80.5, 72.1, 71.8, 63.3, 58.9, 30.6, 29.7, 23.3. MS (ESI) *m/z* Calcd. for $C_{35}H_{27}Cl_3N_3NiO_5^+$ $[M+H]^+$ 732.0. Found 732.7.

Notes

Acknowledgments and finances. This research was funded by the National Natural Science Foundation of China (No. 21761132021) and IKERBASQUE, Basque Foundation for Science (for Soloshonok).

The authors declare no conflict of interest.

Author contributions. **Yupiao Zou, Zizhen Yin**: Synthesis of compounds, Investigation, Formal analysis, writing experimental section. **Haibo Mei, Hiroyuki Konno**: Investigation, Formal analysis, writing most of the manuscript. **Hiroki Moriwaki, Vadim A. Soloshonok and Jianlin Han**: Conceptualization, Supervision, Writing - review & editing. **Zizhen Yin**: X-ray analysis.

Supporting information

The characterization data, NMR spectra and single crystal for **14**.

References

1. For the definition of "tailor-made amino acids", see: Soloshonok, V. A.; Cai, C.; Hruby, V. J.; Meervelt, L. V. Asymmetric synthesis of novel highly sterically constrained (2*S*,3*S*)-3-methyl-3-trifluoromethyl- and (2*S*,3*S*,4*R*)-3-trifluoromethyl-4-methylpyroglutamic acids. *Tetrahedron* **1999**, *55*, 12045-12058.
2. a) Zhou, Y.; Wang, J.; Gu, Z.; Wang, S.; Zhu, W.; Aceña, J. L.; Soloshonok, V. A.; Izawa, K.; Liu, H. Next Generation of Fluorine-Containing Pharmaceuticals, Compounds Currently in Phase II-III Clinical Trials of Major Pharmaceutical Companies: New Structural Trends and Therapeutic Areas. *Chem. Rev.* **2016**, *116*, 422-518; b) Zhu, W.; Wang, J.; Wang, S.; Gu, Z.; Aceña, J.L.; Izawa, K.; Liu, H.; Soloshonok, V. A. Recent advances in the trifluoromethylation methodology and new CF3-containing drugs. *J. Fluorine Chem.* **2014**, *167*, 37-54; c) Mei, H.; Han, J.; Fustero, S.; Medio-Simon, M.; Sedgwick, D. M.; Santi, C.; Ruzziconi, R.; Soloshonok, V. A. Fluorine-containing drugs approved by the FDA in 2018. *Chem. Eur. J.* **2019**, *25*, 11797-11819; d) Liu, J.; Li, Z.; Mei, H.; Soloshonok, V.

A.; Han, J. Detrifluoroacetylative in Situ Generated Cyclic Fluorinated Enolates for the Preparation of Compounds Featuring a C-F Stereogenic Center. *ACS Omega* **2019**, *4*, 19505-19512; e) Zhu, Y.; Han, J.; Wang, J.; Shibata, N.; Sodeoka, M.; Soloshonok, V. A.; Coelho, J. A. S.; Toste, F. D. Modern Approaches for Asymmetric Construction of Carbon-Fluorine Quaternary Stereogenic Centers: Synthetic Challenges and Pharmaceutical Needs. *Chem. Rev.* **2018**, *118*, 3887-3964.

3. a) Wang, J.; Sánchez-Roselló, M.; Aceña, J. L.; del Pozo, C.; Sorochinsky, A. E.; Fustero, S.; Soloshonok, V. A.; Liu, H. Fluorine in Pharmaceutical Industry: Fluorine-Containing Drugs Introduced to the Market in the Last Decade (2001-2011). *Chem. Rev.* **2014**, *114*, 2432-2506; b) Meanwell, N. A. Fluorine and Fluorinated Motifs in the Design and Application of Bioisosteres for Drug Design. *J. Med. Chem.* **2018**, *61*, 5822-5880; c) Ilardi, E. A.; Vitaku, E.; Njardarson, J. T. Data-Mining for Sulfur and Fluorine: An Evaluation of Pharmaceuticals To Reveal Opportunities for Drug Design and Discovery. *J. Med. Chem.* **2014**, *57*, 2832-2842; d) Mei, H.; Han, J.; Klika, K. D.; Izawa, K.; Sato, T.; Meanwell, N. A.; Soloshonok, V. A. Applications of fluorine-containing amino acids for drug design. *Eur. J. Med. Chem.* **2020**, *186*, 111826.

4. a) Soloshonok, V. A.; Izawa, K. (Eds.) Asymmetric Synthesis and Application of α-Amino Acids. ACS Symposium Series 1009, Oxford University Press: Oxford, UK, **2009**; b) Henninot, A.; Collins, J. C.; Nuss, J. M. The Current State of Peptide Drug Discovery: Back to the Future? *J. Med. Chem.* **2018**, *61*, 1382-1414; c) Blaskovich, M. A. T. Unusual Amino Acids in Medicinal Chemistry. *J. Med. Chem.* **2016**, *59*, 10807-10836; d) Soloshonok, V. A.; Sorochinsky, A. E. Practical Methods for the Synthesis of Symmetrically α,α-Disubstituted α-Amino Acids. *Synthesis* **2010**, 2319-2344.

5. a) Ma, J. S. Unnatural amino acids in drug discovery. *Chim. Oggi* **2003**, *21*, 65-68; b) Hodgson, D. R. W.; Sanderson, J. M. The synthesis of peptides and proteins containing non-natural amino acids. *Chem. Soc. Rev.* **2004**, *33*, 422-430; c) Sato, T.; Izawa, K.; Aceña, J. L.; Liu, H.; Soloshonok, V. A. Tailor-Made α-Amino Acids in the Pharmaceutical Industry: Synthetic Approaches to (1R,2S)-1-Amino-2-vinylcyclopropane-1-carboxylic Acid (Vinyl-ACCA). *Eur. J. Org. Chem.* **2016**, 2757-2774; d) Wang, S.; Wang, Y.; Wang, J.; Sato, T.; Izawa, K.; Soloshonok, V. A.; Liu, H. The Second-generation of Highly Potent Hepatitis C Virus (HCV) NS3/4A Protease Inhibitors: Evolutionary Design Based on Tailor-made Amino Acids, Synthesis and Major Features of Bio-activity. *Curr. Pharm. Des.* **2017**, *23*, 4493-4554.

6. Reviews on amino acids, see: a) Sorochinsky, A. E.; Soloshonok, V. A. Asymmetric synthesis of fluorine-containing amines, amino alcohols, α-and β-amino acids mediated by chiral sulfinyl group. *J. Fluorine Chem.* **2010**, *131*, 127-139; b) Aceña, J. L.; Sorochinsky, A. E.; Soloshonok, V. A. Recent advances in the asymmetric synthesis of α-(trifluoromethyl)-containing α-amino acids. *Synthesis* **2012**, *44*, 1591-1602; c) Turcheniuk, K. V.; Kukhar, V. P.; Roeschenthaler, G.-V.; Aceña, J. L.; Soloshonok, V. A.; Sorochinsky, A. E. Recent advances in the synthesis of fluorinated aminophosphonates and aminophosphonic acids. *RSC Adv.* **2013**, *3*, 6693-6716; d) Kukhar, V. P.; Sorochinsky, A. E.; Soloshonok, V. A. Practical synthesis of fluorine-containing α- and β-amino acids: recipes from Kiev, Ukraine. *Future Med. Chem.* **2009**, *1*, 793-819; e) Soloshonok, V. A. Highly diastereoselective michael addition reactions between nucleophilic glycine equivalents and β-substituted-α, β-unsaturated carboxylic acid derivatives a general approach to the stereochemically defined and sterically χ-constrained α-amino acids. *Curr. Org. Chem.* **2002**, *6*, 341-364; f) Mikami, K.; Fustero, S.; Sánchez-Roselló, M.; Aceña, J. L.; Soloshonok, V. A.; Sorochinsky, A. E. Synthesis of fluorinated β-amino acids. *Synthesis* **2011**, 3045-3079; g) Soloshonok, V. A.; Ohkura, H.; Yasumoto, M. Operationally convenient asymmetric synthesis of (*S*)- and (*R*)-3-amino-4,4,4-trifluorobutanoic acid: Part II. Enantioselective biomimetic transamination of 4,4,4-trifluoro-3-oxo-N-[(R)-1-phenylethyl]butanamide. *J. Fluorine Chem.* **2006**, *127*, 930-935; h) Han, J.; Sorochinsky, A. E.; Ono, T.; Soloshonok, V. A. Biomimetic transamination-a metal-free alternative to the reductive amination. Application for generalized preparation of fluorine-containing amines and amino acids. *Curr. Org. Synth.* **2011**, *8*, 281-294; i) Wzorek, A.; Sato, A.; Drabowicz, J.; Soloshonok, V. A.; Klika, K. D. Remarkable magnitude of the self-disproportionation of enantiomers (SDE) via achiral chromatography: application to the practical-scale enantiopurification of *β*-amino acid esters. *Amino Acids* **2016**, *48*, 605-613; j) Han, J.; Romoff, T. T.; Moriwaki, H.; Konno, H.; Soloshonok, V. A. Development of Hamari ligands for practical asymmetric synthesis of tailor-made amino acids. *ACS Omega* **2019**, *4*, 18942-18947; k) Han, J.; Wzorek, A.; Kwiatkowska, M.; Soloshonok, V. A.; Klika, K. D. The self-disproportionation of enantiomers (SDE) of amino acids and their derivatives. *Amino Acids* **2019**, *51*, 865-889.

7. For reviews, see: a) Sorochinsky, A. E.; Aceña, J. L.; Moriwaki, H.; Sato, T.; Soloshonok, V. A. Asymmetric synthesis of α-amino acids via homologation of Ni (II) complexes of glycine Schiff bases. *Amino Acids* **2013**, *45*, 691-718; b) Sorochinsky, A. E.; Aceña, J. L.; Moriwaki, H.; Sato, T.; Soloshonok, V. A. Asymmetric synthesis of α-amino acids via homologation of Ni (II) complexes of glycine Schiff bases. Part 2: Aldol, Mannich addition reactions, deracemization and (*S*) to (*R*) interconversion of α-amino acids. *Amino Acids* **2013**, *45*, 1017-1033; c) Aceña, J. L.; Sorochinsky, A. E.; Moriwaki, H.; Sato, T.; Soloshonok, V. A. Synthesis of fluorine-containing α-amino acids in enantiomerically pure form via homologation of Ni (II) complexes of glycine and alanine Schiff bases. *J. Fluorine Chem.* **2013**, *155*, 21-38; d) Aceña, J. L.; Sorochinsky, A. E.; Soloshonok, V. A. Asymmetric synthesis of α-amino acids via homologation of Ni (II) complexes of glycine Schiff bases. Part 3: Michael addition reactions and miscellaneous transformations. *Amino Acids* **2014**, *46*, 2047-2073; e) Wang, Y.; Song, X.; Wang, J.; Moriwaki, H.; Soloshonok, V. A.; Liu, H. Recent approaches for asymmetric synthesis of α-amino acids via homologation of Ni (II) complexes. *Amino Acids* **2017**, *49*, 1487-1520; f) Mei, H.; Jean, M.; Albalat, M.; Vanthuyne, N.; Roussel, C.; Moriwaki, H.; Yin, Z.; Han, J.; Soloshonok, V. A. Effect of substituents on the configurational stability of the stereogenic nitrogen in metal (II) complexes of α-amino acid Schiff bases. *Chirality* **2019**, *31*, 401-409.

8. For recent paper, see: a) Bergagnini, M.; Fukushi, K.; Han, J.; Shibata, N.; Roussel, C.; Ellis, T. K.; Aceña, J. L.; Soloshonok, V. A. NH-type of chiral Ni (II) complexes of glycine Schiff base: design, structural evaluation, reactivity and synthetic applications. *Org. Biomol. Chem.* **2014**, *12*, 1278-1291; b) Wang, S.; Zhou, S.; Wang, J.; Nian, Y.; Kawashima, A.; Moriwaki, H.; Aceña, J. L.; Soloshonok, V. A.; Liu, H. Chemical dynamic thermodynamic resolution and S/R interconversion of unprotected unnatural tailor-made α-amino acids. *J. Org. Chem.* **2015**, *80*, 9817-9830; c) Li, J.; Zhou, S.; Wang, J.; Kawashima, A.; Moriwaki, H.; Soloshonok, V. A.; Liu, H. Asymmetric Synthesis of Aromatic and Heteroaromatic α-Amino Acids Using a Recyclable Axially Chiral Ligand. *Eur. J. Org. Chem.* **2016**, 999-1006; d) Takeda, R.; Kawamura, A.; Kawashima, A.; Sato, T.; Moriwaki, H.; Izawa, K.; Abe, H.; Soloshonok, V. A. Second-order asymmetric transformation and its application for the practical synthesis of α-amino acids. *Org. Biomol. Chem.* **2018**, *16*, 4968-4972.

9. a) Soloshonok, V. A.; Ellis, T. K.; Ueki, H.; Ono, T. Resolution/deracemization of chiral α-amino acids using resolving reagents with flexible stereogenic centers. *J. Am. Chem. Soc.* **2009**, *131*, 7208-7209; b) Takeda, R.; Kawamura, A.; Kawashima, A.; Sato, T.; Moriwaki, H.; Izawa, K.; Akaji, K.; Wang, S.; Liu, H.; Aceña, J. L.; Soloshonok, V. A. Chemical dynamic kinetic resolution and S/R interconversion of unprotected α-amino acids. *Angew. Chem. Int. Ed.* **2014**, *53*, 12214-12217; c) Sorochinsky, A. E.; Ueki, H.; Aceña, J. L.; Ellis, T. K.; Moriwaki, H.; Soloshonok, V. A. Chemical approach for interconversion of (*S*)-and (*R*)-α-amino acids. *Org. Biomol. Chem.* **2013**, *11*, 4503-4507.

10. Zhou, S.; Wang, J.; Chen, X.; Aceña, J. L.; Soloshonok, V. A.; Liu, H. Chemical kinetic resolution of unprotected β-substituted β-amino acids using recyclable chiral ligands. *Angew. Chem. Int. Ed.* **2014**, *53*, 7883-7886.

11. a) Taylor, S. M.; Yamada, T.; Ueki, H.; Soloshonok, V. A. Asymmetric synthesis of enantiomerically pure 4-aminoglutamic acids via methylenedimerization of chiral glycine equivalents with dichloromethane under operationally convenient conditions. *Tet. Lett.* **2004**, *45*, 9159-9162; b) Ellis, T. K.; Hochla, V. M.; Soloshonok, V. A. Efficient synthesis of 2-aminoindane-2-carboxylic acid via dialkylation of nucleophilic glycine equivalent. *J. Org. Chem.* **2003**, *68*, 4973-4976; c) Wang, J.; Lin, D.; Zhou, S.; Soloshonok, V. A.; Liu, H. Asymmetric synthesis of sterically and electronically demanding linear ω-trifluoromethyl containing amino acids via alkylation of chiral equivalents of nucleophilic glycine and alanine. *J. Org. Chem.* **2011**, *76*, 684-687.

12. a) Yamada, T.; Okada, T.; Sakaguchi, K.; Ohfune, Y.; Ueki, H.; Soloshonok, V. A. Efficient asymmetric synthesis of novel 4-substituted and configurationally stable analogues of thalidomide. *Org. Lett.* **2006**, *8*, 5625-5628; b) Yamada, T.; Sakaguchi, K.; Shinada, T.; Ohfune, Y.; Soloshonok, V. A. Efficient asymmetric

synthesis of the functionalized pyroglutamate core unit common to oxazolomycin and neooxazolomycin using Michael reaction of nucleophilic glycine Schiff base with α,β-disubstituted acrylate. *Tetrahedron: Asymmetry* **2008**, *19*, 2789-2795; c) Soloshonok, V. A.; Cai, C.; Hruby, V. J. (*S*)-or (*R*)-3-(*E*-Enoyl)-4-phenyl-1, 3-oxazolidin-2-ones: ideal Michael acceptors to afford a virtually complete control of simple and face diastereoselectivity in addition reactions with glycine derivatives. *Org. Lett.* **2000**, *2*, 747-750.

13. a) Kawamura, A.; Moriwaki, H.; Röschenthaler, G.-V.; Kawada, K.; Aceña, J. L.; Soloshonok, V. A. Synthesis of (2*S*, 3*S*)-β-(trifluoromethyl)-α, β-diamino acid by Mannich addition of glycine Schiff base Ni (II) complexes to *N*-tert-butylsulfinyl-3,3,3-trifluoroacetaldimine. *J. Fluorine Chem.* **2015**, *171*, 67-72; b) Soloshonok, V. A.; Avilov, D. V.; Kukhar, V. P.; Meervelt, L. V.; Mischenko, N. Highly diastereoselective aza-aldol reactions of a chiral Ni (II) complex of glycine with imines. An efficient asymmetric approach to 3-perfluoroalkyl-2,3-diamino acids. *Tet. Lett.* **1997**, *38*, 4671-4674.
14. a) Jörres, M.; Aceña, J. L.; Soloshonok, V. A.; Bolm, C. Asymmetric carbon-carbon bond formation under solventless conditions in ball mills. *ChemCatChem* **2015**, *7*, 1265-1269; b) Jörres, M.; Chen, X.; Aceña, J. L.; Merkens, C.; Bolm, C.; Liu, H.; Soloshonok, V. A. Asymmetric synthesis of α-amino acids under operationally convenient conditions. *Adv. Synth. Catal.* **2014**, *356*, 2203-2208.
15. a) Kawashima, A.; Shu, S.; Takeda, R.; Kawamura, A.; Sato, T.; Moriwaki, H.; Wang, J.; Izawa, K.; Aceña, J. L.; Soloshonok, V. A.; Liu, H. Advanced asymmetric synthesis of (1*R*, 2*S*)-1-amino-2-vinylcyclopropanecarboxylic acid by alkylation/cyclization of newly designed axially chiral Ni (II) complex of glycine Schiff base. *Amino Acids* **2016**, *48*, 973-986; b) Kawashima, A.; Xie, C.; Mei, H.; Takeda, R.; Kawamura, A.; Sato, T.; Moriwaki, H.; Izawa, K.; Han, J.; Aceña, J. L.; Soloshonok, V. A. Asymmetric synthesis of (1*R*, 2*S*)-1-amino-2-vinylcyclopropanecarboxylic acid by sequential SN 2-SN 2′ dialkylation of (*R*)-*N*-(benzyl) proline-derived glycine Schiff base Ni (II) complex. *RSC Adv.* **2015**, *5*, 1051-1058.
16. Large-scale synthesis, see: a) Yin, Z.; Moriwaki, H.; Abe, H.; Miwa, T.; Han, J.; Soloshonok, V. A. Large-scale asymmetric synthesis of Fmoc-(*S*)-2-amino-6, 6, 6-trifluorohexanoic acid. *ChemistryOpen* **2019**, *8*, 701-704; b) Mei, H.; Yin, Z.; Miwa, T.; Moriwaki, H.; Abe, H.; Han, J.; Soloshonok, V. A. Convenient asymmetric synthesis of Fmoc-(*S*)-6,6,6-trifluoro-Norleucine. *Symmetry* **2019**, *11*, 578; c) Mei, H.; Hiramatsu, T.; Takeda, R.; Moriwaki, H.; Abe, H.; Han, J.; Soloshonok. V. A. Expedient asymmetric synthesis of (*S*)-2-Amino-4, 4, 4-trifluorobutanoic acid via alkylation of chiral nucleophilic glycine equivalent. *Org. Process Res. Dev.* **2019**, *23*, 629-634; d) Han, J.; Takeda, R.; Liu, X.; Konno, H.; Abe, H.; Hiramatsu, T.; Moriwaki, H.; Soloshonok, V. A. Preparative Method for asymmetric synthesis of (*s*)-2-amino-4, 4, 4-trifluorobutanoic acid. *Molecules* **2019**, *24*, 4521.
17. a) Soloshonok, V. A.; Kukhar, V. P.; Galushko, S. V.; Svistunova, N. Y.; Avilov, D. V.; Kuzmina, N. A.; Raevski, N. I.; Struchkov, Y. T.; Pisarevsky, A. P.; Belokon, Y. N. General method for the synthesis of enantiomerically pure β-hydroxy-α-amino acids, containing fluorine atoms in the side chains. Case of stereochemical distinction between methyl and trifluoromethyl groups. X-Ray crystal and molecular structure of the nickel (II) complex of (2*S*, 3*S*)-2 (trifluoromethyl) threonine. *J. Chem. Soc. Perkin Trans 1* **1993**, 3143-3155; b) Soloshonok, V. A.; Avilov, D. V.; Kukhar, V. P. Highly diastereoselective asymmetric aldol reactions of chiral Ni (II)-complex of glycine with alkyl trifluoromethyl ketones. *Tetrahedron: Asymmetry* **1996**, *7*, 1547-1550; c) Soloshonok, V. A.; Avilov, D. V.; Kukhar, V. P. Asymmetric aldol reactions of trifluoromethyl ketones with a chiral Ni (II) complex of glycine: stereocontrolling effect of the trifluoromethyl group. *Tetrahedron* **1996**, *52*, 12433-12442.
18. a) Li, T.; Zhou, S.; Wang, J.; Aceña, J. L.; Soloshonok, V. A.; Liu, H. Asymmetric synthesis of α-(1-oxoisoindolin-3-yl) glycine: Synthetic and mechanistic challenges. *Chem. Commun.* **2015**, *51*, 1624-1626; b) Li, T.; Zhou, S.; Wang, J.; Aceña, J. L.; Soloshonok, V. A.; Liu, H. Asymmetric synthesis of (2 S, 3 S)-α-(1-oxoisoindolin-3-yl) glycines under low-basicity "kinetic" control. *J. Org. Chem.* **2015**, *80*, 11275-11280.
19. Soloshonok, V. A.; Avilov, D. V.; Kukhar, V. P.; Tararov, V. I., et al. Asymmetric aldol reactions of chiral Ni (II)-complex of glycine with aliphatic aldehydes. Stereodivergent synthesis of syn-(2*S*)-and syn-(2*R*)-β-alkylserines. *Tetrahedron: Asymmetry* **1995**, *6*, 1741-1756.
20. a) Nian, Y.; Wang, J.; Moriwaki, H.; Soloshonok, V. A.; Liu, H. Analysis of crystallographic structures of Ni (ii) complexes of α-amino acid Schiff bases: elucidation of the substituent effect on stereochemical preferences. *Dalton Trans.* **2017**, *46*, 4191-4198; b) Romoff, T. T.; Palmer, A. B.; Mansour, N.; Creighton, C. J.; Miwa, T.; Ejima, Y.; Moriwaki, H.; Soloshonok, V. A. Scale-up synthesis of (*R*)-and (*S*)-N-(2-Benzoyl-4-chlorophenyl)-1-(3,4-dichlorobenzyl) pyrrolidine-2-carboxamide hydrochloride, a versatile reagent for the preparation of tailor-made α-and β-amino acids in an enantiomerically pure form. *Org. Process Res. Dev.* **2017**, *21*, 732-739.
21. a) Takeda, R.; Abe, H.; Shibata, N.; Moriwaki, H.; Izawa, K.; Soloshonok, V. A. Asymmetric synthesis of α-deuterated α-amino acids. *Org. Biomol. Chem.* **2017**, *15*, 6978-6983; b) Yamamoto, J.; Kawashima, A.; Kawamura, A.; Abe, H.; Moriwaki, H.; Shibata, N.; Soloshonok, V. A. Operationally Convenient and Scalable Asymmetric Synthesis of (2*S*)-and (2*R*)-α-(Methyl) cysteine Derivatives through Alkylation of Chiral Alanine Schiff Base NiII Complexes. *Eur. J. Org. Chem.* **2017**, 1931-1939.
22. a) Nian, Y.; Wang, J.; Zhou, S.; Wang, S.; Moriwaki, H.; Kawashima, A.; Soloshonok, V. A.; Liu, H. Recyclable ligands for the non-enzymatic dynamic kinetic resolution of challenging α-amino acids. *Angew. Chem. Int. Ed.* **2015**, *54*, 12918-12922; b) Nian, Y.; Wang, J.; Zhou, S.; Dai, W.; Wang, S.; Moriwaki, H.; Kawashima, A.; Soloshonok, V. A.; Liu, H. Purely chemical approach for preparation of D-α-amino acids via (*S*)-to-(*R*)-interconversion of unprotected tailor-made α-amino acids. *J. Org. Chem.* **2016**, *81*, 3501-3508; c) Mei, H.; Han, J.; Takeda, R.; Sakamoto, T.; Miwa, T.; Minamitsuji, Y.; Moriwaki, H.; Abe, H.; Soloshonok, V. A. Practical method for preparation of (*S*)-2-Amino-5,5,5-trifluoropentanoic acid via dynamic kinetic resolution. *ACS Omega* **2019**, *4*, 11844-11851.

Каскадні реакції альдольного приєднання та циклізації на основі хірального комплексу Ni(II) основи Шифа гліцину

Ю. Чжоу[1], Ц. Їнь[1], Х. Мей[1], Х. Конно[2], Х. Моріваки[3], В. А. Солошонок[4,5]*, Ц. Хань[1]*

[1] *Нанкінський лісотехнічний університет, вул. Лонпан роуд, 159, Нанкін, 210037, КНР*
[2] *Вища школа науки і технології, Ямагатський університет, Йонезава, Ямагата, 992-8510, Японія*
[3] *Гамарі Кемікалс Лтд., 1-19-40, Нанкоіта, Суміное-ку, Осака, 559-0034, Японія*
[4] *Університет Країни Басків, вул. Пасео Мануель Лардізабаля, 3, Сан-Себастьян, 20018, Іспанія*
[5] *ІКЕРБАСК, Баскський фонд науки, вул. Марії Діас де Аро, Більбао, 48013, Іспанія*

Резюме: На базі хірального комплексу Ni(II) основи Шифа гліцину нового типу було розроблено каскадні реакції приєднання-циклізації з метою вивчення аспектів кінетичного/термодинамічного утворення відповідних (*S*)(2*S*,3*S*)/(*S*)(2*S*,3*R*) діастереомерів. Було знайдено, що утворені лактони в значній мірі є продуктами термодинамічно контрольованої діастереоселективності завдяки значному внеску зворотньої реакції альдольного приєднання порівняно із подальшою циклізацією. Досить несподіваним виявився факт температурної залежності стереохімічних співвідношень продуктів реакції: при низькій температурі утворювався переважно (2*S*,3*R*) діастереомер, у той час як при підвищеній – (2*S*,3*S*). Спостережувана діастереоселективність становила 4/1 (*S*)(2*S*,3*S*)/(*S*)(2*S*,3*R*), що є значно кращим показником порівняно із попередніми даними (1.7/1). Подібний рівень діастереоселективності, а також сумарний вихід продуктів реакції (більш ніж 90%), свідчать про великий синтетичний потенціал даного методу, що однозначно заслуговує на всебічне та цілеспрямоване дослідження.

Ключові слова: асиметричний синтез; альдольне приєднання; специфічні неприродні амінокислоти; Ni(II) комплекси; основи Шифа; каскадні/доміно/тандемні реакції.

ISSN 1814-9758. Ukr. Bioorg. Acta, 2021, Vol. 16, N 1
UDC 547.783 + 615.281.8 + 615.277.3
DOI: hpps://doi.org/10.15407/bioorganica2021.01.010

Ukrainica Bioorganica Acta
www.bioorganica.org.ua

RESEARCH ARTICLE

New 4-iminohydantoin sulfamide derivatives with antiviral and anticancer activity

Yurii Eu. Kornii[1], Oleh V. Shablykin[1], Olga V. Shablykina[1,2]*, Volodymyr S. Brovarets[1]

[1] *V. P. Kukhar Institute of Bioorganic Chemistry and Petrochemistry of the NAS of Ukraine, 1 Murmanska St., Kyiv, 02094, Ukraine*
[2] *Taras Shevchenko National University of Kyiv, 60 Volodymyrska St., Kyiv, 01601, Ukraine*

Abstract: A number of sulfamides were obtained by reaction interaction of (5-(dichloromethylene)-2-oxoimidazolidin-4-ylidene)sulfamoyl chloride with anilines, benzylamines, Boc-protected piperazine, methylalylamine, and amino acids methyl esters with primary and secondary amino group. The antiviral and anticancer activity of new derivatives was evaluated. The most effective compounds against *Human cytomegalovirus* were sulfamides based on anisidine (**1b**), *N*-Boc-piperazine (**1h**), and the derivatives **1n, o** with fragments of nipecotic and azetidine-3-carboxylic acids, respectively. Anticancer activity was most significant for sulfamides based on *p*-methoxybenzylamine (compound **1d**), benzylmethylamine (compound **1f**), and allylmethylamine (compound **1g**).

Keywords: hydantoins; sulfamides; antiviral activity; anticancer activity.

Introduction

The hydantoin motif often appears in bioactive molecules of both natural and synthetic origin (Figure 1) [1-2]. This heterocyclic system, due to its low aromaticity, can be consider as a cyclic combination of an α-amino acid and urea with all the resultant consequences, such as the possibility of assembly with a variation of substituents [3], the relative ease of combinatorial libraries creation [4], the possibility of further modification, as well as bioavailability and environmental friendliness [5]. These factors make hydantoin derivatives very attractive objects for medicinal chemistry, and a brief overview of the achievements in this area over the past decade can be found in the work [6]. At the same time, the possibility disagreeable side effects of a number of hydantoin drugs cannot be ignored [7-9]. However, it is also obvious that the main reason for the toxicity of some derivatives is not the hydantoin fragment (for example, Allantoin exhibits almost no undesirable effects), but the effect of substituents. Consequently, the creation of new substances with a hydantoin fragment and

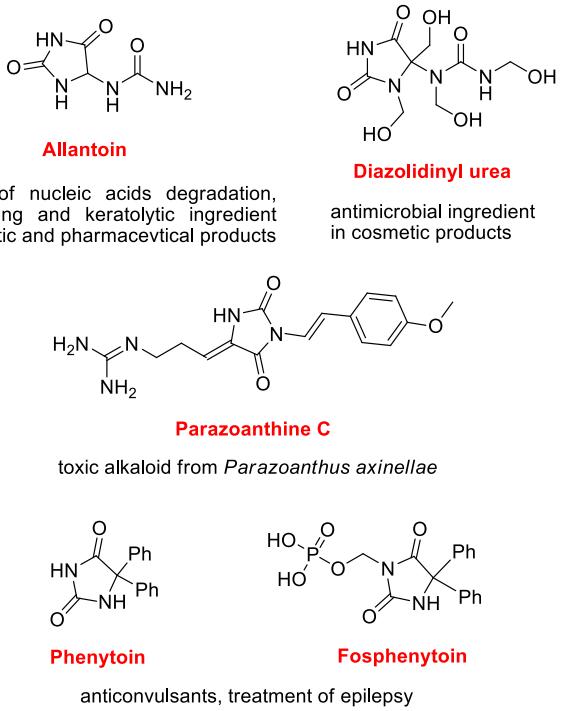

Figure 1. Practically used natural and synthetic hydantoin derivatives [1-2].

Received: 15.04.2021
Revised: 29.04.2021
Accepted: 13.05.2021
Published online: 30.06.2021

* Corresponding author. Tel.: +380-66-167-9812;
e-mail: shablykina@ukr.net (O. V. Shablykina)
ORCID: 0000-0002-5362-0831

the study of possible areas of their practical application is a crucial task.

Earlier, we established a convenient way to synthesize the novel sulfamides with a hydantoin fragment and found anticancer [10] and antiviral [11] activity for some of these compounds (Figure 2, general structure **1**). The results of studies of the anticancer activity of hydantoin sulfonamides were quite optimistic in terms of further prospects for this class of substances: for example, all of the first six synthesized derivatives were selected for single-dose assay, and five-dose assay were led for two compounds [10, 12]. Data on antiviral activity were less demonstrative [11], but also showed a significant dependence of the level of activity on the nature of the substituents R^1 and R^2.

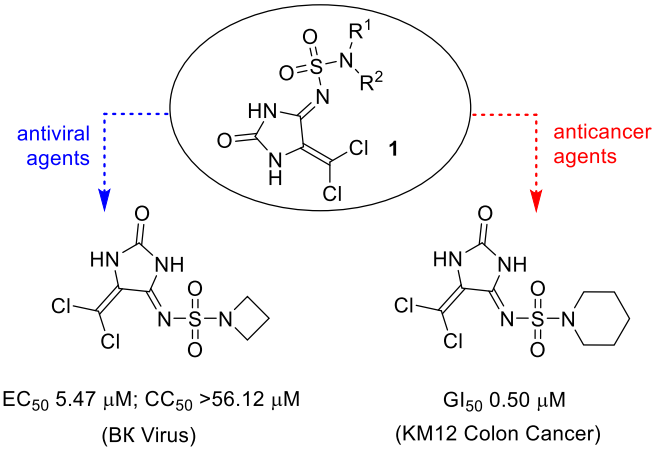

Figure 2. Bioactive (5-(dichloromethylene)-2-oxoimidazolidin-4-ylidene)sulfamides [10-12].

This has become a weighty reason for us to keep this research course; therefore, the aim of this work was to create new derivatives of general formula **1** (Figure 2), and study their antiviral and anticancer effects. This course is also supported by the data summarized in the review [13] concerning the anticancer and antiviral activity of sulfonamides: the varying the substituents can stimulate the displaying one or another type of activity.

Results and Discussion

Chemistry

The starting sulfamoyl chloride **2** is formed by the reaction of chlorosulfonylisocyanate (**3**) with 2-amino-3,3-dichloroacrylonitrile (ADAN, **4**) through the steps of acylation of the ADAN amino group with isocyanate, heterocyclization with the ADAN CN-group and the nitrogen atom of the newly formed urea, and, at last, recyclization [10]. Despite the presence of a several active functional fragments, compound **2** is relatively stable and suitable for long-term storage (at low temperature), therefore, it is a convenient "building block".

Compared with previous works, we have significantly expanded the list of amines that were involved in the interaction with sulfamoyl chloride **2** to obtain the target sulfamides **1a-o**. Substituted anilines, benzylamines, Boc-protected piperazine, methylalylamine, and amino acids methyl esters with primary and secondary amino group were used. The focus on a series of amino acid derivatives obtaining was due to previous results: a sulfamide of similar structure with a residue of ester nipecotic acid showed strong anticancer activity [10], and the corresponding acid exhibited antiviral action [11]. The formation of compounds **1** occurred under the action of 5-6 eq. amine on chloride **2** in THF solution, and the nature of the amine didn't have much effect on the yield of the product. Removal of Boc-protection of compound **1h** was applied in organic solvent with dry HCl.

Biological Assay

To establish antiviral activity *in vivo* against some strains of cytomegalovirus compounds **1b-h, k, l, n, o** were selected. Unfortunately, a number of investigated substances revealed low activity and insufficient chemotherapeutic index; namely *Human cytomegalovirus* was not suppressed by sulfamides **1c-g, k, l**. Compounds **1b, h** couldn't effectively suppress the growth of *H. cytomegalovirus* strain GDGr K_{17}, but proved to be quite effective against *H. cytomegalovirus* strain AD169 (see Table 1). The derivatives **1n, o** with a fragment of nipecotic and azetidine-3-carboxylic acids, respectively, also acted selectively only on certain species and strains of cytomegaloviruses and weren't active against the others ones. In particular the sulfamides **1n, o** weren't effective against *Guinea pig cytomegalovirus* (22122), *Murine cytomegalovirus* (Smith), but active against *H. cytomegalovirus* (see Table 1). The indexes of antiviral activity also depended on the detection method. For example, when determining the EC_{50} value of the compounds **1n, o** to *H. cytomegalovirus* (AD169) by quantitative polymerase chain reaction these substances were classified as inefficient, while when determining EC_{50} by the method of CellTiter-Glo the value were nearby to the comparison drugs (Table 1). Therefore, four substances showed worthy of interest antiviral activity; these data are shown in Table 1, where the EC_{50} – compound concentration that reduces viral replication by 50%, EC_{90} – concentration that reduces viral replication by 90%, CC_{50} – concentration that reduces cell viability by 50%, SI_{50} – CC_{50} / EC_{50}, SI_{90} – CC_{50} / EC_{90}. The EC_{50} value of the sulfamides **1b, h, n, o** were comparable to the Ganciclovir and Cidofovir. But they have an unremarkable chemotherapy index, especially SI_{90}

The possible anticancer effect was investigated not only for the sulfamides **1a-o** synthetized in this work, but also for the isopropylamine and tryptamine derivatives **1r**, **s**, described in the article [11]. As a result of the primary analysis, a number of biological screening substances were selected (see Table 2).

According to single-dose assay, not all of the studied derivatives had significant anticancer activity. The average percentage inhibition of cancer cell growth, the range of values, as well as the number of lines (from 60 studying ones) that experienced a growth inhibition of more than 50%, and the number of cell lines for which the test compo-

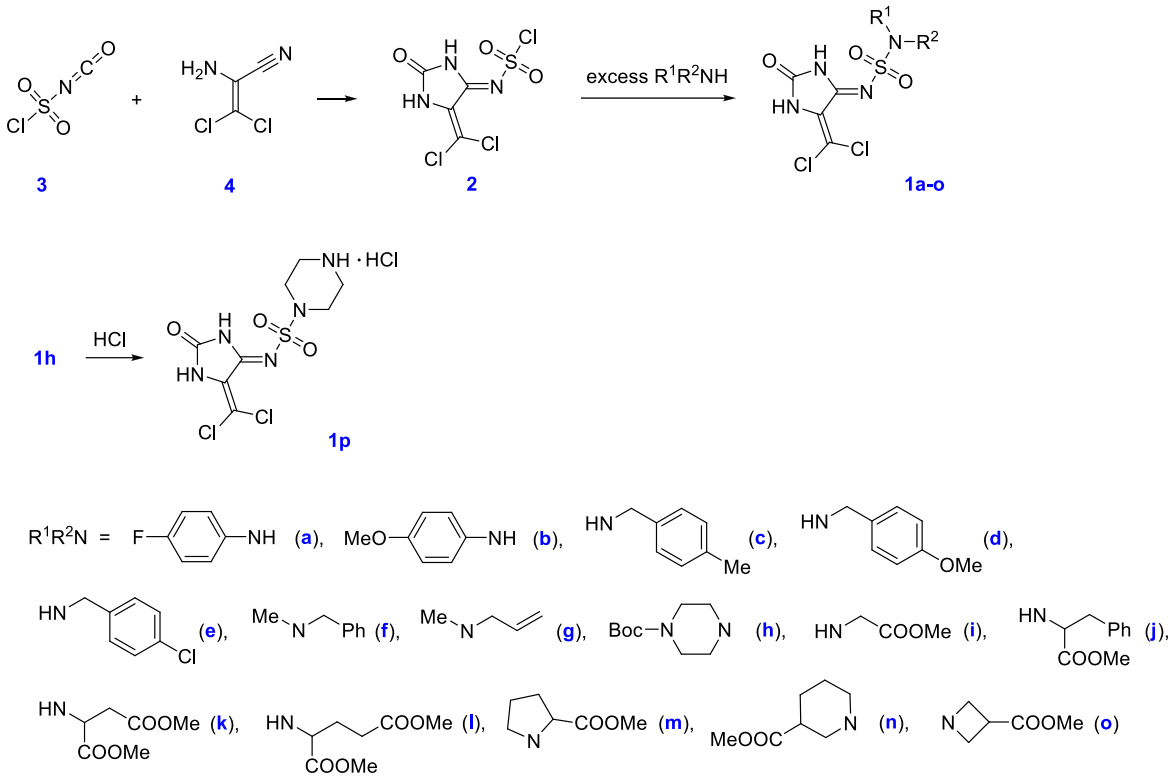

Scheme 1. Synthesis of new (5-(dichloromethylene)-2-oxoimidazolidin-4-ylidene)sulfamides.

unds were lethal are shown in Table 2. In the latter case, the record values of mortality rates are also reported.

Even in a such small list of compounds, the following tendency can be observed: sulfamides based on aliphatic and aromatic amines show, on average, low anticancer activity, and, on the other hand, the derivatives of benzylamines, allylmethylamine and tryptamine very effectively inhibit the growth of numerous cancer cell lines. It is noteworthy that two compounds – **1f** and **1g**, which were obtained from similar amines (benzylmethylamine and allylmethylamine, respectively), showed the highest anticancer activity against the same cancer cell lines (Table 2) with very similar values.

Table 1. The antiviral activity data of sulfamides **1b, h, n, o** against *H. cytomegalovirus*.*

Virus Strain	Compd	EC_{50}	EC_{90}	CC_{50}	SI_{50}	SI_{90}
AD169	**Ganciclovir**	0.39	1.13	>150.00	>383	>133
	1b	0.21	>6.00	14.42	69	<2
	1h	0.95	>6.00	15.87	17	<3
	1n	0.15	>6.00	14.34	96	<2
	1o	0.19	>30.00	68.08	353	<2
GDGr K_{17}	**Ganciclovir**	13.44	>150.00	>150.00	>11	1
	Cidofovir	0.11	>30.00	117.81	1061	<4
	1n	0.13	>6.00	15.99	119	<3
	1o	0.54	>30.00	70.90	131	<2

* Cell Line: HFF; control assay: CellTiter-Glo (cytopathic effect/toxicity).

It is also interesting that the values of the activity of sulfamides **1f** and **1g** activity are in a plenty wide range. These compounds have shown very selective cytotoxicity against various cancer lines. As shown in Table 3, the growth inhibition rates of 8 melanoma lines were observed. It is easy to see that the compounds **1f, g** only slightly inhibit the growth of some lines, but a high percentage of lethality was recorded for LOX IMVI cells. Similar strong differences in the activity of compounds **1f, g** can be observed to different cell lines of colorectal, renal and ovarian cancers. But these substances were found to be highly effective against all studied lines of leukemia (Table 3) – from almost discontinuing of growth to significant lethality.

For substances **1d, f, g**, a five-dose assay of their anticancer activity were performed. In the Table 4 the average concentrations of GI_{50}, TGI, LC_{50} and the corresponding values for cancer lines that were inhibited most effectively in a single-dose experiment are shown (compare with Table 2; Melanoma LOX IMVI for compounds **1f, g** wasn't investigate), as well as values for the lines with the highest inhibition (marked in a color).

In average values, compound **1f** exhibits the highest anticancer activity, and the effect of sulfonamide **1g** is slightly less. Substance **1f** was able to inhibit growth by 50% at a concentration of less than 10^{-6} M (respectively, lg GI_{50} < -6) of 5 lines out of 59 tested in a five-dose experiment, including Colon Cancer KM12 (see Table 3), Leukemia RPMI-8226 and SR, Breast Cancer MCF7 and MDA-MB-468; and the substance **1g** in less than 10^{-6} M concentration inhibited the growth by 50% the same 5 lines.

Substance **1d** in less than micromolar concentrations inhibited by 50% the growth of 11 lines from 59, but TGI and LC_{50} values wasn't so conductive.

Table 2. The effect of compounds **1a-h, p-s** on the growth of cancer cells, determined by single-dose assay (C = 10^{-5} M); GP – Growth Percent, %; N_{50} – number of lines with GP <50%; N_0 – number of lines with GP <0%.

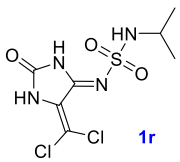

1r

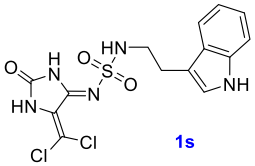

1s

Compd (NCS code)	GP, Mean	GP, Range	N_{50}	N_0	The most significant inhibition, GP
1a (827223)	100.8	58.9	–	–	69.7 SNB-75 (CNS Cancer)
1b (827225)	93.8	108.7	4	–	15.4 MDA-MB-468 (Breast Cancer)
1c (827227)	52.9	121.6	29	3	-8.7 BT-549 (Breast Cancer) -3.0 SNB-75 (CNS Cancer) -1.1 HOP-92 (Non-Small Cell Lung Cancer)
1d (827226)	26.8	106.4	47	7	-23.2 SNB-75 (CNS Cancer) -22.9 SF-295 (CNS Cancer) -11.1 HL-60(TB) (Leukemia)
1e (827224)	98.7	82.7	1	–	44.1 MDA-MB-468 (Breast Cancer)
1f (828790)	36.0	201.2	30	13	-90.8 ACHN (Renal Cancer) -84.5 LOX IMVI (Melanoma) -81.7 OVCAR-3 (Ovarian Cancer)
1g (828791)	20.88	200.41	35	21	-96.7 ACHN (Renal Cancer) -88.3 LOX IMVI (Melanoma) -84.3 OVCAR-3 (Ovarian Cancer)
1h (827229)	83.9	176.1	7	1	-52.4 NCI-H522 (Non-Small Cell Lung Cancer)
1p (827228)	102.0	48.3	–	–	72.5 SNB-75 (CNS Cancer)
1r (812426)	95.5	102.6	1	–	19.7 SR (Leukemia)
1s (812428)	56.4	135.9	23	3	-3.3 MDA-MB-468 (Breast Cancer) -4.6 KM12 (Colon Cancer) -25.8 OVCAR-3 (Ovarian Cancer)

Conclusions

Thus, the diversity of the sulfamides obtained on the base of (5-(dichloromethylene)-2-oxoimidazolidin-4-ylidene)sulfamoyl chloride was significantly supplemented by us, and the antiviral and anticancer activity of new derivatives was determined. It was found that the antiviral activity against *H. cytomegalovirus* is inherent for esters of nipecotic and azetidine-3-carboxylic acids **1n** and **1o**, respectively, as well as for anisidine **1b** and Boc-piperazine **1h** sulfamides, but, unfortunately, these compounds have a low chemotherapy index. Most of the tested compounds can effectively inhibit the growth of tumor cells, and strongest inhibition was observed for sulfamides based on *p*-methoxybenzylamine (compo-und **1d**), benzylmethylamine (compound **1f**), and allyl-methylamine (compound **1g**). The substances **1f, g** also have high selectivity for certain cancer cells lines. So, using various amines in the synthesis of *N*-[5-(dichloro-methylene)-2-oxoimidazolidin-4-ylidene]sulfa-mides, it has been indeed possible to obtain compounds with either antiviral or anticancer activity.

Table 3. The effect of compounds **1f, g** on the growth of Melanoma and Leukemia cells.

	Growth Percent, %	
	1f (NSC 828790)	**1g** (NSC 828791)
Melanoma		
LOX IMVI	-84.5	-88.3
MALME-3M	-19.9	-69.4
MDA-MB-435	79.6	34.4
SK-MEL-2	87.8	90.0
SK-MEL-28	11.2	-83.6
SK-MEL-5	95.7	91.6
UACC-257	68.2	57.4
UACC-62	62.2	32.9
Leukemia		
CCRF-CEM	-12.9	-27.1
HL-60(TB)	-29.8	-51.7
K-562	1.1	-3.5
MOLT-4	10.3	-19.7
RPMI-8226	-1.1	5.2
SR	-0.4	-18.7

Table 4. The effect of compounds **1d, f, g** on the growth of cancer cells, determined by five-dose assay (the concentrations GI_{50}, TGI and LC_{50}*, mol/l, given as **lg**).

Compd (NCS code)	Cell line	Value of cancer cell lines' growth inhibition		
		lg GI_{50}	lg TGI	lg LC_{50}
1d (827226)	***Mean value***	-5.75	-4.46	-4.07
	SNB-75 (CNS Cancer)	-5.87	> -4.00	> -4.00
	SF-295 (CNS Cancer)	-5.54	> -4.00	> -4.00
	HL-60(TB) (Leukemia)	-6.12	-5.25	> -4.00
	MDA-MB-468 (Breast Cancer)	-6.74	-6.19	-4.11
1f (828790)	***Mean value***	-5.74	-5.26	-4.69
	ACHN (Renal Cancer)	-5.75	-5.50	-5.24
	OVCAR-3 (Ovarian Cancer)	-5.75	-5.47	-5.18
	KM12 (Colon Cancer)	-6.57	-6.13	-4.44
1g (828791)	***Mean value***	-5.66	-5.14	-4.61
	ACHN (Renal Cancer)	-5.75	-5.50	-5.24
	LOX IMVI (Melanoma)	-	-	-
	OVCAR-3 (Ovarian Cancer)	-5.72 -	5.42	-
	MCF7 (Breast Cancer)	-6.41	> -4.00	> -4.00
	RPMI-8226 (Leukemia)	-6.39	-5.01	> -4.00
	KM12 (Colon Cancer)	-6.36	-4.59	> -4.00

* GI_{50} (growth inhibitory activity) – concentration of the compound causing 50 % decrease in net cell growth; TGI (cytostatic activity) – concentration of the compound resulting in total growth inhibition; LC_{50} (cytotoxic activity) – concentration of the compound causing net 50 % loss of initial cells at the end of the incubation period of 48 h.

Experimental section

Chemistry

The solvents were purified according to the standard procedures. All materials were purchased from commercial sources and used without further purification. The success rate was calculated as the number of successful experiments divided by the total number of experiments. NMR spectra were recorded on Varian Union Plus spectrometer (400 MHz for ^{1}H and 100 MHz for ^{13}C) in DMSO-d_6 solution. Chemical shifts are reported in ppm downfield from TMS as internal standards. Mass spectra were recorded on an LC-MS instrument with chemical ionization (CI). LC-MS data were acquired on an Agilent 1200 HPLC system equipped with DAD/ELSD/LCMS-6120 diode matrix and mass-selective detector. Melting points were measured on a MPA100 OptiMelt automated melting point system. Elemental analyses were performed at the Analytical Laboratory of the V.P. Kukhar Institute of Bioorganic Chemistry and Petrochemistry of the NAS of Ukraine, their results were found to be in good agreement (±0.4%) with the calculated values.

The method of sulfamoyl chloride **2** synthesis and general method of sulfamides **1a-o** synthesis from 1 g (3.59 mmol) sulfamoyl chloride **2** were given in publication [10]. The synthesis and the data of sulfamides **1r, s** see at [11].

*(Z)-N-[5-(Dichloromethylene)-2-oxoimidazolidin-4-yl-idene]-N′-(4-fluorophenyl)sulfamide (**1a**).*

Yield: 0.36 g, 28%; mp 220-221 °C. ^{1}H NMR δ 11.47 (br s, 1H, NH), 11.15 (br s, 1H, NH), 9.92 (s, 1H, SO_2NH), 7.05-7.28 (m, 4H, Ar). ^{13}C NMR δ 158.91 (d, J_{CF} 240.1 Hz, C-F), 152.2 (C=N or C=O), 151.1 (C=N or C=O), 134.4 (d, J_{CF} 1.6 Hz, NH-S), 129.7 (C=CCl_2), 122.85 × 2 (d, J_{CF} 8.2 Hz, CHCHCF), 115.56 × 2 (d, J_{CF} 22.5 Hz, CHCF), 107.3 (CCl_2). HPLC (CI) m/z (I_{rel}, %) 353.0 $[M+1]^+$ (100).

*(Z)-N-[5-(Dichloromethylene)-2-oxoimidazolidin-4-yl-idene]-N′-(4-methoxyphenyl)sulfamide (**1b**).*

Yield: 0.97 g, 74%; mp 195 °C (decomp.). ^{1}H NMR δ 11.38 (br s, 1H, NH), 11.13 (s, 1H, NH), 9.60 (s, 1H, SO_2NH), 7.13 (d, *J* 8.6 Hz, 2H, Ar), 6.87 (d, *J* 8.6 Hz, 2H, Ar), 3.70 (s, 3H, CH_3O). ^{13}C NMR δ 156.5 ($C_{Ar}O$), 152.2 (C=N or C=O), 150.9 (C=N or C=O), 130.6 (Ar), 129.7 (C=CCl_2), 123.8 × 2 (Ar), 114.1 × 2 (Ar), 107.2 (CCl_2), 55.2 (CH_3O). HPLC (CI) m/z (I_{rel}, %) 363.0 $[M-1]^-$ (100).

*(Z)-N-[5-(Dichloromethylene)-2-oxoimidazolidin-4-yl-idene]-N′-(4-methylbenzyl)sulfamide (**1c**).*

Yield: 0.91 g, 70%; mp 165-166 °C. ^{1}H NMR δ 11.02 (m, 2H, 2NH), 7.80 (t, *J* 6.6 Hz, 1H, $NHCH_2$), 7.19 (d, *J* 6.8 Hz 2H, Ar), 7.08 (d, *J* 6.8 Hz, 2H, Ar), 4.12 (d, *J* 6.6 Hz, 2H, $NHCH_2$), 2.26 (s, 3H, CH_3). ^{13}C NMR δ 152.2 (C=N or C=O), 150.2 (C=N or C=O), 136.3 (Ar), 134.4 (Ar), 129.5 (C=CCl_2), 128.5 × 2 (Ar), 127.8 × 2 (Ar), 106.9 (CCl_2), 46.3 (CH_2), 20.7 (CH_3). HPLC (CI) m/z (I_{rel}, %) 361.0 $[M-1]^-$ (100).

*(Z)-N-[5-(Dichloromethylene)-2-oxoimidazolidin-4-yl-idene]-N′-(4-methoxybenzyl)sulfamide (**1d**).*

Yield: 1.22 g, 90%; mp 190-191 °C. ^{1}H NMR δ 11.03 (br s, 2H, NH), 7.76 (t, *J* 5.6 Hz, 1H, $NHCH_2$), 7.22 (d, *J* 7.9 Hz, 2H, Ar), 6.83 (d, *J* 7.9 Hz, 2H, Ar), 4.09 (d, *J* 5.6 Hz, 2H, $NHCH_2$), 3.72 (s, 3H, CH_3O). ^{13}C NMR δ 158.5 (C_{Ar}–O), 152.2 (C=N or C=O), 150.1 (C=N or C=O), 129.6 (C=CCl_2), 129.4 (Ar), 129.2 × 2 (Ar), 113.4 × 2 (Ar), 106.9 (CCl_2), 55.1 (CH_3O), 46.0 (CH_2). HPLC (CI) m/z (I_{rel}, %) 379.0 $[M-1]^-$ (100).

*(Z)-N′-(4-Chlorobenzyl)-N-[5-(dichloromethylene)-2-oxo-imidazolidin-4-ylidene]sulfamide (**1e**).*

Yield: 1.13 g, 82%; mp 202-203 °C. ^{1}H NMR δ 11.12 (br s, 1H, NH), 11.06 (s, 1H, NH), 7.93 (t, *J* 5.7 Hz, 1H, $NHCH_2$), 7.29-7.41 (m, 4H, Ar), 4.16 (d, *J* 5.7 Hz, 2H,

$NHCH_2$). ^{13}C NMR δ 152.2 (C=N or C=O), 150.3 (C=N or ($C=CCl_2$), 128.0 × 2 (Ar), 107.0 (CCl_2), 45.7 (CH_2). HPLC (CI) m/z (I_{rel}, %) 383.0 $[M+1]^+$ (100).

*(Z)-N′-Benzyl-N-[5-(dichloromethylene)-2-oxoimidazolidin-4-ylidene]-N′-methylsulfamide (**1f**).*

Yield: 1.15 g, 88%; mp 180-181 °C. ^1H NMR δ 11.41 (br s, 1H, NH), 11.13 (br s, 1H, NH), 7.22-7.46 (m, 5H, Ph), 4.19 (s, 2H, CH_2), 2.63 (s, 3H, CH_3). ^{13}C NMR δ 152.4 (C=N or C=O), 151.5 (C=N or C=O), 136.0 (Ph), 129.8 ($C=CCl_2$), 128.4 × 4 (Ph), 127.6 (Ph), 107.2 (CCl_2), 54.2 (CH_3N), 35.1. HPLC (CI) m/z (I_{rel}, %) 363.0 $[M+1]^+$ (100).

*(Z)-N′-Allyl-N-[5-(dichloromethylene)-2-oxoimidazolidin-4-ylidene)-N′-methylsulfamide (**1g**).*

Yield: 0.78 g, 69%; mp 102-103 °C. ^1H NMR δ 11.52 (br s, 1H, NH), 11.12 (br s, 1H, NH), 5.77-5.93 (m, 1H, –CH=), 5.28 (d, J_{trans} 17.1 Hz, 1H, $=CH_2$), 5.21 (d, J_{cis} 10.1 Hz, 1H, $=CH_2$), 3.66 (d, J 5.7 Hz, 2H, NCH_2), 2.67 (s, 3H, CH_3). ^{13}C NMR δ 152.4, 151.5, 132.8, 129.8, 118.9, 107.1 (CCl_2), 53.2, 34.8. HPLC (CI) m/z (I_{rel}, %) 313.0 $[M+1]^+$ (100).

*tert-Butyl (Z)-4-(N-(5-(dichloromethylene)-2-oxoimidazolidin-4-ylidene)sulfamoyl)piperazine-1-carboxylate (**1h**).*

Yield: 1.02 g, 66%; mp 198-199 °C. ^1H NMR δ 11.64 (br s, 1H, NH), 11.13 (br s, 1H, NH), 3.37-3.50 (m, 4H, $N(CH_2)_2$), 2.96-3.09 (m, 4H, $N(CH_2)_2$), 1.39 (s, 9H, $C(CH_3)_3$). ^{13}C NMR δ 153.8 (CO_2), 152.5 (C=N or C=O), 152.3 (C=N or C=O), 130.0 ($C=CCl_2$), 107.1 (CCl_2), 79.3 (O–C), 46.1 × 4 (2 $N(CH_2)_2$), 28.0 × 3 ($C(CH_3)_3$). HPLC (CI) m/z (I_{rel}, %) 426.0 $[M-1]^-$ (100).

*Methyl (Z)-(N-(5-(dichloromethylene)-2-oxoimidazolidin-4-ylidene)sulfamoyl)glycinate (**1i**).*

Yield: 0.83 g, 70%; mp 179-180 °C. ^1H NMR δ 11.16 (m, 2H, 2NH), 7.79 (t, J 5.8 Hz, 1H, $NHCH_2$), 3.84 (d, J 5.8 Hz, 2H, $NHCH_2$), 3.62 (s, 3H, CH_3O). ^{13}C NMR δ 169.7 (CO_2), 152.4 (C=N or C=O), 151.2 (C=N or C=O), 129.8 ($C=CCl_2$), 107.3 (CCl_2), 51.9 (CH_3O), 44.0 (CH_2). HPLC (CI) m/z (I_{rel}, %) 331.0 $[M+1]^+$ (100).

*Methyl (Z)-(N-(5-(dichloromethylene)-2-oxoimidazolidin-4-ylidene)sulfamoyl)phenylalaninate (**1j**).*

Yield: 1.24 g, 82%; mp 174-175 °C. ^1H NMR δ 10.82-11.18 (m, 2H, 2NH), 7.96 (d, J 9.0 Hz, 1H, NHCH), 7.13-7.30 (m, 5H, Ph), 4.10-4.23 (m, 1H, NHCH,), 2.99 (dd, J_{hem} 13.6 Hz, J_{vic} 5.8 Hz, 1H, CH_2), 2.87 (dd, J_{hem} 13.6 Hz, J_{vic} 8.8 Hz, 1H, CH_2). ^{13}C NMR δ 171.6 (CO_2), 152.3 (C=N or C=O), 151.1 (C=N or C=O), 136.2 (Ph), 129.6 ($C=CCl_2$), 129.1 × 2 (Ph), 128.1 × 2 (Ph), 126.6 (Ph), 107.4 (CCl_2), 57.3 (NHCH), 51.9 (CH_3O), 38.0 (CH_2). HPLC (CI) m/z (I_{rel}, %) 421.0 $[M+1]^+$ (100).

*Dimethyl (Z)-(N-(5-(dichloromethylene)-2-oxoimidazolidin-4-ylidene)sulfamoyl)aspartate (**1k**).*

Yield: 1.11 g, 77%; mp 168-169 °C. ^1H NMR δ 11.27 (br s, 1H, NH), 11.20 (br s, 1H, NH), 7.98 (d, J 7.9 Hz, 1H, CHNH), 4.23-4.38 (m, 1H, CHNH), 3.62 (s, 3H, CH_3O), 3.59 (s, 3H, CH_3O), 2.83 (d, J 4.9 Hz, 2H, $CHCH_2$). ^{13}C NMR δ 170.5 (CO_2), 170.1 (CO_2), 152.3 (C=N or C=O), 151.3 (C=N or C=O), 129.7 ($C=CCl_2$), 107.4 (CCl_2), 52.4 (CH_3O), 52.3 (CH_3O), 51.7 (CHNH). HPLC 36.8 (CH_2), (CI) m/z (I_{rel}, %) 403.0 $[M+1]^+$ (100).

*Dimethyl (Z)-(N-(5-(dichloromethylene)-2-oxoimidazolidin-4-ylidene)sulfamoyl)glutamate (**1l**).*

Yield: 1.17 g, 78%; mp 175-176 °C. ^1H NMR δ 11.07-11.25 (m, 2H, 2NH), 7.97 (d, J 9.0 Hz, 1H, SO_2NH), 3.91-4.03 (m, 1H, CH), 3.61 (s, 3H, CH_3O), 3.58 (s, 3H, CH_3O), 2.34-2.46 (m, 2H, $CH_2CH_2CO_2Me$), 1.90-2.02 (m, 1H, $CHCH_2$), 1.75-1.88 (m, 1H, $CHCH_2$). ^{13}C NMR δ 172.4 (CO_2), 171.6 (CO_2), 152.2 (C=N or C=O), 151.0 (C=N or C=O), 129.7 ($C=CCl_2$), 107.3 (CCl_2), 54.8 (NHCH), 52.1 (CH_3O), 51.4 (CH_3O), 29.2 (CH_2), 27.2 (CH_2). HPLC (CI) m/z (I_{rel}, %) 415.0 $[M-1]^-$ (100).

*Methyl (Z)-(N-(5-(dichloromethylene)-2-oxoimidazolidin-4-ylidene)sulfamoyl)prolinate (**1m**).*

Yield: 0.84 g, 63%; mp 142-143 °C. ^1H NMR δ 11.52 (br s, 1H, NH), 11.12 (br s, 1H, NH), 4.15-4.25 (m, 1H, NCH), 3.65 (s, 3H, CH_3O), 3.30 (m, 2H, NCH_2, with H_2O signal), 2.12-2.27 (m, 1H, H_{Pyr}), 1.78-1.98 (m, 3H, H_{Pyr}). ^{13}C NMR δ 172.3 (CO_2), 152.4 (C=N or C=O), 152.2 (C=N or C=O), 130.0 ($C=CCl_2$), 107.2 (CCl_2), 60.9 (NCH), 52.1 (CH_3O), 49.7 (NCH_2), 30.6 (CH_2), 24.5 (CH_2). HPLC (CI) m/z (I_{rel}, %) 371.2 $[M+1]^+$ (100).

*Methyl (Z)-1-(N-(5-(dichloromethylene)-2-oxoimidazolidin-4-ylidene)sulfamoyl)piperidine-3-carboxylate (**1n**).*

Yield: 0.77 g, 56%; mp 151-152 °C. ^1H NMR δ 10.39-11.98 (br s, 2H, 2NH), 3.45-3.65 (m, 4H, CH_3O, H_{Pip}), 2.78-2.96 (m, 1H, H_{Pip}), 2.62-2.78 (m, 1H, H_{Pip}), 1.80-1.99 (m, 1H, H_{Pip}), 1.63-1.80 (m, 1H, H_{Pip}), 1.29-1.63 (m, 4H, H_{Pip}). ^{13}C NMR δ 173.0, 152.7, 152.1, 130.2, 107.6, 51.9, 48.2, 46.7, 26.0, 23.3. HPLC (CI) m/z (I_{rel}, %) 385.0 $[M+1]^+$ (100).

*Methyl (Z)-1-(N-(5-(dichloromethylene)-2-oxoimidazolidin-4-ylidene)sulfamoyl)azetidine-3-carboxylate (**1o**).*

Yield: 0.74 g, 58%; mp 211-212 °C. ^1H NMR δ 11.74 (br s, 1H, NH), 11.17 (br s, 1H, NH), 4.06-3.92 (m, 4H, $N(CH_2)_2$), 3.65 (s, 3H, OCH_3), 3.59-3.49 (m, 1H, $CHCO_2Me$). ^{13}C NMR δ 171.9 (CO_2Me), 152.9 (C=N or C=O), 152.4 (C=N or C=O), 130.0 ($C=CCl_2$), 107.5 (CCl_2), 53.2 (OCH_3), 52.1 × 2 ($N(CH_2)_2$), 30.8 ($CHCO_2Me$). HPLC (CI) m/z (I_{rel}, %) 355.0 $[M-1]^-$ (100).

*Hydrochloride of (Z)-N-(5-(dichloromethylene)-2-oxoimidazolidin-4-ylidene)piperazine-1-sulfonamide (**1p**).*

The substance **1h** (0.50 g, 1.17 mmol) was dissolved in 10 mL of dry CH_2Cl_2, and the 1.5 mL (5 eq.) of 4 M HCl in 1,4-dioxane was added. The reaction mixture was stirred for 8 h, than was evaporated, and the dry residue was triturated in 15 ml of MTBE, filtered and washed with MTBE (2 × 10 ml). Yield: 0.36 mg, 85%; mp 218-219 °C. ^1H NMR δ 11.94 (br s, 1H, NH), 11.19 (br s, 1H, NH), 9.50 (br s, 2H,

NH_2^+), 3.30-3.38 (m, 4H, $N(CH_2)_2$), 3.13-3.25 (m, 4H, $N(CH_2)_2$). ^{13}C NMR δ 152.6 (C=N or C=O), 152.3 (C=N or C=O), 129.6 ($C=CCl_2$), 108.2 (CCl_2), 43.4 × 2 ($N(CH_2)_2$), 41.7 × 2 ($N(CH_2)_2$). HPLC (CI) m/z (I_{rel}, %) 328.0 $[M+1]^+$ (100).

Biological Assay

The antiviral activity of synthesized compounds was tested in the Department of Pediatrics, University of Alabama, Birmingham; description of the technique see in [11].

The anticancer activity of synthesized compounds was tested according to the International Program of the National Institutes of Health – DTP (Developmental Therapeutic Program) of the National Cancer Institute (NCI, Bethesda, Maryland, USA) on 60 cancer cell lines [14]; a description of the technique is also given in [15].

Notes

Acknowledgments and finances. The study of antiviral activity was performed according to the contract HHSN2722011000191 from Virology Branch DMID, NIAID, NIH (USA). We would like to thank US Public Health Service and National Cancer Institute, USA, for *in vitro* evaluation of anticancer activity (providing the NCI-60 cell testing) within the framework of Developmental Therapeutic Program (http://dtp.cancer.gov), and ENAMINE Ltd. for the material and technical support for this work.

Disclaimer. This material should not be interpreted as representing the viewpoint of the U.S. National Institutes of Health, or the National Cancer Institute.

The authors declare that there is no conflict of interest.

References

1. Lehmann, S. V.; Hoeck, U.; Breinholdt, J.; Olsen, C. E.; Kreilgaard, B. Characterization and chemistry of imidazolidinyl urea and diazolidinyl urea. *Cont. Dermat.* **2006**, *54*, 50-58.
2. Cachet, N.; Genta-Jouve, G.; Regalado, E. L.; Mokrini, R.; Amade, P.; Culioli, G.; Thomas, O. P. Parazoanthines A–E, Hydantoin Alkaloids from the Mediterranean Sea Anemone *Parazoanthus axinellae*. *J. Nat. Prod.* **2009**, *72*, 1612-1615.
3. Meusel, M.; Gütschow, M. Recent developments in hydantoin chemistry. A review. *Org. Prep. Proced. Int.* **2004**, *36*, 391-443.
4. Bogolubsky, A. V.; Moroz, Y. S.; Savych, O.; Pipko, S.; Konovets, A.; Platonov, M. O.; Vasylchenko, O. V.; Hurmach, V. V.; Grygorenko, O. O. An Old Story in the Parallel Synthesis World: An Approach to Hydantoin Libraries. *ACS Comb. Sci.* **2018**, 20, 35-43.
5. Colacino, E.; Porcheddu, A.; Charnay, C.; Delogu, F. From enabling technologies to medicinal mechanochemistry: an eco-friendly access to hydantoin-based Active Pharmaceutical Ingredients. *React. Chem. Eng.* **2019**, *4*, 1179-1188.
6. Cho, S.; Kim, S.-H.; Shin, D. Recent applications of hydantoin and thiohydantoin in medicinal chemistry. *Eur. J. Med. Chem.* **2018**, *164*, 517-545.
7. Schachter, S. C. Anticonvulsant Agents: Phenytoin and Fosphenytoin. In: NeuroPsychopharmacotherapy. Riederer, P.; Laux, G.; Mulsant, B.; Le, W.; Nagatsu, T., Eds.; Springer, Cham., 2020, pp 1-6.
8. Danielsson, B.; Sköld, A.-C.; Azarbayjani, F.; Öhman, I.; Webster, W. Pharmacokinetic Data Support Pharmacologically Induced Embryonic Dysrhythmia as Explanation to Fetal Hydantoin Syndrome in Rats. *Toxicol. Appl. Pharmacol.* **2000**, *163*, 164-175.
9. Kammuller, M. E.; Bloksma, N.; Seinen, W. Chemical-induced autoimmune reactions and spanish toxic oil syndrome. Focus on hydantoins and related compounds. *J. Toxicol.: Clin. Toxicol.* **1988**, *26*, 157-174.
10. Shablykin, O. V.; Kornii, Y. Eu.; Dyakonenko, V. V.; Shablykina, O. V.; Brovarets, V. S. Synthesis and anticancer activity of new substituted imidazolidinone sulfonamides. *Curr. Chem. Lett.* **2019**, *8*, 199-210.
11. Kornii, Y.; Chumachenko, S.; Shablykin, O.; Prichard, M. N.; James, S. H.; Hartline, C.; Zhirnov, V.; Brovarets, V. New 2-Oxoimidazolidine Derivatives: Design, Synthesis and Evaluation of Anti-BK Virus Activities *in Vitro*. *Chem. Biodiversity* **2019**, *16*, e1900391.
12. Shablykin, O. V.; Kornii, Y. E.; Brovarets, V. S.; Shablykina, O. V.; Khilya, V. P. Synthesis of new oxoimidazolidine sulfonamides with anticancer activity. *Dopov. Nac. akad. nauk Ukr.* **2019**, *1*, 79-85 (in Ukrainian).
13. Scozzafava, A.; Owa, T.; Mastrolorenzo, A.; Supuran, C. T. Anticancer and antiviral sulfonamides. *Curr. Med. Chem.* **2003**, *10*, 925-953.
14. NCI-60 Human Tumor Cell Lines Screen. DTP Developmental Therapeutics Program, NIH website [Internet]. Available from: https://dtp.cancer.gov/discovery_development/nci-60/default.htm (accessed on April 15, 2021).
15. Velihina, Ye. S.; Pil'o, S. G.; Zyabrev, V. S.; Moskvina, V. S.; Shablykina, O. V.; Brovarets, V. S. 2-(Dichloromethyl)pyrazolo[1,5-*a*][1,3,5]triazines: synthesis and anticancer activity. *Biopolym. Cell.* **2020**, *36*, 61-74.

Нові сульфамідні похідні 4-іміногідантоїну з противірусною та протираковою активністю

Ю. Є. Корній[1], О. В. Шабликін[1], О. В. Шабликіна[1,2]*, В. С. Броварець[1]

[1] *Інститут біоорганічної хімії та нафтохімії ім. В.П. Кухаря НАН України, вул. Мурманська, 1, Київ, 02094, Україна*
[2] *Київський національний університет імені Тараса Шевченка, вул. Володимирська, 60, Київ, 01601, Україна*

Резюме: Взаємодією (5-(дихлорометилен)-2-оксоімідазолідін-4-іліден)сульфамоїлхлориду з анілінами, бензиламінами, Boc-захищеним піперазином, метилаліламіном та метиловими естерами амінокислот з первинною та вторинною аміногрупами отримано ряд сульфамідів. Для встановлення противірусної активності *in vivo* щодо окремих штамів цитомегаловірусу сполук було відібрано 11 сполук. На жаль, низьку противірусну активність та хіміотерапевтичний індекс виявили похідні на основі *пара*-заміщених бензиламінів, бензилметил- та алілметиламіну, а також естерів аспарагінової та глутамінової кислоти. Сульфаміди, отримані за участю естерів ніпекотинової та азетидин-3-карбонової кислот, діяли селективно лише на певні види та штами цитомегаловірусів і не були активними щодо інших: зокрема, були неефективними проти цитомегаловірусу морської свинки (22122), цитомегаловірусу миші (Сміт), але активні щодо цитомегаловірусу людини. Показники противірусної активності також залежали від методу виявлення. Значення EC_{50} сульфамідів естерів ніпекотинової та азетидин-3-карбонової кислот, а також сульфамідів *пара*-анізидину та *N*-Boc-піперазину були близькі до показників препаратів порівняння Ганцикловіру та Цидофовіру, хоча досліджувані сполуки мали невисокі хіміотерапевтичні індекси, особливо SI_{90}. При аналізі протиракової активності синтезованих сульфамідів за результатами однодозових випробувань була встановлена висока активність похідних на основі заміщених бензиламінів, бензилметил- та алілметиламіну, *N*-Boc-піперазину та раніше синтезованого сульфаміду з фрагментом триптаміну. Найбільш перспективними у якості протиракових агентів виявились похідні бензилметил- та алілметиламіну, оскільки окрім активності в цілому вони виявляють високу селективність по відношенню до окремих ліній ракових клітин. У порівнянні із цими двома речовинами сульфамід на основі *пара*-метоксибензиламіну здатен до ефективного інгібування меншої кількості ліній ракових клітин; хоча середні показники EC_{50}, отримані внаслідок п'ятидозових випробувань, для усіх трьох похідних були близькі.

Ключові слова: гідантоїни; сульфаміди; противірусна активність; протипухлинна активність.

ISSN 1814-9758. Ukr. Bioorg. Acta, 2021, Vol. 16, N 1
UDC 616-093 + 547.789.1
DOI: hpps://doi.org/10.15407/bioorganica2021.01.018

Ukrainica Bioorganica Acta
www.bioorganica.org.ua

RESEARCH ARTICLE

Synthesis of novel pyrazoline-thiazolidin-4-one hybrids and evaluation of their biological activity

Serhii M. Holota[1,2]*

[1] *Danylo Halytsky Lviv National Medical University, 69 Pekarska St., Lviv, 79010, Ukraine*
[2] *Lesya Ukrainka Volyn National University, 13 Voli Ave., Lutsk, 43025, Ukraine*

Abstract: In the present work, the synthesis of pyrazoline-thiazolidin-4-one hybrids and their pharmacological properties are described. The structure of compounds is characterized using ^{1}H, ^{13}C NMR, and LC-MS spectra. The antioxidant (DPPH assay), antimicrobial (Gram-positive bacterium *Lactobacillus plantarum*, Gram-negative bacterium *Escherichia coli*, and yeasts *Candida albicans*, MIC determination), redox (cyclic voltammetry) as well as herbicidal activity (against grass species *Agrostis stolonifera*) of compounds have been studied. All derivatives have demonstrated radical scavenging activity with IC_{50} values in the range of 4.67-7.12 mM that were measured by the DPPH test. The tested compounds showed very low antimicrobial and herbicidal activity and no redox peaks were observed in the cyclic voltammetry studies.

Keywords: pyrazoline-thiazolidin-4-ones hybrids; DPPH assay; antimicrobial/herbicidal activity; cyclic voltammetry.

Introduction

The last decade has witnessed a growing interest in the development of redox modulating agents as effective tool in therapy oxidative-stress associated processes: cancers, diabetes, inflammatory diseases, neurological disorders, and others [1-4]. In this context, the structure modified thiazolidin-4-one and pyrazoline nucleus are prospective molecular platforms for design antioxidants and redox-modulating agent design [5-8]. For example, the application of the mentioned scaffolds is an attractive direction for the development of selective modulators of Nrf2 and NF-kB transcription factors, that play a key role in the regulation of cellular responses to oxidative-stress factors and are potential drug targets [9-11].

In our early-described researches some types thiazolidin-4-one hybrids linked through “enamine” linker at C-5 has been synthesized and several compounds been have been identified with a high level of antibacterial and antifungal [12-14], anticancer and trypanocidal [15], and anti-inflammatory activity [16] (Figure 1). In our opinion, the 5-aminomethylidene derivatives have several important advantages in synthetic variability and structure optimization processes compared to 5-ylidene analogous.

On the other hand, the pyrazolines possess a wide range of biological activities and belong to unsaturated heterocycles that can be oxidized to the corresponding pyrazoles [17]. These properties are of great interest in the design and development of potential redox-active compounds as possible pharmacological agents.

Taking into account the above reasons, the main goal of the present work was the design and synthesis of novel “enamine”-bearing pyrazoline-thiazolidin-4-one hybrid molecules and further evaluation of their antioxidant, antimicrobial, herbicidal, and redox activities.

Results and Discussion

The synthetic design included two key routes (Scheme 1). Initially, the derivatives **2a, b** were easily obtained using Holmberg’s protocol (*i*) [18] from corres-

Received: 10.02.2021
Revised: 25.03.2021
Accepted: 12.04.2021
Published online: 30.06.2021

* Corresponding author. Tel.: +380-97-226-0066;
e-mail: golota_serg@yahoo.com (S. M. Holota)
ORCID: 0000-0002-9892-437X

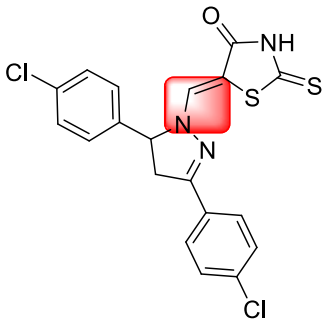

In vivo activity on carrageenan- and formaline-induced oedema models in dose 50 mg/kg. No ulcerogenic, hepatotoxic action

Antiinflammatory activity
Holota S. et al.
Biopolymers&Cell, **2019**

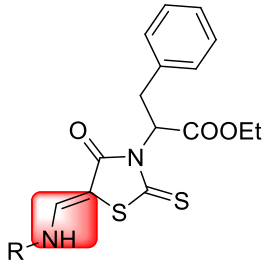

R=4-COOEt-C_6H_4;

Trypanosoma brucei brucei
IC_{50}=0.091μM, SI = 409.4;
Trypanosoma brucei gambiense
IC_{50}=0.027 μM, SI = 1396.2

R=5-(2,4-Cl_2-C_6H_3)thiazol-2-yl;

NCI DTP assay:
MG_MID GI_{50}/TGI=2.57/57.27 μM

Trypanocidal and anticancer activity
Holota S. et al.
Bioorganic Chemistry, **2019**

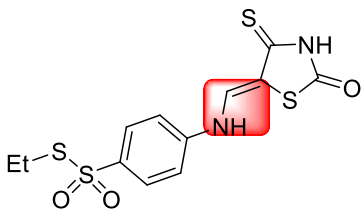

Wide spectrum of antibacterial and antifungal activity with MIC values in μM range

Antimicrobial activity
Derkach G. et al. *JOrgPhCh*, **2016**

Figure 1. The "enamine"-bearing thiazolidin-4-one hybrids as potential pharmacological agents.

ponding aminobenzoic acids **1a, b**. The procedure (*ii*) [15] was used for synthesis **3a, b** from obtained derivatives **2a, b**. The convenient synthetic approach [19] starting from aromatic aldehyde **4a, b**, and acetophenone (*iii* and *iv*) was used for the synthesis of diarylpyrazolines **6a, b**. The target pyrazoline-thiazolidin-4-one hybrids **7a-d** were synthesized in satisfactory yields and purity by reacting compounds **3a, b** and **6a, b** under reflux in ethanol for 30-45 min.

The structures of all synthesized compounds were confirmed by ^1H, ^{13}C NMR spectroscopy, and LC-MS-spectrometry. Esterification of the carboxylic group of compounds **3a, b** under condition *ii* was observed by the appearance of signals from the protons of the ethyl group at ~ 4.31 (q, J = 6.3 Hz) and ~ 1.31 (t, J = 6.3 Hz) ppm in the ^1H NMR spectra. In the ^1H NMR spectra of derivatives **3a, b** and **7a-d** the proton signal at C-5 double bond appears mainly in the field of aromatic protons, and only for derivative **7b** it was observed as a singlet at 7.60 ppm. The pyrazoline fragment of compounds **7a-d** shows the characteristic patterns of the AMX system for CH_2-CH protons.

The synthesized compounds **7a-d** have been evaluated for their antioxidant activity in vitro in the DPPH (1,1-diphenyl-2-picrylhydrazyl) radical scavenging assay [20] in the conditions close to physiological (serial dilutions of stock methanol solutions at six concentrations of 1.0, 2.0, 4.0, 6.0, 8.0, 10.0 mM + Tris-HCl buffer pH = 7.40, measurements after 60 min). Ascorbic acid was used as a reference compound (standard). The IC_{50} values have been determined for compounds **7a-d** as well as ascorbic acid to characterize their antioxidant activity (Figure 2).

As a result, the tested compounds **7a-d** have low-moderate activity in DPPH assay, and the established IC_{50} values of the synthesized compounds were: 4.67 mM (**7a**), 5.90 mM (**7b**), 6.05 mM (**7c**), 7.12 mM (**7d**), and for ascorbic acid IC_{50} = 0.045 mM. It should be noted that this level of antioxidant activity may be more likely associated with the presence of phenolic (-OH), and dimethylamino groups (-$N(CH_3)_2$) in compounds **7a-d** than with other molecular fragments. Nevertheless, all tested derivatives show activity from 8.38 to 13.43 mg/mL that is promising for searching for new potential antioxidants among this subtype of hybrid molecules.

Compounds **7a-d** were preliminary screened for their potential antimicrobial activity against Gram-positive bacteria as *Lactobacillus plantarum*, Gram-negative bacteria as *Escherichia coli*, and yeasts (*Candida albicans)*. Antimicrobial activity was evaluated in terms of minimum inhibitory concentrations (MICs), and the values were compared with standard reference antimicrobial agents [21-22]. Overall, the tested compounds showed very low antimicrobial activity against the *E. coli* and *C. albicans* compared to the reference drugs (36.5 μM for ampicillin and 38.96 μM for fluconazole), Table 1. Only derivative **7c** showed activity with MIC value of 1.25 mM against *E. coli*, and derivative **7d** showed antifungal activity against *C. albicans* with MIC value of 1.25 mM. It is also worth noting that compounds **7a-d** were inactive against *L. plantarum.*

The herbicidal activity of the compounds **7a-d** was tested against the monocot grass species Creeping bentgrass (*Agrostis stolonifera*). Methanol solutions at the concentration of 1mg/ml of all compounds were added to

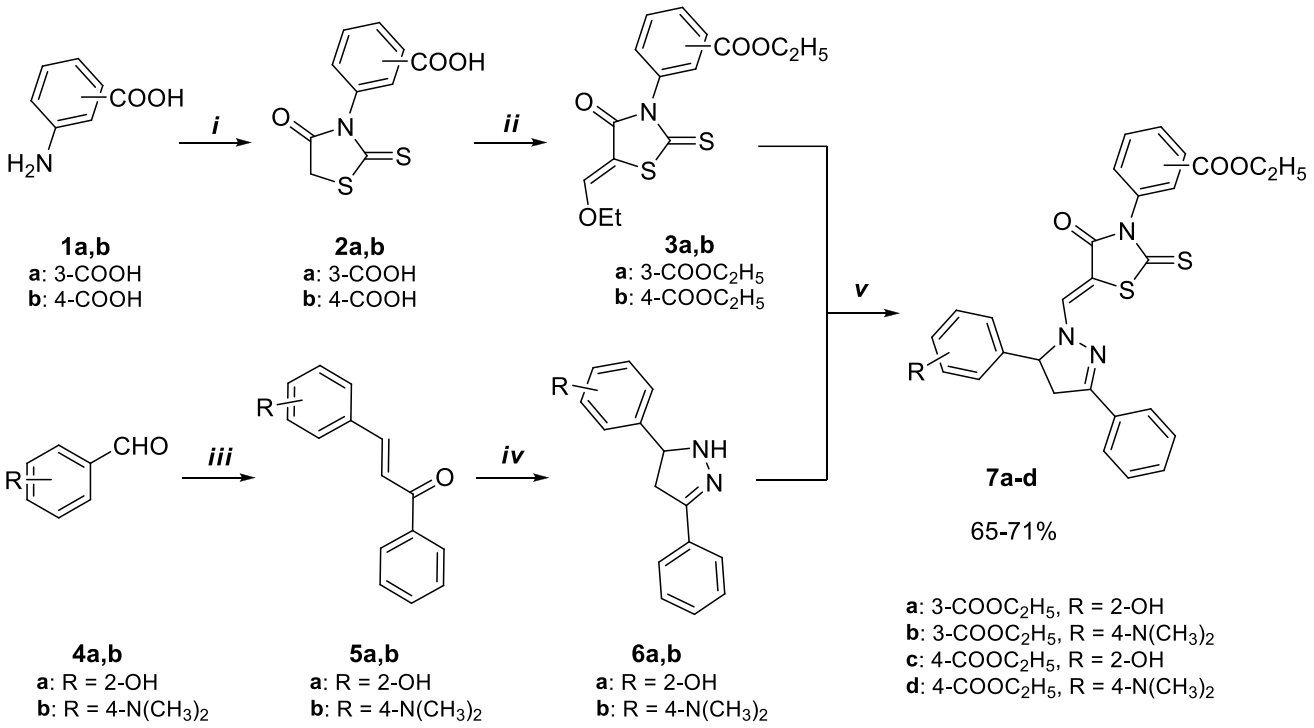

Scheme 1. Synthesis of target pyrazoline-thiazolidin-4-one hybrids **7a-d.** Reagents and conditions: *i*) **1a, b** (10 mmole), $CS(SCH_2COOH)_2$ (10 mmole), C_2H_5OH:H_2O, reflux, 5h; *ii*) **2a, b** (10 mmole), $HC(OC_2H_5)_3$ (10 mmole), Ac_2O, reflux, 3h; *iii*) **4a, b** (10 mmole), acetophenone (10 mmole), NaOH (10 mmole); *iv*) **5a, b** (10 mmole), NH_2-NH_2 (10 mmole), KOH (10 mmole), C_2H_5OH; *v*) **3a, b** (10 mmole), **6a, b** (10 mmole), C_2H_5OH, reflux, 2h.

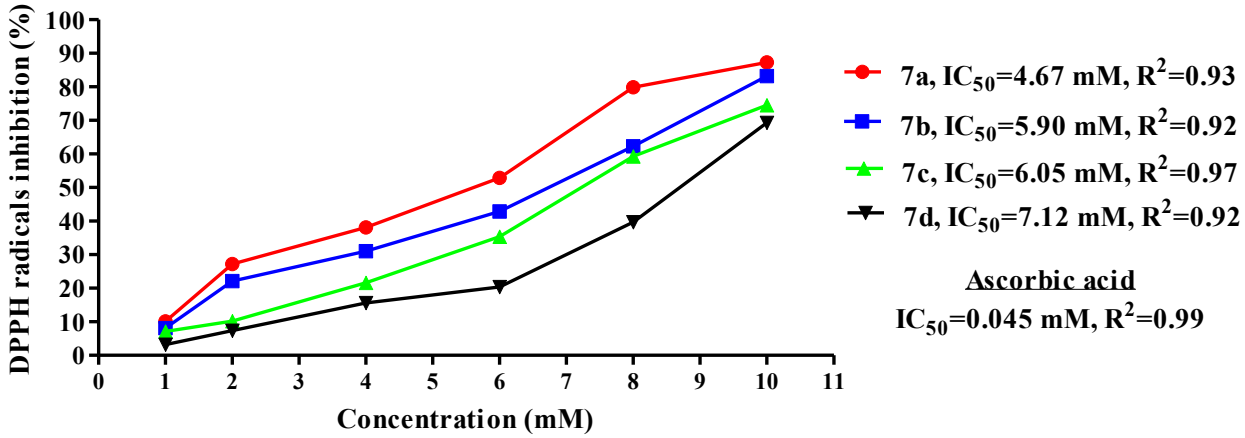

Figure 2. The dose-depending DPPH radical inhibition and IC_{50} values for compounds **7a-d**.

the plant seeds and incubated in a minimal medium. Seed germination was observed after 3 days, and only compound **7b** inhibited of grass growth by 15 %. No inhibitory effect on *A. stolonifera* was observed in the case of compounds **7a**, **7c**, and **7d**.

The redox activity of **7a-d** was evaluated by cyclic voltammetry technique using stock solutions of compounds in methanol (C = 5 mM) with the addition of phosphate buffer solution (pH = 6.40). The glassy carbon working electrode, a platinum wire counter, and a saturated calomel electrode were used, and the measurements were performed at 0 min and after 60 min in the potential range from -1500 mV to 1500 mV with scan rates between 10 and 100 mV/s. No redox peaks were observed under mentioned experimental conditions in cyclic voltammetry studies for tested compounds **7a-d**.

Table 1. Antimicrobial properties of compounds **7a-d** (MICs values)

Compounds/ Microorganisms	*E.coli*	*L. plantarum*	*C. albicans*
7a	2.5 mM	>2.5 mM	>2.5 mM
7b	>2.5 mM	>2.5 mM	2.5 mM
7c	1.25 mM	>2.5 mM	2.5 mM
7d	2.5 mM	>2.5 mM	1.25 mM
References[a,b]	36.5 μM[a]	39.8 μM[a]	38.96 μM[b]

- [a] – ampicillin
- [b] – fluconazole

Conclusions

In the present paper, a synthesis of the series of new pyrazoline-thiazolidin-4-one hybrids has been reported. The structure of the compounds was confirmed using ^{1}H, ^{13}C NMR, and LC-MS spectra. All synthesized compounds were evaluated for their antioxidant, antibacterial, antifungal, herbicidal, and redox properties. The synthesized hybrid compounds have promising free radical scavenging activities, and obtained results argue to the next development of antioxidant agents among these types of molecules.

Experimental section

General

Commercial reagents were purchased from Merck and used without purification. Melting points were measured in open capillary tubes on a BŰCHI B-545 melting point apparatus and are uncorrected. The elemental analyses (C, H, N) was performed using the Perkin-Elmer 2400 CHN analyzer and was within ±0.4% of the theoretical values. The ^{1}H and ^{13}C NMR spectra were recorded on a Bruker-500 spectrometer at 500 MHz and 126 MHz using a mixture of DMSO-d6+CCl4 as a solvent and TMS as an internal standard. Chemical shift values are reported in ppm units with use of δ scale. Mass spectra were obtained using electrospray ionization (ESI) techniques on an Agilent 1100 Series LCMS. The purity of the compounds was checked by thin-layer chromatography performed with Merck Silica Gel 60 F254 aluminum sheets. Spots were detected by their absorption under UV light.

Synthesis

General procedure for the synthesis derivatives ***7a-d.***

In a round bottom flask is placed by 0.01 mole of **3a** or **3b** and **6a** or **6b**, add 10 ml of ethanol. The mixture was heated at reflux for 2 hours. After cooling, the precipitate formed is filtered off and recrystallized from DMF-ethanol.

*Ethyl (Z)-3-(5-(ethoxymethylene)-4-oxo-2-thioxothiazolidin-3-yl)benzoate (**3a**)*

Yield 52%, mp 163-165 °C. ^{1}H NMR (500 MHz, DMSO-d_6) δ 7.99 (s, 1H), 7.90 (s, 1H), 7.47-7.55 (m, 2H), 4.35 (q, *J* 6.2 Hz, 2H), 4.15 (q, *J* 6.3 Hz, 2H), 1.35 (t, *J* 6.2 Hz, 3H), 1.15 (t, *J* 6.3 Hz, 3H). LC/MS m/z 338 $(M+H)^{+}$. Anal. Calcd. for $C_{15}H_{15}NO_4S_2$: C, 53.40; H, 4.48; N, 4.15. Found: C, 53.50; H, 4.60; N, 4.20.

*Ethyl (Z)-4-(5-(ethoxymethylene)-4-oxo-2-thioxothiazolidin-3-yl)benzoate (**3b**)*

Yield 63%, mp 187-189 °C. ^{1}H NMR (500 MHz, DMSO-d_6) δ 7.90 (s, 1H), 7.84 (d, *J* 8.6 Hz, 2H), 7.69 (d, *J* 8.6 Hz, 2H), 4.35 (q, *J* 6.2 Hz, 2H), 4.15 (q, *J* 6.3 Hz, 2H), 1.35 (t, *J* 6.2 Hz, 3H), 1.15 (t, *J* 6.3 Hz, 3H). LC/MS m/z 338 $(M+H)^{+}$. Anal. Calcd. for $C_{15}H_{15}NO_4S_2$: C, 53.40; H, 4.48; N, 4.15. Found: C, 53.60; H, 4.50; N, 4.30.

*Ethyl (Z)-3-(5-((5-(2-hydroxyphenyl)-3-phenyl-4,5-dihydro-1H-pyrazol-1-yl)methylene)-4-oxo-2-thioxothiazolidin-3-yl)benzoate (**7a**)*

Yield 65%, mp 212-214 °C. ^{1}H NMR (500 MHz, DMSO-d_6) δ 9.53 (s, 1H), 8.10-8.00 (m, 2H), 7.99-7.91 (m, 2H), 7.69-7.57 (m, 3H), 7.49-7.39 (m, 3H), 7.28-7.22 (m, 2H), 6.81-6.75 (m, 2H), 5.56 (dd, *J* 11.3, 7.0 Hz, 1H), 4.31 (q, *J* 6.3 Hz, 2H), 4.00 (dd, *J* 18.4, 11.3 Hz, 1H), 3.51 (dd,
J 18.4, 7.0 Hz, 1H), 1.00 (t, *J* 6.3 Hz, 3H). ^{13}C NMR (126 MHz, DMSO-d_6) δ 186.5, 179.3, 167.2, 164.1, 161.4, 159.4, 157.2, 154.0, 151.1, 149.4, 142.2, 139.0, 137.4, 129.7, 128.3, 127.0, 126.2, 121.2, 118.4, 113.9, 92.4, 88.7, 62.5, 13.4. LC/MS m/z 530 $(M+H)^{+}$. Anal. Calcd. for $C_{28}H_{23}N_3O_4S_2$: C, 63.50; H, 4.38; N, 7.93. Found: C, 63.70; H, 4.50; N, 8.00.

*Ethyl (Z)-3-(5-((5-(4-(dimethylamino)phenyl)-3-phenyl-4,5-dihydro-1H-pyrazol-1-yl)methylene)-4-oxo-2-thioxothiazolidin-3-yl)benzoate (**7b**)*

Yield 67%, mp 228-231 °C. ^{1}H NMR (500 MHz, DMSO-d_6) δ 8.00 (dt, *J* 7.8, 1.4 Hz, 1H), 7.94-7.89 (m,

2H), 7.78 (t, *J* 1.9 Hz, 1H), 7.70-7.59 (m, 2H), 7.60 (s, 1H), 7.62-7.56 (m, 1H), 7.58-7.51 (m, 1H), 7.41 (s, 1H), 7.26-7.21 (m, 2H), 6.79-6.73 (m, 2H), 5.57 (dd, *J* 11.3, 7.1 Hz, 1H), 4.31 (q, *J* 6.3 Hz, 2H), 4.00 (dd, *J* 18.4, 11.3 Hz, 1H), 3.51 (dd, *J* 18.5, 7.1 Hz, 1H), 2.90 (s, 6H), 1.31 (t, *J* 6.3 Hz, 3H). ^{13}C NMR (126 MHz, DMSO-d_6) δ 184.4, 179.5, 166.5, 163.6, 160.9, 159.5, 156.8, 154.1, 150.5, 148.5, 141.7, 138.5, 137.1, 129.2, 128.1, 127.3, 125.8, 120.6, 116.3, 112.6, 91.5, 88.7, 64.4, 35.2, 13.1. LC/MS m/z 557 $(M+H)^+$. Anal. Calcd. for $C_{30}H_{28}N_4O_3S_2$: C, 64.73; H, 5.07; N, 10.06. Found: C, 64.90; H, 5.20; N, 10.20.

*Ethyl (Z)-4-(5-((5-(2-hydroxyphenyl)-3-phenyl-4,5-dihydro-1H-pyrazol-1-yl)methylene)-4-oxo-2-thioxothiazolidin-3-yl)benzoate (**7c**)*

Yield 68%, mp 230-232 °C. ^{1}H NMR (500 MHz, DMSO-d_6) δ 9.50 (s, 1H), 8.11-8.02 (m, 2H), 7.96-7.89 (m, 2H), 7.64-7.53 (m, 3H), 7.48-7.38 (m, 3H), 7.25-7.20 (m, 2H), 6.81-6.74 (m, 2H), 5.56 (dd, *J* 11.3, 7.0 Hz, 1H), 4.31 (q, *J* 6.3 Hz, 2H), 4.00 (dd, *J* 18.4, 11.3 Hz, 1H), 3.51 (dd, *J* 18.4, 7.0 Hz, 1H), 1.05 (t, *J* 6.3 Hz, 3H). ^{13}C NMR (126 MHz, DMSO-d_6) δ 184.0, 179.1, 166.8, 162.9, 160.7, 159.2, 156.8, 153.3, 150.4, 141.5, 138.3, 137.2, 129.7, 129.4, 128.3, 127.5, 126.9, 113.1, 91.1, 86.5, 64.0, 13.2. LC/MS m/z 530 $(M+H)^+$. Anal. Calcd. for $C_{28}H_{23}N_3O_4S_2$: C, 63.50; H, 4.38; N, 7.93. Found: C, 63.80; H, 4.60; N, 8.10.

*Ethyl (Z)-4-(5-((5-(4-(dimethylamino)phenyl)-3-phenyl-4,5-dihydro-1H-pyrazol-1-yl)methylene)-4-oxo-2-thioxothiazolidin-3-yl)benzoate (**7d**)*

Yield 71%, mp 244-246 °C. ^{1}H NMR (500 MHz, DMSO-d_6) δ 8.09-8.00 (m, 2H), 7.94-7.88 (m, 2H), 7.65-7.55 (m, 3H), 7.48-7.38 (m, 3H), 7.26-7.20 (m, 2H), 6.79-6.72 (m, 2H), 5.56 (dd, *J* 11.3, 7.0 Hz, 1H), 4.31 (q, *J* 6.3 Hz, 2H), 4.00 (dd, *J* 18.4, 11.3 Hz, 1H), 3.51 (dd, *J* 18.4, 7.0 Hz, 1H), 2.90 (s, 6H), 1.05 (t, *J* 6.3 Hz, 3H). ^{13}C NMR (126 MHz, DMSO-d_6) δ 183.7, 178.6, 165.7, 162.7, 160.1, 158.8, 156.2, 153.7, 150.0, 141.3, 138.1, 137.0, 129.9, 129.2, 128.1, 127.3, 126.4, 112.6, 90.8, 86.3, 63.7, 39.0, 13.0. LC/MS m/z 557 $(M+H)^+$. Anal. Calcd. for $C_{30}H_{28}N_4O_3S_2$: C, 64.73; H, 5.07; N, 10.06. Found: C, 65.00; H, 5.10; N, 10.30.

Antioxidant activity (DPPH assay)

DPPH inhibition was determined by using the protocol [20]. The DPPH radical is stable due to the delocalization of a spare electron over the molecule, thus preventing dimer formation. This radical is used in the DPPH radical scavenging capacity assay to quantify the ability of antioxidants to quench the DPPH radical. The dark purple color of DPPH will be lost when it is reduced to its non-radical form stable organic nitrogen centered free radical with a dark purple color which when reduced to its non-radical form by antioxidants becomes colorless. DPPH radicals are widely used in the model system to investigate the scavenging activities of several natural compounds. When the DPPH radical is scavenged, the color of the reaction mixture changes from purple to yellow with decreasing of absorbance at wavelength 517 nm. The stock solutions of compounds were prepared in mixture methanol + Tris-HCl buffer pH = 7.40. Then 1 mL of DPPH (8 mg/100 mL of methanol) solution was added to the sample and the blank. This setup was left at room temperature for 30 min (vortexed in between). Absorbance was taken at 517 nm against the ethanol by using UV-1800 spectrophotometer (Shimadzu, Japan). Each sample was analyzed in triplicate. The percentage of inhibition was calculated against blank:

$$I\% = (A_{blank} - (A_{sample + dpph} - A_{sample}))/A_{blank} \times 100\%,$$

where A_{blank} – is the absorbance of the control reaction (containing all reagents except the tested compounds); $A_{sample+dpph}$ – is the absorbance of the tested compounds after 60 min incubation with DPPH solution;
A_{sample} – is the absorbance of the tested compounds without DPPH solution.

Antimicrobial activity

The minimal inhibitory concentrations (MICs) were determined by the standard microdilution method in cation-adjusted Mueller-Hinton II Broth (MHB, Becton-Dickinson, Germany) according to the recommendations of the Clinical and Laboratory Standard Institute. The tested compounds were evaluated for their antimicrobial activity against Gram-positive bacteria (*L. plantarum*), Gram-negative bacteria (*E. coli*), and yeasts (*C. albicans*). Ampicillin was used as a reference antibacterial agent and fluconazole as antifungal one. A representative colony was lifted off with a wire loop and placed in 5 mL of nutrient broth medium, which was then incubated with shaking at 37 °C for 5 h. Then, 1×10^6 cells/mL were suspended in a nutrient broth medium to generate the working suspension. Different concentrations of peptides were prepared in a 96-well plate using nutrient broth medium, and each well contained 100 µL compound solutions. A 100-µL cell working suspension was then added to each well. The plate was incubated at 37 °C for 24 h, and the optical density (OD) of each well was then measured at 600 nm after gently shaking the plate for 10s using a Hybrid Multi-Mode Microplate reader (BioTek, Synergy H4). Wells containing medium only (blank) and wells containing cells in medium without peptides (positive control) were included on the same plate. The values of MIC were recorded after 20 h and 24 h of incubation with the compounds for bacteria and yeasts, respectively. Experiments were performed in triplicate and on three different occasions (i.e., a total of nine repeats for each individual measurement).

Herbicidal activity - Herbicidal Pre-emergence Test

Seeds of *A. stolonifera* (JuliwaHESA, Heidelberg, Germany) were placed into the wells of a 96-well microtiter plate (Sarstedt, Nümbrecht, Germany). A solution containing 2.2 g/l Murashige & Skoog plant salts (Serva, Heidelberg, Germany) and 1.6 g/l Gamborg's B5

plant medium (Serva, Heidelberg, Germany) was added to the wells. The stock solutions in concentration 1 mg/ml in methanol were prepared for compounds **7a-d** and were added to the wells. Identical volumes of methanol without compounds were used as a toxicity test of the organic solvent. The solution containing the plant medium was used as a negative control. The plate was closed and incubated at room temperature under constant light (Osram Fluora lamp) in a humidity chamber. After 3 days of incubation, the plate lid was removed and a container with tap water was placed inside the chamber for increasing the air humidity. The plate was incubated up to 6 days. Three technical replicates were performed.

Voltammetric parameters and electrochemical cells

Voltammetric experiments were performed using BAS 100W Potentiostat.A glassy carbon (GC) (A = 0.07 cm^2) was used as working electrode. Pt wire and saturated calomel electrode (SCE) were used as counter and reference electrodes. Before each experiment, the surface of GCE was polished with diamond spray (particle size 1 μm) followed by thorough rinsing with distilled water. All the voltammetric experiments were conducted in a high purity nitrogen atmosphere at room temperature (25 ± 1 °C) potential range from -1500 mV to 1500 mV, scan rates between 10 and 100 mV/s; stock solutions in methanol
C = 5 mM, PBS pH = 6.40; measurements at 0 and after 60 min. For reproducible experimental results, the polished working electrode was used to place in the desired electrolyte solution followed by recording of various voltammograms until the achievement of steady state baseline.

Notes

Acknowledgments and finances. This work was partially supported by COST Action NutRedOx-CA16112 "Personalized Nutrition in ageing society: redox control of major age-related diseases". The author is grateful to A. Luzhetskyy, A. Palusczak and M. Stierhof (Department of Pharmaceutical Biotechnology, Saarland University, Germany), for support with LC-MS, NMR spectra, and herbicidal activity study.

The author declare no conflict of interest.

References

1. Sies, H.; Jones, D. P. Reactive oxygen species (ROS) as pleiotropic physiological signalling agents. *Nat. Rev. Mol. Cell. Biol.* **2020**, *21*, 363-383.
2. Zarkovic, N. Roles and Functions of ROS and RNS in Cellular Physiology and Pathology. *Cells* **2020**, *9*, 767.
3. Sova, M.; Saso, L. Design and development of Nrf2 modulators for cancer chemoprevention and therapy: a review. *Drug. Des. Devel. Ther.* **2018**, *12*, 3181-3197.
4. Freitas, R. H. C. N.; Fraga, C. A. M. NF-kB-IKKβ Pathway as a Target for Drug Development: Realities, Challenges and Perspectives. *Curr. Drug. Targets.* **2018**, *19*, 1933-1942.
5. Ottanà, R.; Maccari, R.; Giglio, M.; Del Corso; A., Cappiello; M., Mura, U.; Cosconati, S.; Marinelli, L.; Novellino, E.; Sartini, S. et al. Identification of 5-arylidene-4-thiazolidinone derivatives endowed with dual activity as aldose reductase inhibitors and antioxidant agents for the treatment of diabetic complications. *Eur. J. Med. Chem.* **2011**, *46*, 2797-806.
6. Kumar, V.; Sharma, A.; Sharma, P. C. Synthesis of some novel 2,5-disubstituted thiazolidinones from a long chain fatty acid as possible anti-inflammatory, analgesic and hydrogen peroxide scavenging agents. *J. Enzyme Inhib. Med. Chem.* **2011**, *26*, 198-203.
7. Raut, D. G.; Lawand, A. S.; Kadu, V. D.; Hublikar, M. G.; Patil, S. B.; Bhosale, D. G.; Bhosale, R. B. Synthesis of Asymmetric Thiazolyl Pyrazolines as a Potential Antioxidant and Anti-Inflammatory Agents. *Polycycl. Arom. Comp.* **2020**, 1-10.
8. Upadhyay, N.; Tilekar, K.; Loiodice, F.; Anisimova, N. Y.; Spirina, T. S.; Sokolova, D. V.; Smirnova, G. B.; Choe, J. Y.; Meyer-Almes, F. J.; Pokrovsky, V. S.; Lavecchia, A.; Ramaa, C. S. Pharmacophore hybridization approach to discover novel pyrazoline-based hydantoin analogs with anti-tumor efficacy. *Bioorg. Chem.* **2020**, *107*, 104527.
9. Borcherding, D. C.; Siefert, M. E., Lin, S., Brewington, J., Sadek, H., Clancy, J. P., Plafker, S. M., Ziady, A. G. Clinically approved CFTR modulators rescue Nrf2 dysfunction in cystic fibrosis airway epithelia. *J. Clin. Invest.* **2019**, *129*, 3448-3463.
10. Robledinos-Antón, N.; Fernández-Ginés, R.; Manda, G.; Cuadrado, A. Activators and Inhibitors of NRF2: A Review of Their Potential for Clinical Development. *Oxid. Med. Cell. Longev.* **2019**, *2019*, 9372182.
11. Lu, M.; Zhang, X., Zhao, J.; You, Q.; Jiang, Z. A hydrogen peroxide responsive prodrug of Keap1-Nrf2 inhibitor for improving oral absorption and selective activation in inflammatory conditions. *Redox Biol.* **2020**, *34*, 101565.
12. Derkach, G. O.; Golota, S. M.; Trufin, Y. O.; Roman, O. M.; Sementsiv, G. M.; Demchuk, I. L.; Soronovych, I. I.; Kutsyk, R. V.; Grellier, P.; Lesyk, R. B. Synthesis and biological activity of 5-aminomethylene-2-thioxotiazolidin-4-ones derivatives. *Pharm. Rev.* **2017**, *2*, 5-11 (In Ukrainian).
13. Derkach, G. O.; Golota, S. M.; Zasidko, V. V.; Soronovych, I. I.; Kutsyk, R. V.; Lesyk, R. B. The synthesis and the study of antimicrobial properties of 5-r,r'-aminometylene derivatives of thiazolidine-2, 4-dione and 4-thioxothiazolidine-2-one. *J. Org. Pharm. Chem.* **2016**, *14*, 32-37.
14. Holota, S. M.; Derkach, G. O.; Zasidko, V. V.; Trokhymchuk, V. V.; Furdychko, L. O.; Demchuk, I. L.; Semenciv, G. M.; Soronovych, I. I.; Kutsyk, R. V.; Lesyk, R. B. Features of antimicrobial activity of some 5-aminomethylene-2-thioxo-4-thiazolidinones. *Biopolym. Cell.* **2019**, *35*, 371-380.
15. Holota, S.; Kryshchyshyn, A.; Derkach, H.; Trufin, Y.; Demchuk, I.; Gzella, A.; Grellier, P.; Lesyk, R. Synthesis of 5-enamine-4-thiazolidinone derivatives with trypanocidal and anticancer activity. *Bioorg Chem.* **2019**, *86*, 126-136.
16. Holota, S.M.; Derkach, H. O.; Demchuk, I. L.; Vynnytska, R. B.; Antoniv, O. I.; Furdychko, L. O.; Nektegayev, I.O.; Lesyk, R. B. Synthesis and *in vivo* evaluation of pyrazoline-thiazolidin-4-one hybrid Les-5581 as a potential non-steroidal anti-inflammatory agent. *Biopolym.Cell.*, **2019**, *35*, 437-447.
17. Ajantha, J.; Varathan, E.; Bharti, V.; Subramanian, V.; Easwaramoorthi, S.; Chand, S. Photophysical and charge transport properties of pyrazolines. *RSC Adv.* **2016**, *6*, 786-795.
18. Radi, M.; Botta, L.; Casaluce, G.; Bernardini, M.; Botta, M. Practical One-Pot Two-Step Protocol for the Microwave-Assisted Synthesis of Highly Functionalized Rhodanine Derivatives. *J. Comb. Chem.* **2010**, *12*, 200-205.
19. Chebanov, V. A.; Desenko, S. M.; Gurley, T. W. *Azaheterocycles based on a,ß-unsaturated carbonyls,* Springer-Verlag Berlin Heidelberg, 2008.
20. Brand-Williams, W.; Cuvelier, M.; Berset, C. Use of a free radical method to evaluate antioxidant activity. *LWT – Food Science and Technology*, **1995**, *28*, 25-30.
21. Humphries, R.M.; Ambler, J.; Mitchell, S.L.; Castanheira, M.; Dingle, T.; Hindler, J.A.; Koeth, L.; Sei, K. CLSI Methods Development and Standardization Working Group Best Practices for Evaluation of Antimicrobial Susceptibility Tests. *J. Clin. Microbiol.* **2018**, *56*, e01934-1917.
22. Nenoff, P.; Oswald, U.; Haustein, U.F. *In vitro* susceptibility of yeasts for fluconazole and itraconazole. Evaluation of a microdilution test. *Mycoses*, **1999**, *42*, 629-639.

Синтез нових піразолін-тіазолідин-4-онових гібридних молекул та оцінка їх біологічної активності

С. М. Голота[1,2]*

[1] *Львівський національний медичний університет імені Данила Галицького, вул. Пекарська, 69, Львів, 79010, Україна*
[2] *Волинський національний університет імені Лесі Українки, просп. Волі, 13, Луцьк, 43025, Україна*

Резюме: Протягом останніх десятиріч гібридні молекули на основі піразолінових та тіазолідин-4-онових каркасів є об'єктом інтенсивних досліджень в медичній хімії як джерело потенційних біологічно активних сполук із широким фармакологічним профілем. В даній роботі запропонований та представлений ефективний підхід до синтезу піразолін-тіазолідин-4-онових гібридних молекул з єнаміновим лінкером у молекулах. Структура синтезованих сполук підтверджена з використанням методів ^{1}H-, ^{13}C-ЯМР спектроскопії та РХ-МС-спектрометрії. Для всіх сполук досліджена антиоксидантна (DPPH метод), протимікробна (по відношенню до грам-позитивних *Lactobacillus plantarum*, грам-негативних *Escherichia coli* та грибів *Candida albicans*, визначення МІК), редокс (метод циклічної вольтметрії) та гербіцидна активності (по відношенню до *Agrostis stolonifera*). Всі тестовані сполуки продемонстрували здатність інгібувати радикали в умовах DPPH-тесту з IC_{50} в межах 4.67-7.12 mM. Отримані результати скринінгу антирадикальної активності є аргументом для поглиблених досліджень із застосуванням додаткових/альтернативних експериментальних моделей, а також оптимізації молекулярної структури. Всі тестовані сполуки проявили низьку протимікробну та гербіцидну активності, а також не володіють редокс-властивостями.

Ключові слова: піразолін-тіазолідин-4-онові гібриди; метод DPPH; протимікробна/гербіцидна активність; циклічна вольтметрія.

ISSN 1814-9758. Ukr. Bioorg. Acta, 2021, Vol. 16, N 1
UDC 547.78 + 577.152.24
DOI: hpps://doi.org/10.15407/bioorganica2021.01.025

Ukrainica Bioorganica Acta
www.bioorganica.org.ua

UBA

RESEARCH ARTICLE

In vitro and *in silico* study of 1,3-oxazol-4-yltriphenylphosphonium salts as potential inhibitors of *Candida albicans* transglycosylase

Ivan V. Semenyuta*, Maria M. Trush, Diana M. Hodyna, Maryna V. Kachaeva, Larysa O. Metelytsia, Volodymyr S. Brovarets

V.P. Kukhar Institute of Bioorganic Chemistry and Petrochemistry of the NAS of Ukraine, 1 Murmanska St., Kyiv, 02094, Ukraine

Abstract: The previously established *in vitro* high antimicrobial activity of triphenylphosphonium salts (TPPs) against bacterial (*Staphylococcus aureus* ATCC 25923 and multi-drug resistant (MDR)) and fungal (*Candida albicans* ATCC 10231 and MDR) strains made it possible to propose a molecular mechanism of action of these compounds associated with transglycosylase (TG) activity. The hypothesis was based on the well-known literature data on TPPs as inhibitors of *S. aureus* TG. The created homology model of TG *C. albicans* is optimal in terms of quality indicators such as GMQE (0.61), ERRAT (overall quality factor 95.904) and Ramachandran plot analysis (90% amino acid residues in the favored regions). The modeling of molecular docking of the most active ligands **1a-d**, **3c** into the active center of the created homology *C. albicans* TG model demonstrated the formation of stable ligand-protein complexes with calculated binding energies from -8.9 to -9.7 kcal/mol due to the various types of interactions. An important role in complex formation belongs to amino acid residues TYR307, TYR107, GLU275, ALA108 and PRO136. The presented qualitative homologous model of *C. albicans* TG can be used to search and create new agents with a dual mechanism of antimicrobial action. 1,3-oxazol-4-yltriphenylphosphonium salts **1a-d**, **3c** are the perspective objects for further study as antimicrobials against infectious MDR pathogens.

Keywords: transglycosylase; triphenylphosphonium salts; 1,3-oxazole; *Candida albicans; Staphylococcus aureus*.

Introduction

Hospital infections, which often lead to systemic damage and mortality in patients with various types of diseases, are an important problem in the modern healthcare system [1]. The increase in the number of hospital infections is directly related to patients with reduced immunity of various etiologies. The rapid development of multidrug resistance in most microbial pathogens is the main motivation for the rapid development and creation of drugs with new alternative molecular mechanisms of action [2]. It is known that bacterial TG are used as a promising target for the development of new antimicrobial drugs [3-4]. On the other hand, such antifungal agents as caspofungin, anidulafungin and micafungin are inhibitors of 1,3-beta-glucan synthase (EC 2.4.1.34) from the transglycosylase family and participate in the formation of the main component of the fungal cell wall - beta-1,3-glucan polymer [5-6].

Many transglycosylases inhibitors are known as drugs or antibiotics. There is evidence about echinocandins as inhibitors of fungal β-1,3-glucan synthases [6], ethambutol as an inhibitor of mycobacterial arabinotransferases [7], moenomycin as an inhibitor of peptidoglycan glycosyltransferases [8] and niccomycins as inhibitors of chitin synthases [9]. Phosphonium salts have also demonstrated transglycosylase activity as antimicrobial agents against methicillin-resistant *S. aureus* [10]. Analysis of the structure-activity relationship of salts in the online chemical database ChEMBL confirmed this fact as well [11]. As pharmacological agents, a number of phosphonium salts have shown high activity against parasites of the genus *Leishmania* [12], *Trypanosoma brucei* [13], *Trypanosoma cruzi* [14] and *Schistosoma mansoni* [15]. Particular interest in the TPPs is due to a number of other unique properties. They can act as intracellular antioxidants [16], acetylcholinesterase inhibitors [17], chemotherapeutic

Received: 16.04.2021
Revised: 23.04.2021
Accepted: 17.05.2021
Published online: 30.06.2021

* Corresponding author. Tel.: +380-44-573-2595;
e-mail: ivan@bpci.kiev.ua (I. V. Semenyuta)
ORCID: 0000-0001-8464-3692

agents [18], some studies have demonstrated the antiglycemic properties and antiproliferative activity of phosphonium salts [19, 20].

In our work, the results of *in silico* and *in vitro* studies of a number of 1,3-oxazol-4-yltriphenylphosphonium salts are presented as effective antimicrobial agents with a high activity potential against bacterial and fungal strains with a special type of molecular action.

Results and discussion

The synthesis of 5-amino- and 5-sulfanyl-1,3-oxazol-4-yl(triphenyl)phosphonium salts **1-4** was based on convenient approaches developed by B. S. Drach and coworkers [21-23]. 5-Alkylsulfanyl-1,3-oxazol-4-yl(triphenyl)phosphonium iodides **1a-d** were synthesized from available 1-acylamino-2,2-dichloroethenyl (triphenyl)phosphonium chlorides **A** of the general formula $Cl_2C{=}C(NHC(O)Ar)P^+Ph_3Cl^-$ [21] by the reaction with sodium hydrosulfide followed by alkyl iodide treatment [21] (Scheme 1).

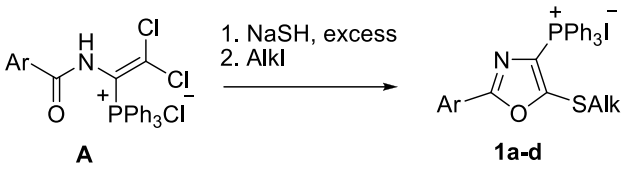

	Ar	Alk
1a	4-MeC_6H_4	Et
1b	4-ClC_6H_4	Et
1c	4-MeC_6H_4	$CH_2CH{=}CH_2$
1d	C_6H_5	$CH_2CH{=}CH_2$

Scheme 1. Synthesis of 5-alkylsulfanyl-1,3-oxazol-4-yl(triphenyl)phosphonium iodides **1a-d.**

For the synthesis of 5-(4-chlorophenylsulfanyl)-2-(4-methylphenyl)-1,3-oxazol-4-yl(triphenyl)phosphonium perchlorate (**2**) 2,2-dichloro-1-((4-methylbenzoyl)amino) ethenyl(triphenyl)phosphonium chloride **A** was converted into the corresponding ylide betaine **B.** The reaction of compound **B** with methyl iodide with subsequent hydrogen peroxide oxidation and sodium perchlorate treatment leads to 5-mesyl-substituted 1,3-oxazol-4-yl(triphenyl)-phosphonium chloride **C.** By the substitution of mesyl group with sodium 4-chlorobenzenethiolate we obtained compound **2** [22] (Scheme 2).

Interaction of the 1-acylamino-2,2-dichloroethenyl-(triphenyl)phosphonium chlorides **A** with amines leads to formation of 5-amino-1,3-oxazol-4-yl(triphenyl)-phosphonium chlorides converted to the corresponding phosphonium iodides or perchlorates **3a-e** [21, 24] (Scheme 3). Cyclization of urea derivatives **D** with morpholine leads to 2-anilino-5-morpholino-1,3-oxazol-4-yl(triphenyl) phosphornium perchlorate (**4**) [23] (Scheme 4).

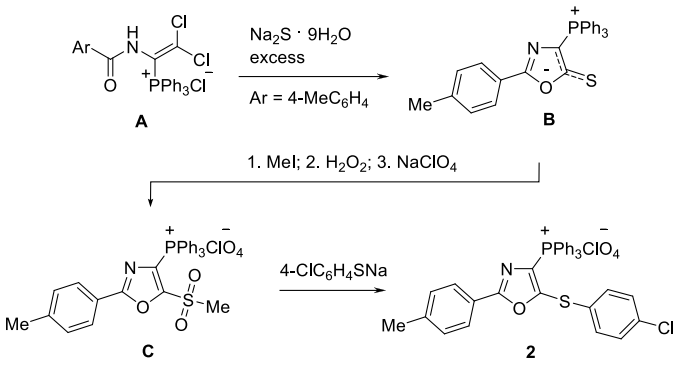

Scheme 2. Synthesis of 5-(4-chlorophenylsulfanyl)-2-(4-methylphenyl)-1,3-oxazol-4-yl(triphenyl)phosphonium perchlorate (**2**).

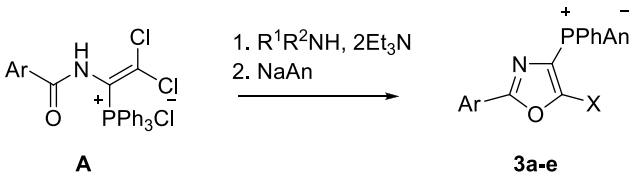

	Ar	X	An
3a	Ph	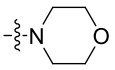	
3b	Ph	4-MeC_6H_4NH	I^-
3c	Ph	Me_2N	I^-
3d	4-MeC_6H_4	PhNH	ClO_4^-
3e	4-MeC_6H_4	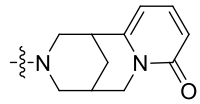	ClO_4^-

Scheme 3. Synthesis of 5-aminosubstituted 2-aryl-1,3-oxazol-4-yl(triphenyl)phosphonium iodides or perchlorates **3a-e.**

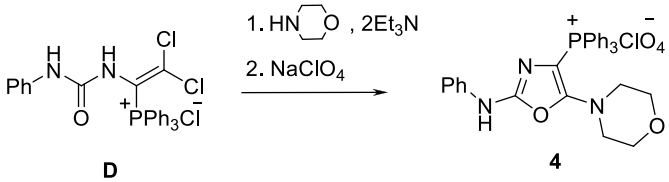

Scheme 4. Synthesis of 2-anilino-5-morpholino-1,3-oxazol-4-yl(triphenyl)phosphonium perchlorate (**4**).

Earlier, we have obtained and published the results of *in silico* and *in vitro* studies of a number of TPPs as effective antimicrobial agents against *S. aureus* and *C. albicans*, including against their clinical drug-resistant isolates [25, 26], presented in Table 1.

Table 1 demonstrates that salts **1a-d, 3c** are the most active against both bacterial *S. aureus* and fungal *C. albicans* strains. It is important to note the high antimicrobial potential of these compounds against clinical drug-resistant strains. Many authors associate the anti-staphylococcal potential of TPPs with their transglycosylase activity [10]. A similarly high potential was noted in our

Table 1. Antimicrobial activity of TPPs.

Compound	Antibacterial activity*		Antifungal activity*	
	S. aureus ATCC 25923	*S. aureus* MDR	*C. albicans* ATCC 10231	*C. albicans* MDR
1	38,7±0,3	32,3±0,3	36,0 ± 0,3	30,3 ± 0,3
2	34,3±0,9	31,0±0,9	35,3 ± 0,9	30,0 ± 0,6
3	34,7±0,6	34,7±0,6	36,7 ± 0,3	37,3 ± 0,6
4	37,3±0,6	34,7±0,6	29,3 ± 0,6	31,3 ± 0,3
5	20,3 ± 0,3	34,3±0,6	22,0 ± 0,3	17,0 ± 0,6
6	32,3±0,6	24,3±0,3	14,3 ± 0,3	15,3 ± 0,3
7	30.3±0.6	28.3±0.3	22,3 ± 0,3	21,0 ± 0,3
8	35.0±0.6	31.3±0.3	38,0 ± 0,9	34,7 ± 0,3
9	36.3±0.9	32.0±0.3	25,7 ± 0,3	27,0 ± 0,6
10	20,7±0,3	19,3±0,3	21,3 ± 0,3	16,0 ± 0,3
11	27,5±0,3	22,0±0,6	18,0 ± 0,3	14,0 ± 0,6
Fluconazole	-	-	21,6±0,3	n/a
Ampicillin	29,0±0,6	n/a	-	-
Oxacillin	30,3±0,3	n/a	-	-
Ceftriaxone	11,3±0,6	n/a	-	-

work against the fungi (Table 1). Hence, it was possible to assume a similar target-oriented molecular mechanism of TPPs action. Based on this hypothesis, we conducted *in silico* studies including the creation of a homology model *C. albicans* TG.

A preliminary search of amino acid sequences associated with *C. albicans* TGs was conducted by the SWISS-MODEL template library. 1726 templates were created, from which the 5oa6.1.A template with 48.65% sequence identity was selected and a homology model was built. The created model (Figure 1) is the most optimal considering the resolution (1.94Å) and the estimation quality QMEAN (-1.75), GMQE (0.61).

At the next stage, the quality of the homology model was assessed using the online resources ERRAT and PROCHECK-web server data analysis has been also confirmed the 3D model structure TG good quality using Ramachandran plot analysis (Figure 2). Ramachandran plot results indicated that 90.0 % of the amino acid residues were distributed in the favored regions, 9.5 % – in the additionally allowed regions, 0.3 % – in the generously allowed regions and only 0.3 % – in the disallowed regions.

Thus, the created 3D structure of TG *C. albicans* has good stereochemically quality and was used for molecular docking. Molecular docking of ligands **1a-d** and **3c**, as the most active antimicrobials, was carried out into the active site of the created homology *C. albicans* TG model (Figure 3, 4). Ligand-protein complex formation of the studied TPPs was provided by various types of interactions (Table 2).

Thus, the formation of ligand-protein complexes is accompanied by estimated binding energies in a certain range from -8.9 to -9.7 kcal/mol (Table 2). The ligand-protein complexes were stabilized through strong hydrogen bonds (2.59-2.75 Å), electrostatic (3.38-4.55 Å) and hydrophobic (3.94-5.26 Å) interactions. The amino acid residues TYR307, TYR107, GLU275, ALA108 and PRO136 play a key role in this complexation.

Conclusions

Thus, we have experimentally established the presence of high antibacterial and antifungal activity of TPPs **1a-d**, **3c**, including the activity against drug-resistant clinical isolates obtained from biomaterial. The formation of stable ligand-protein complexes is provided by strong hydrogen bonds between amino acid residues and the oxazole ring of the ligands. The triphenylphosphonium group also plays a special role in the stabilization of the complexes. Other substituents in the structure of salts also form a number of electrostatic (3.38-4.55 Å) and hydrophobic interactions (3.94-5.26 Å).

Thus, a qualitative homology model of *C. albicans* TG can be used as a tool for the successful construction of new agents with the double antimicrobial action mechanism.

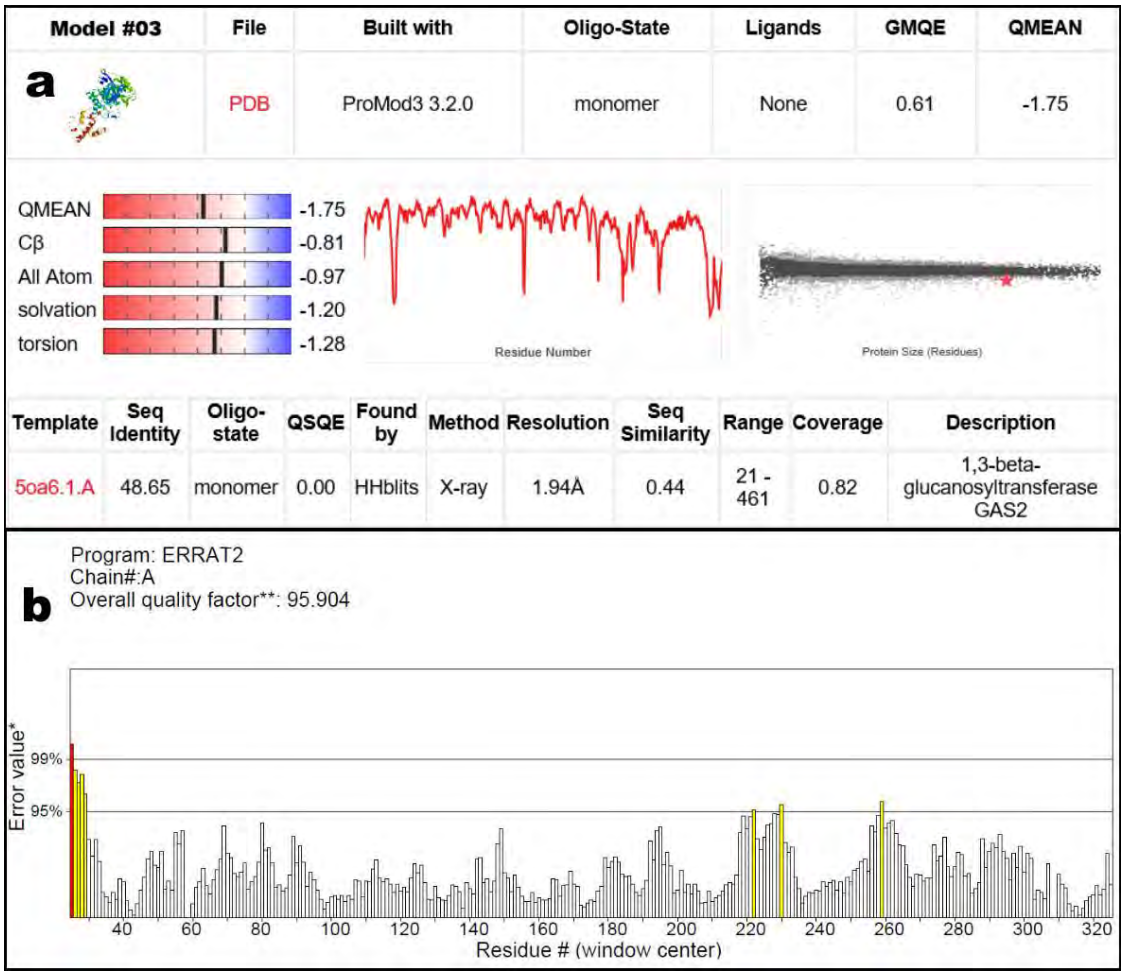

Figure 1. Quality assessment of the created homology model TG *C. albicans*. a) QMEAN quality plot of the homology model; b) the 3D profile of subunit A TG verified by using ERRAT server.

Table 2. Docking results of ligands **1a-d, 3c** into TG *C. albicans* active sites.

Compound	ΔG, kcal/mol	Hydrogen bonds	Electrostatic interaction	Hydrophobic interactions
1a	−9.2	TYR307 (2.59Å)	GLU275 (3.61Å), GLU275 (3.38Å), GLU176 (4.12Å)	TYR307 (5.20Å), TYR107 (4.41Å), TYR244 (4.92Å), TYR307 (5.18Å), TYR107 (5.18Å), TYR107 (3.94Å), ALA108 (5.27Å), PRO136 (4.45Å), PRO136 (4.60Å)
1b	−9.3	TYR307 (2.65Å)	TYR307 (3.60Å), TYR307 (3.38Å), GLU275 (4.12Å), TYR107 (4.08Å)	GLU275 (5.20Å), TYR107 (4.41Å), TYR107 (3.96Å), ALA108 (5.22Å), PRO136 (4.35Å), PRO136 (4.53Å)
1c	−8.9	TYR307 (2.75Å)	GLU275 (3.64Å), TYR107 (3.94Å)	TYR244 (4.89Å), TYR307 (5.26Å), TYR107 (4.41Å), TYR107 (3.97Å), ALA108 (5.26Å), PRO136 (4.32Å), PRO136 (4.55Å)
1d	−9.1	TYR307 (2.76Å)	GLU275 (3.58Å), TYR107 (4.00Å)	TYR307 (5.25Å), TYR107 (4.39Å), ALA108 (5.22Å), PRO136 (4.29Å), PRO136 (4.54Å)
3c	−9.7	TYR307 (2.74Å)	GLU275 (3.70Å), GLU275 (4.99Å), ARG142 (4.55Å)	TYR307 (5.05Å), TYR107 (4.88Å), TYR107 (5.10Å), PRO136 (5.21Å), PRO136 (5.16Å)

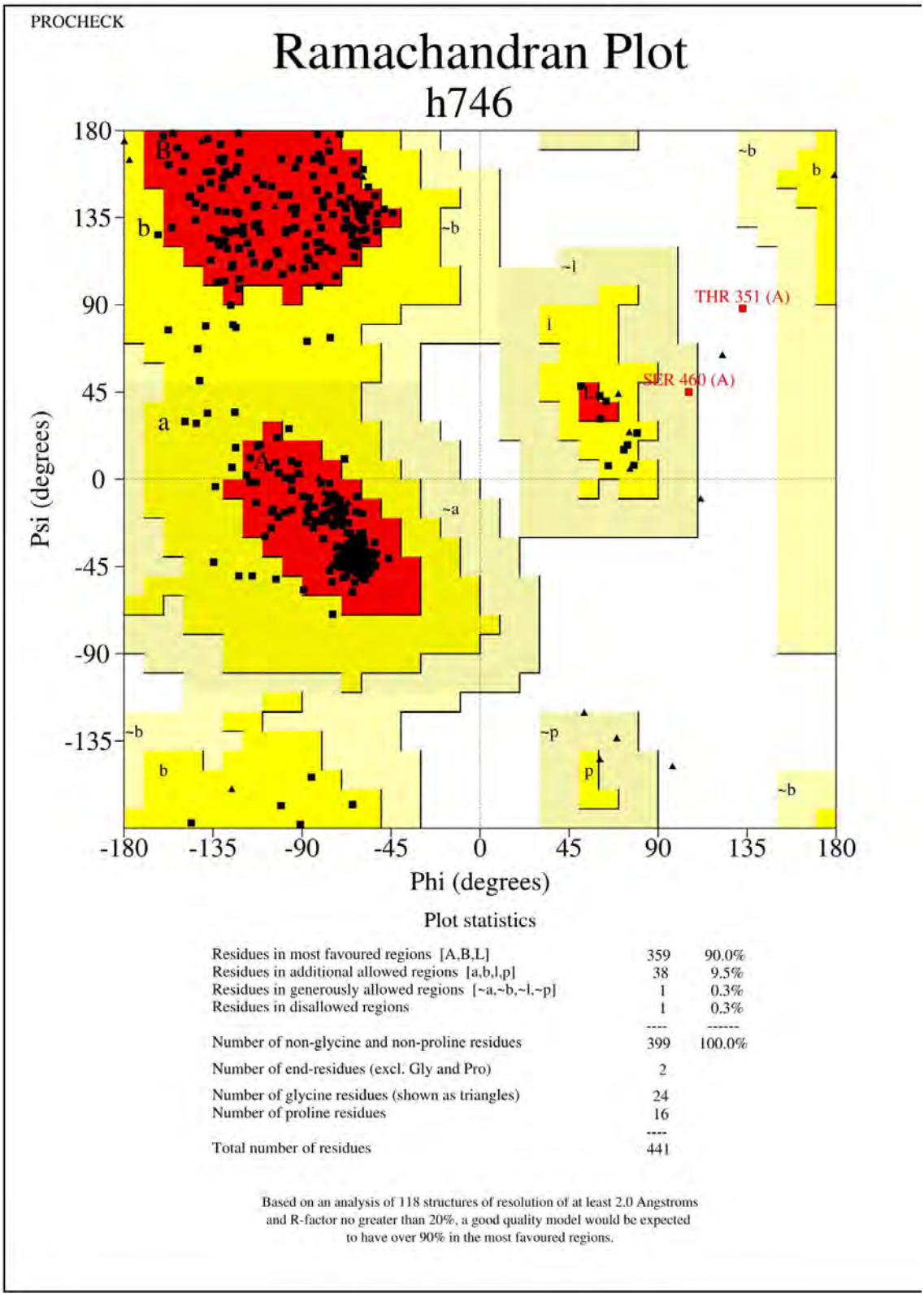

Figure 2. Quality assessment of the created homology model TG *C. albicans*. Ramachandran plot analysis of the stereochemical quality of TG model generated by PROCHECK validation server.

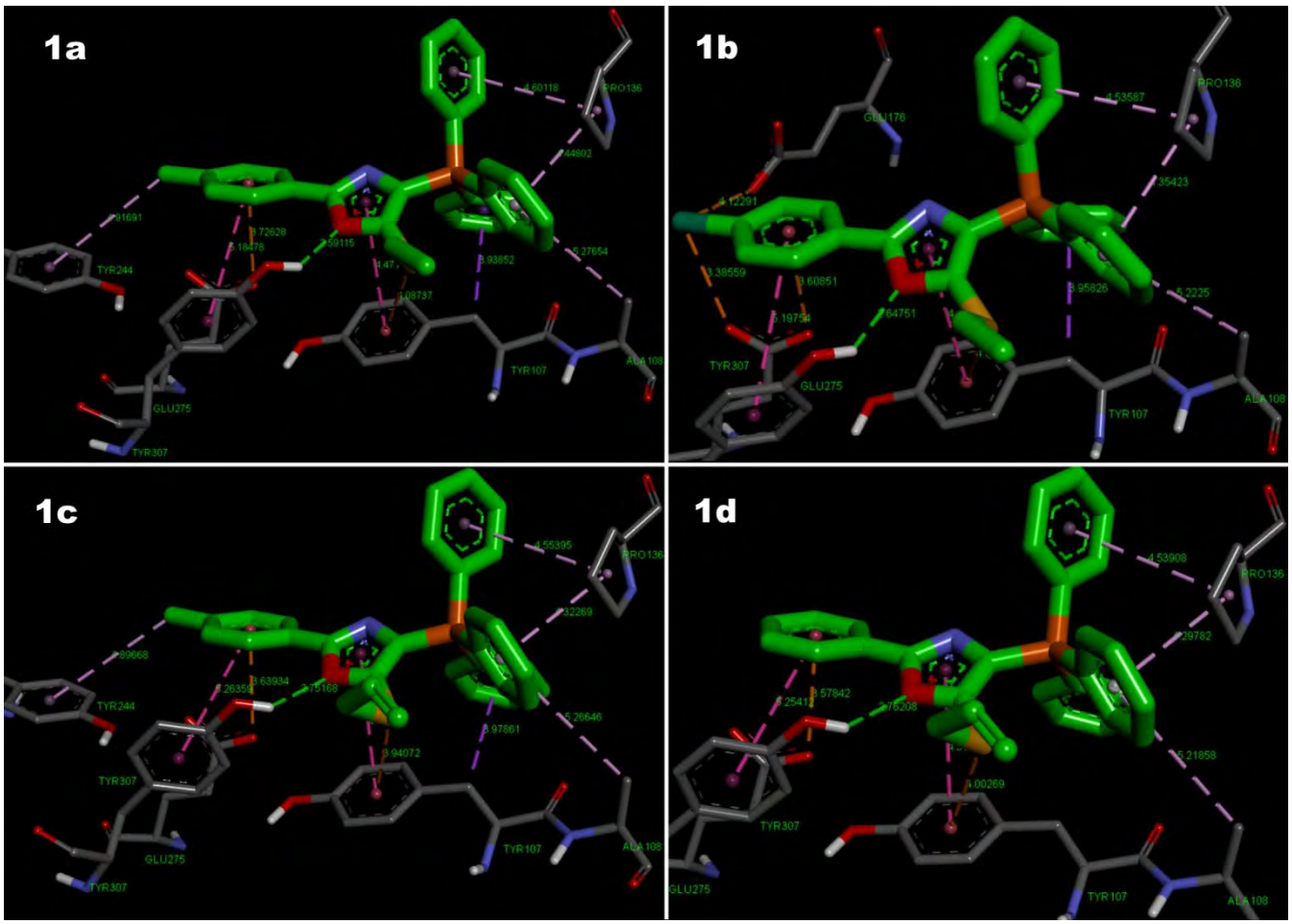

Figure 3. Molecular docking of the ligands **1a-d** into the active site of TG *C. albicans*.

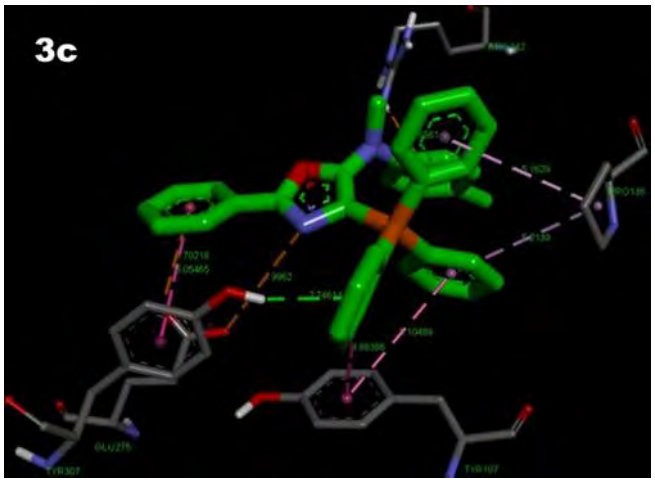

Figure 4. Molecular docking of the ligand **3c** into the active site of TG *C. albicans*.

1,3-oxazol-4-yltriphenylphosphonium salts **1a-d**, **3c** are promising candidates for the development of new antimicrobials against infectious pathogens MDR *S. aureus* and *C. albicans*.

Experimental section

General chemistry methods

Melting points were determined on a Fisher-Johns apparatus. IR spectra were recorded on a Vertex-70 spectrometer from KBr pellets. ^{1}H and ^{13}C NMR spectra were recorded on Varian Mercury 400 (400 MHz) and Bruker Avance DRX 500 (500 and 125 MHz, respectively) spectrometers in $(CD_3)_2SO$ or $CDCl_3$ taking its residual protons signal as a standard. LCMS analysis was performed on an Agilent 1200 Series system equipped with a diode array and a G6130A mass-spectrometer (atmospheric pressure electrospray ionization). Combustion elemental analysis was performed in the V.P. Kukhar Institute of Bioorganic Chemistry and Petrochemistry of the NAS of Ukraine analytical laboratory.

The structure of investigated 1,3-oxazole derivatives **1a-d** [26, 27], **2** [27, 22], **4** [28], **3a** [29, 30], **3b,c** [21], **3d** [26] and **3e** [24] have been confirmed by NMR (1H and 13C NMR), IR spectroscopy, chromato-mass and elemental analysis and corresponded to previously described.

Biology

The antimicrobial activity of the studied triphenylphosphonium salts (TPPs) was estimated against *C. albicans* (ATCC 10231 and fluconazole-resistant clinical isolate) and *S. aureus* (ATCC 25923 and multi-drug (MDR) resistant clinical isolate) received from the Museum of Microbial Culture Collection of the P.L. Shupyk National Medical Academy of Postgraduate Education.

Antimicrobial properties were determined by the disc diffusion method in Mueller-Hinton and Sabouraud agar [31]. A final inoculum concentration of $1 \cdot 10^5$ colony-forming unit (CFU) per mL was established using a 0.5 McFarland turbidity standard and subsequent dilution of 0.02 ml of the tested compounds was applied on standard paper disks (6 mm) which were placed on the agar plate. The compound content on a disk was 0.3 μM. The known antifungal Fluconazole and antibacterial Ampicilline, Oxacilline and Ceftriaxone were used as positive controls.

The activity of tested compounds was identified by measuring the zone diameter of the growth inhibition, which indicates the degree of susceptibility or resistance of all microbial pathogens against the test compounds. The compounds, which formed zones > 15 mm of growth inhibition of microorganisms, were selected as active.

Homology modeling

Homology modeling of the aminoacid sequence of *C. albicans* TG (UniProt: C4YFM5) [32] was performed using web server SWISS-MODEL [33]. First, a preliminary search for evolutionarily related aminoacids sequences was performed using the SWISS-MODEL template library. Search and analysis of structures homologous to *C. albicans* TG were performed using the methods of BLAST [34] and HHBlits [35]. Templates for building a homology model were selected based on the overall rating of the created templates. The quality of the created homology model of *C. albicans* TG was estimated using internal methods of testing the web server SWISS-MODEL [36] and web servers ERRAT [37] and PROCHECK [38].

Molecular docking

The created homology model of *C. albicans* TG was used for docking studies. AutoDock Tools (ADT) 1.5.6 [39] was used to prepare the protein and ligands. All polar hydrogens were added to the protein molecules by ADT. The renumbering of all atoms with included new hydrogen atoms were performed by the noBondOrder method. The Gasteiger method was applied for the calculation and addition of partial charges. The made protein and ligands were saved in PDBQT format. The ChemAxon Marvin Sketch 5.3.735 program [40] was used to create, optimize and save the ligand structures in Mol2 format. The ligands optimization and energy minimization were performed by Avogadro v1.1.1 [41] using an auto-optimization tool by applying MMFF94s force field with the steepest descent algorithm. The partial charges and torsion angles of the ligands were altered by ADT and saved in PDBQT format. Docking was performed by AutoDock Vina 1.1.2 program [42]. The grid map (30*30*30 points) with a grid spacing of 1Å was used. The analysis and visualization of protein-ligand interactions were conducted by Accelrys DS 4.0 [43].

Notes

Acknowledgments and finances. We thank the National Research Foundation of Ukraine (NRFU competition "Science for the Security of Human and Society" №2020.01/0075) for financial support.

The authors declare no conflict of interest.

Author contributions. **I. V. S**: molecular docking, homology modeling, analysis results, conceptualization, writing and editing. **M. M. T., D. M. H.** the investigation of bioactivity. **M. V. K**: synthesis of compounds, writing experimental section. **V. S. B**: synthesis of compounds, conceptualization. **L. O. M**: the investigation of bioactivity, conceptualization, results analysis, writing and editing.

References

1. Boev, C.; Kiss, E. Hospital-Acquired Infections: Current Trends and Prevention. *Crit. Care Nurs. Clin.* **2017**, *1*, 51-65.
2. Jacopin, E.; Lehtinen, S.; Débarre, F.; Blanquart, F. Factors favouring the evolution of multidrug resistance in bacteria. *J. R. Soc. Interface*. **2020**, 1720200105.
3. Xiaorui, C.; Chi-Huey, W.; Che, M. Targeting the Bacterial Transglycosylase: Antibiotic Development from a Structural Perspective. *ACS Infect. Dis.* **2019**, *9*, 1493-1504.

4. Raghavan, R.; Mandal, J. Use of Bacterial Cell Wall Recycle Inhibitors to Combat Antimicrobial Resistance. In: Thomas S. (eds) Antimicrobial Resistance. Springer: Singapore, **2020**.
5. Liu, J.; Balasubramanian, MK. 1,3-beta-Glucan synthase: a useful target for antifungal drugs. *Curr. Drug. Targets Infect. Disord*. **2001**, *2*, 159-169.
6. Handbook of Pharmacogenomics and Stratified Medicine, Padmanabhan, S., Academic Press / Elsevier: London, **2014**.
7. Goude, R.; Amin, AG.; Chatterjee, D.; Parish, T. The arabinosyltransferase EmbC is inhibited by ethambutol in Mycobacterium tuberculosis. *Antimicrob. Agents Chemother*. **2009,** *10*, 4138-4146.
8. Ostash, B.; Doud, E.; Fedorenko, V. The molecular biology of moenomycins: towards novel antibiotics based on inhibition of bacterial peptidoglycan glycosyltransferases. *Biol. Chem*. **2010**, *5*, 499-504.
9. Gaughran, J.P.; Lai, M.H.; Kirsch, D.R.; Silverman, S.J. Nikkomycin Z is a specific inhibitor of Saccharomyces cerevisiae chitin synthase isozyme Chs3 *in vitro* and *in vivo*. *J. Bacteriol.* **1994**, *18*, 5857-5860.
10. Cheng, T.J.; Wu, Y.T.; Yang, S.T.; Lo, K.H.; Chen, S.K.; Chen, Y.H.; Huang, W.I.; Yuan, C.H.; Guo, C.W.; Huang, L.Y.; Chen, K.T.; Shih, H.W.; Cheng, Y.S.; Cheng, W.C.; Wong, C.H. High-throughput identification of antibacterials against methicillin-resistant Staphylococcus aureus (MRSA) and the transglycosylase. *Bioorg. Med. Chem*. **2010**, *24*, 8512-8529.
11. Bioassay ID=CHEMBL1640432. In ChEMBL Database. European Molecular Biology Laboratory [Internet]. Available from: https://www.ebi.ac.uk/chembl/assay_report_card/CHEMBL1640432/ (accessed on April 16, 2021).
12. Manzano, J.I.; Cueto-Díaz, E.J.; Olías-Molero, A.I.; Perea, A.; Herraiz, T.; Torrado, J.J.; Alunda, J.M.;, Gamarro, F.; Dardonville, C. Discovery and Pharmacological Studies of 4-Hydroxyphenyl-Derived Phosphonium Salts Active in a Mouse Model of Visceral Leishmaniasis. *J. Med. Chem.* **2019**, *23*, 10664-10675.
13. Taladriz, A.; Healy, A.; Flores Pérez, E.J.; Herrero García, V.; Ríos Martínez, C.; Alkhaldi, A.A.; Eze, A.A.; Kaiser, M.; de Koning, H.P.; Chana, A.; Dardonville, C. Synthesis and structure-activity analysis of new phosphonium salts with potent activity against African trypanosomes. *J. Med. Chem.* **2012**, *6*, 2606-2622.
14. Long, T.E.; Lu, X.; Galizzi, M.; Docampo, R.; Gut, J.; Rosenthal, P.J. Phosphonium lipocations as antiparasitic agents. *Bioorg. Med. Chem. Lett.* **2012**, *8*, 2976-2979.
15. McAllister, P.R.; Dotson, M.J.; Grim, S.O.; Hillman, G.R. Effects of phosphonium compounds on Schistosoma mansoni. *J. Med. Chem.* **1980**, *8*, 862-865.
16. Korshunova, G.A.; Shishkina, A.V.; Skulachev, M.V. Design, synthesis, and some aspects of the biological activity of mitochondria-targeted antioxidants. *Biochemistry (Moscow).* **2017**, *82*, 760-777.
17. Levi-Schaffer, F.; Tarrab-Hazdai, R.; Meshulam, H.; Arnon, R.; Effect of phosphonium salts and phosphoranes on the acetylcholinesterase activity and on the viability of Schistosoma mansoni parasites. *Int. Immunopharmacol.* **1984**, *6*, 619-627.
18. Bergeron, K.L.; Murphy, E.L.; Majofodun, O.; Muñoz, L.D.; Williams, J.C.; Almeida, K.H. Arylphosphonium salts interact with DNA to modulate cytotoxicity. *Mutat. Res.* **2009**, *2*, 141-148.
19. Blank, B.; DiTullio, N.W.; Deviney, L.; Roberts, J.T.; Saunders, H.L. Synthesis and hypoglycemic activity of phenacyl-triphenylphosphoranes and phosphonium salts. *J. Med. Chem.* **1975**, *9*, 952-954.
20. Rideout, D.C.; Calogeropoulou, T.; Jaworski, J.S.; Dagnino, R.; McCarthy, M.R. Phosphonium salts exhibiting selective anti-carcinoma activity in vitro. *Anticancer Drug Des.* **1989**, *4*, 265-280.
21. Lobanov, O. P.; Martyn'yuk, A. P.; Drach, B. S. Reactions of (2,2-dichloro-1-acylaminovinyl)triphenylphosphonium chlorides with nucleophiles. *Zh. Obshch. Khim.* **1980**, *50*, 2248-2257.
22. Golovchenko, A. V.; Brovarets, V. S.; Drach, B. S. A Convenient Procedure for Introducing Arylsulfanyl and Heterylsulfanyl Groups into the 5 Position of the Oxazole Ring. *Rus. J. Gen. Chem.* **2004**, *74,* 1414-1417.
23. Martynyuk, A. P.; Brovarets, V. S.; Lobanov, O. P.; Drach, B. S. Phosphorus-containing derivatives of N-2,2-dichlorovinylurea. *Zh. Obshch. Khim.* **1984**, *54*, 2186-2200.
24. Abdurakhmanova, E. R.; Pil'o, S. G.; Kondratyuk, K. M.; Golovchenko, A. V.; Brovarets, V. S. 1,3-Oxazole derived cytisines. *Russ. J. Gen. Chem.,* **2017**, *87*, 244-251.
25. Trush, M.M.; Kovalishyn, V.; Ocheretniuk, A.D.; Kovalishyn, V.; Ocheretniuk, A.D.;Kachaeva, M.V.; Brovarets, V.S.; Metelytsia, L.O. QSAR Study of Some 1,3-Oxazolylphosphonium Derivatives as New Potent Anti-Candida Agents and Their Toxicity Evaluation. *Curr. Drug Discov. Technol.* **2019**, *16*, 204-209.
26. Trush, M.M.; Kovalishyn, V.; Ocheretniuk, A.D.; Kalashnikova, L.E.; Prokopenko, V.M.; Holovchenko, O.V.; Kobzar, O.L.; Brovarets V.S.; Metelytsia, L.O. New 1,3-oxazolylphosphonium Salts as Potential Biocides: QSAR Study, Synthesis, Antibacterial Activity and Toxicity Evaluation. *Lett Drug Des Discov.* **2018**, *15*, 1259.
27. Trush, M. M.; Kovalishyn, V.; Hodyna, D.; Golovchenko, O. V.; Chumachenko, S.; Tetko, I. V.; Brovarets, V. S.; Metelytsia, L. In silico and in vitro studies of a number PILs as new antibacterials against MDR clinical isolate Acinetobacter baumannii *Chem. Biol. Drug Des.* **2020**, *95*, 624-630.
28. WO Patent No 2006105669 A1. Antimicrobial solution comprising a metallic salt and a surfactant / Tessier, D.; Filteau, M.; Radu I. Patent appl. No PCT/CA2006/000543 07.04.2006. Publ. 12.10.2006.
29. Brovarets, V. S.; Lobanov, O. P.; Drach, B. S. Syntheses of 2,5-substituted azoles from (2,2-dichloro-1-acylaminovinyl) triphenylphosphonium chlorides. *Zh. Obshch. Khim.* **1983**, *53*, 2015-2020.
30. Drach, B. S.; Sviridov, E. P.; Kirsanov, A. V. Reaction of 1,2,2,2-tetrachloroethylamides of acids with the ethyl ester of diphenylphosphinous acid and with triphenylphosphene. *Zh. Obshch. Khim.* **1975**, *45*, 12-16.
31. A. W. Bauer, W. M. Kirby, J. C. Sherris, M. Turck. Am. J. Clin. Pathol. **1966**, *45*, 493-496.
32. The UniProt Consortium, UniProt: the universal protein knowledgebase in 2021. *Nucleic Acids Res.* **2021**, *49*, 480–489, Available from: https://www.uniprot.org/uniprot/C4YFM5 (accessed on April 16, 2021).
33. Waterhouse, A.; Bertoni, M.; Bienert, S.; Studer, G.; Tauriello, G.; Gumienny, R.; Heer, F.T.; de Beer, T.A.P.; Rempfer, C.; Bordoli, L.; Lepore, R.; Schwede, T. SWISS-MODEL: homology modelling of protein structures and complexes. *Nucleic Acids Res.* **2018**, *46*, 296-303.
34. Camacho, C.; Coulouris, G.; Avagyan, V.; Ma, N.; Papadopoulos, J.; Bealer, K.; Madden, T.L. BLAST+: architecture and applications. *BMC Bioinformatics*, **2009**, *10*, 421-430.
35. Steinegger, M.; Meier, M.; Mirdita, M.; Vöhringer, H.; Haunsberger, S. J.; Söding, J. HH-suite3 for fast remote homology detection and deep protein annotation. *BMC Bioinformatics.* **2019**, *20*, 473.
36. Benkert, P.; Biasini, M.; Schwede, T. Toward the estimation of the absolute quality of individual protein structure models. *Bioinformatic.* **2011**, *27*, 343-350.
37. C. Colovos, T.O. Yeates, Verification of protein structures: patterns of nonbonded atomic interactions. *Protein Sci*. **1993**, *2*, 1511-1519.
38. R.A. Laskowski, M.W. MacArthur, D.S. Moss, J.M. Thornton, PROCHECK - a program to check the stereochemical quality of protein structures. *J. App. Cryst.* **1993**, *26*, 283-291.
39. Sanner, M.F.; Python: A programming language for software integration and development. *J. Mol. Graph. Model.* **1999**, 17, 57-61.
40. Marvin Sketch was used for drawing, displaying and optimization chemical structures; MarvinSketch 5.3.735, 2017, ChemAxon website [Internet]. Available from: http://www.chemaxon.com (accessed on April 16, 2021).
41. Hanwell, M.D.; Curtis, D.E.; Lonie, D.C.; Vandermeersch, T.; Zurek, T.; Hutchison, G.R. Avogadro: an advanced semantic chemical editor, visualization, and analysis platform. *J. Cheminform*. **2012**, *4*, 17.
42. Trott, O.; Olson, A.J. AutoDock Vina: improving the speed and accuracy of docking with a new scoring function, efficient optimization, and multithreading. *J. Comput. Chem.* **2010**, *31*, 455-461.
43. Dassault Systèmes BIOVIA, Discovery Studio Visualizer, v4.0.100.13345, San Diego: Dassault Systèmes, **2020.**

In vitro та *in silico* дослідження 1,3-оксазол-4- ілтрифенілфосфонієвих солей як потенційних інгібіторів трансглікозилази *Candida albicans*

І. В. Семенюта*, М. М. Труш, Д. М. Година, М. В. Качаєва, Л. О. Метелиця, В. С. Броварець

Інститут біоорганічної хімії та нафтохімії ім. В.П. Кухаря НАН України, вул. Мурманська, 1, Київ, 02094, Україна

Резюме: У роботі запропоновано новий потенційний молекулярний механізм дії 1,3-оксазол-4-ілтрифенілфосфонієвих солей як інгібіторів трансглікозилази. За результатами біологічних досліджень встановлено високий антимікробний потенціал досліджених солей трифенілфосфонію як проти бактеріальних (*Staphylococcus aureus* ATCC 25923 та мультирезистентний), так і проти грибкових (*Candida albicans* ATCC 10231 та мультирезистентний) штамів. Отримані експериментальні дані щодо їх антимікробної активності дозволили запропонувати молекулярний механізм дії цих сполук, пов'язаний з трансглікозилазною активністю. В основу гіпотези було покладено результати аналізу «структура-активність» солей трифосфонію в онлайн хімічній базі ChEMBL, а також за відомими літературниими джерелами щодо антимікробної активності солей як інгібіторів трансглікозилази *S. aureus*. Створена гомологічна модель трансглікозилази *C. albicans* продемонструвала високі показники якості та була використана для молекулярного докінгу. Молекулярний докінг найбільш активних лігандів **1a-d**, **3c** в активний центр створеної гомологічної моделі *C. albicans* засвідчив утворення стабільних ліганд-білкових комплексів з ΔG в діапазоні від -8,9 до -9,7 ккал/моль шляхом формування різних типів взаємодій. Представлена якісна гомологічна модель трансглікозилази *C. albicans* може бути використана для пошуку та створення нових агентів з подвійним механізмом антимікробної дії. Солі 1,3-оксазол-4-ілтріфенілфосфонію **1a-d**, **3c** є перспективними об’єктами для подальшого вивчення в якості антимікробних засобів проти мультирезистентних інфекційних збудників.

Ключові слова: трансглікозилаза; трифенілфосфонієві солі; 1,3-оксазол; *Candida albicans*; *Staphylococcus aureus*.

ISSN 1814-9758. Ukr. Bioorg. Acta, 2021, Vol. 16, N 1
UDC 544.6 + 541.138.3: 539.2: 539.216
DOI: hpps://doi.org/10.15407/bioorganica2021.01.034

Ukrainica Bioorganica Acta
www.bioorganica.org.ua

RESEARCH ARTICLE

In silico study the interaction of heterocyclic bases with peptide moieties of proteins in "fragment-to-fragment" approach

Yevheniia S. Velihina[1], Nataliya V. Obernikhina[2]*, Stepan G. Pilyo[1], Maryna V. Kachaeva[1], Oleksiy D. Kachkovsky[1]

[1]*V. P. Kukhar Institute of Bioorganic Chemistry and Petrochemistry of the NAS of Ukraine, 1 Murmanska St., Kyiv, 02094, Ukraine*
[2]*O. O. Bogomolets National Medical University, 13 Shevchenko Blvd., Kyiv, 01601, Ukraine*

Abstract: The binding affinity of model peptide moieties (*Pept*) and heterocyclic bases involving 1,3-oxazoles that are condensed with pyridine and pyrimidine as pharmacophores (*Pharm*) was investigated *in silico* and analyzed within the "fragment-to-fragment" approach. The anellation of the heterocyclic rings increasing their acceptor properties is accompanied by gaining stability of the [*Pharm-Pept*] complexes formed by the π,π-stacking interaction. It was found that elongation of the polypeptide chain led to a twofold increase of the stabilization energy of the [*Pharm-Pept*] complexes. The stability of the hydrogen bonding ([HB]) [*Pharm-BioM*] complexes formed by means of the interaction between the dicoordinated nitrogen atom of the heterocycle and the functional groups of peptide amino acids (-OH, -NH_2, -SH) was evaluated. It was demonstrated that [HB]-complexes that were formed by hydrogen bonds formation with amino acid that contained OH groups had the largest stabilization effect. The anellation with pyridine and pyrimidine rings led to stability increase of the complexes formed by the hydrogen bonding mechanism. The binding energy of [HB]-complexes for compounds **2b** and **3** with a "free" peptide bond of the extended part of the protein is lower compared to amino acids with OH-functional groups. On the contrary, the binding energy of compound **4** with peptides was 2 kcal/mol higher. Compound **4** demonstrated the most pronounced biological activity *in vitro* studies.

Keywords: fragment-to-fragment approach; peptide bond; biological affinity; [*Pharm-BioM*] complex; π,π-stacking interaction; hydrogen bonding.

Introduction

The heterocyclic ring systems containing both nitrogen and oxygen, such as substituted 1,3-oxazoles, are very suitable for use in drug design and library design, which has allowed the introduction of a number of novel pharmacological agents in medical practice (see for example reviews [1-2]). The 1,3-oxazoles with branched conjugated systems have revealed higher biological activity including antibacterial and antiviral activities [3-4], and multiple drug resistance pump inhibition [5-6].

Received: 27.04.2021
Revised: 06.05.2021
Accepted: 08.05.2021
Published online: 30.06.2021

* Corresponding author. Tel.: +380-96-225-7764;
e-mail: nataliya.obernikhina@gmail.com (N. V. Obernikhina)
ORCID: 0000-0003-1143-8924

It was found that these compounds can be considered as a promising component in the development of new biologically active substances that exhibit antitumor activity in a strong dependence on the nature of the substituents in the heterocycle [7-10]. This has enabled the wide introduction of novel pharmacological remedies in clinical practice [11-12]. The QSAR models have been developed for a large series of 1,3-oxazole derivatives showing inhibitory effect on some cancer cell lines and demonstrating a good correlation between many descriptors and biological activity [14].

Determination of a mechanism of multiple ligand binding affinity for amino acids in binding and regulatory proteins is currently an actual task for researches. Binding cavities on protein surfaces are important for protein function because they are usually the sites at which a protein binds to other biological macromolecules such as other proteins and nucleic acids, or small molecules such as metabolites and pharmacophores [15].

Table 1. Chemical structures of the compounds **1-2(a-c)** and **3-6**.

Compd	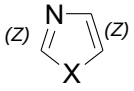	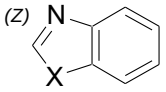	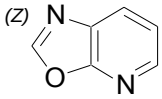	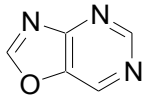	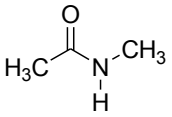	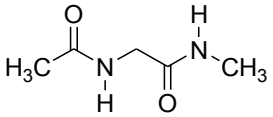
	1	**2**	**3**	**4**	**5**	**6**
X=NH	a	a	-	-	-	-
X=O	b	b	-	-	-	-
X=S	c	c	-	-	-	-

Therefore, in order to minimize energy of formation of the Pharmophore Biomolecule ([*Pharm-BioM*]) complex, structure and electronic properties of the pharmacophore should be as close as possible to the corresponding real protein cavities [16]. The interaction between ligands and proteins usually induces changes in structure and conformational flexibility of the protein. These modifications are due to the coupling of unfolding with binding equilibrium [17-18]. In this regard, it could be expected that modifications in protein stability correlate with changes in the protein packaging caused by ligand-pharmacophore binding due to various types of bond formation, including the formation of a pharmacophore-ligand bond with a "free" peptide bond, not untwisted part of the protein.

Over the past two decades, the Fragment-Based Drug Discovery (FBDD) strategy has been considered in the pharmaceutical industry as a successful key technology for early-stage drug discovery and development [19-20]. This strategy consists of screening low molecular weight compounds (pharmacophores) against macromolecular targets (usually proteins) of clinical relevance. Previously, the "fragment-to-fragment" approach has been used for studying interactions between oxazole and its derivatives with aromatic acid residues in the protein molecule in [*Pharm-BioM*] complexes formed on the basis of the π,π-stacking interactions [21-23]. The oxazole cycle contains two-coordinated nitrogen atom with a lone electron pair (LEP); therefore, it can be considered as a donor center for the formation of [*Pharm-BioM*] complex with amino acid residues of proteins such as lysine, arginine and histidine by the mechanism of hydrogen bonds interaction.

This paper presents the results of *in-silico* studies of the stability of the *[Pharmophore-Peptide*] complex formed between peptide moieties in a model protein and heterocycles as pharmacophores using the "fragment-to fragment" approach.

Materials and calculation method

It was found that oxazole derivatives demonstrated their biological activity [24-26] associated with their ability to form a stable [*Pharm-BioM*] complex. The oxazole molecule has two distinctive features: 1) it contains a branched π-system, therefore, it can form a complex due to the π,π-stacking interactions with suitable conjugated fragments of biomolecules; 2) it contains the dicoordinated nitrogen atom with the LEP and, therefore, can form the complex due to a hydrogen bond when this atom is a proton acceptor. Then, in this paper, the possible expansion of the conjugate system and the increase the number of the LEPs in the anellated compounds **1-4** were investigated. Of course, the real pharmacophore molecules contain both the conjugated and non-conjugated substituents. However, in this study, only the heterocyclic moieties will be considered.

Regarding the polypeptide chain, only the model molecules containing one and two peptide bonds are studied (Table 1, structures **5** and **6**).

The double bond of the >C=O group and the LEP of the nitrogen atom form a short conjugated system, while the LEPs of the oxygen atom could take part in the formation of hydrogen bonds with hydrogen atoms. So, here we will consider only the complex of molecules **1-4** with model molecules **5, 6** formed by the π,π-stacking interactions and hydrogen bonds.

The main characteristics of the electron structure (optimized molecular geometry, charge distribution, energies and shapes of molecular orbitals) were calculated by DFT [wB97XD/6-31G(d.p.)] method (package GAUSSIAN 03 [27]).

Results and Discussion

Possible interaction compounds 1-4 and its derivatives with the peptide bonds

According to theoretical conception, the capacity of the organic molecules to form stable complex with biomolecules is essential condition of the biological activity; it is designated as its *affinity* or *biological affinity* [28-29]. Then, pharmacophore [*Pharm*] and biological molecule Peptide [*Pept*] form the stable complex [*Pharm-Pept*]:

$$[\ \text{Pharm}\ ] + [\ \text{Pept}\ ] \rightleftharpoons [\ \text{Pharm-Pept}\ ]$$

The complex stability depends on the electronic environment of both components. We supposed that the complex and its component are neutral and hence no electron redistribution between the components upon complexation occurs [30]. Stabilization energy of the complex (or binding energy E_{bind}) was estimated as the difference of the total energies of the complex its components:

$$E_{bind} = E_{[Complex]} - E_{[Comp\ 1]} - E_{[Comp\ 2]} \quad (1)$$

where $E_{[Complex]}$ is energy of the optimized complex, while $E_{[Comp\ 1]}$ and $E_{[Comp\ 2]}$ are energies of both optimized components.

Recently, the "fragment-to-fragment" approach was proposed [22-23], which could be considered as the next step *in silico* modeling. It divides the total interaction into the particular components and hence enables estimating the interaction energies between fragments by the more correct non-empirical quantum-chemical methods, i.e. it taken into consideration the chemical and electronic structures of the complex and those of the both components.

In this paper, the so-called hydrophobic interaction is not considered. It should also be noted that the formation of conformational formations of the polypeptide chain is accompanied by the stabilization of protein structures through the formation of hydrogen bonds between -NH•••O=C peptide fragments. In the helix, then, the peptide bonds that form the protein conformation do not interact effectively with the pharmacophore molecules. Pharmacophores can form complexes only with "free" peptide bonds of the untwisted part of the protein.

Generally, the stack interaction between two π-electron systems A (*Pharmacophore*) and B (*Biomolecule*) is determined by the relative positions of the molecular levels of both molecules, can be estimated by perturbation theory [31], using the following equation (2):

$$\Delta E \approx \sum_{\mu}^{A}\sum_{i}^{A}\sum_{\nu}^{B}\sum_{j}^{B}\left[\frac{C_{i\mu}C_{j\nu}}{\varepsilon_i - \varepsilon_j}\right] \quad (2)$$

where ε_i and ε_j are MO energies; $C_{i\mu}$ and $C_{j\nu}$ are MO coefficients; nieces i, $\mu\in$ system A, while indices j,$\nu\in$ system B; the first two sums run over all levels, whereas second two sums run over all atoms (π-centers).

Equation (2) implies that interactions between the occupied levels of one component (*Pharmacophore*) with the vacant levels of another component (*Peptide*) should be effective, while interactions between the occupied levels or vacant levels of both components should not be effective. Of course, the interaction amplitude depends on the overlap of the orbitals (or more exactly, on the coefficients $C_{i\mu}$). The molecular levels of the components will be discussed later.

Molecular characteristics of complex components

Planarity and geometrical dimensions of molecules studied

Optimized structures of molecules **1-6** and corresponding complexes are planar, what is typical for the conjugated systems; this planarity is not disturbed upon complexation. Molecular dimension of the complex components are in the same order; they are presented in Figure 1.

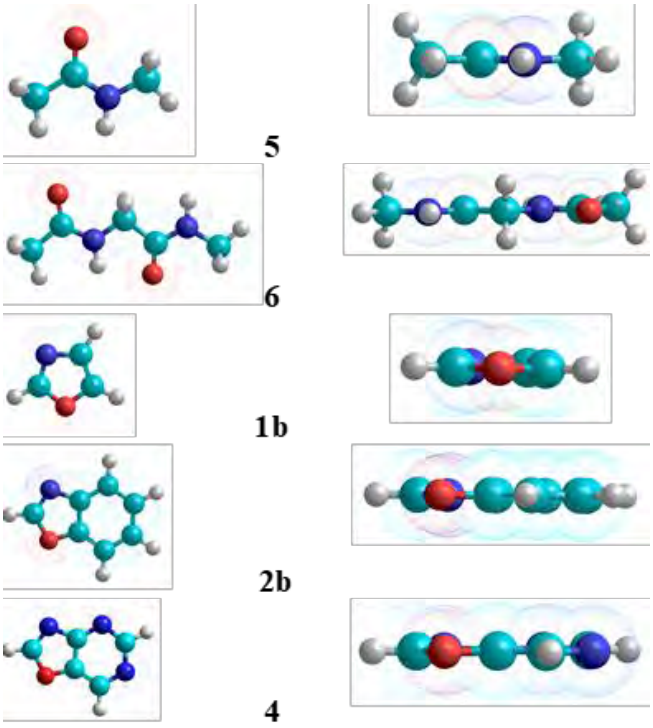

Figure 1. Optimized geometry of the compounds **1b, 2b, 4-6** (modeled using the HyperChem package).

Azoles **1** and their derivatives **2-4** take the molecular volume: the thickness of π-electron shell is ≈3.4 Å; then the estimated values for the oxazole cycle is ≈ [6x6x3,4] Å^3; for the anellated derivatives it is ≈ [7x8,5x3,4] Å^3; for the model peptide **5** it is ≈ [7x5x3,4] Å^3; for the model dipeptide **6** it is ≈ [11x7x3,4] Å^3. The hetero-substitution O → S → NH_2 somewhat increases the molecular volume.

As it follows from Figure 1, molecules **1-4** can form the binary [*Pharm-Pept*] complex by π,π-stacking interactions with only one π-system of the peptide; the bicyclic molecules **2-4** could form the complex with two π-moieties in dipeptide **6**.

The Lone electron pair (LEP) and n-molecular orbitals (MO) dicoordinated nitrogen atoms.

As the molecules **1-4** contain dicoordinated nitrogen atoms, then *n*-MOs occurs in the electron shell beside π-levels. The corresponding LEPs can participate in hydrogen bonds; the corresponding interaction energy depends on the dispositions of the *n*-levels. For sake of illustration, the

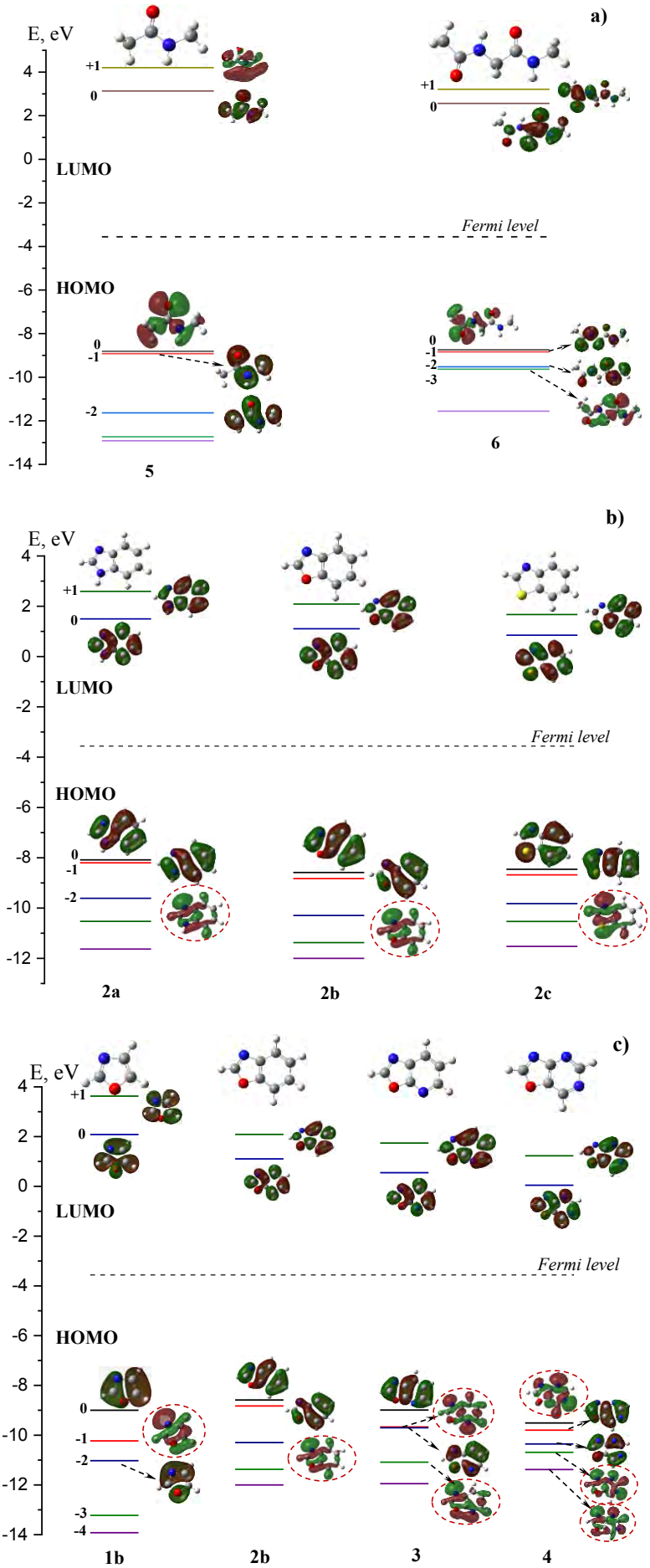

Figure 2. Shape of frontier MO and *n*-MO in the peptides **5-6** (a), compounds **2a-2c** (b) and **1b, 2b, 3, 4** (c)

energies and shapes of the frontier and nearest MOs in the oxazole **1** and its anellated derivatives **2-4** as well as the model peptide **5** and dipeptide **6** are pictured in Figure 2.

Elongation of the polypeptide chain (introduction of the second peptide unit), as shown in Figure 2a, leads to an asymmetric distribution of electron density in the dipeptide. This distribution must be taken into account when interacting with the pharmacophore by the π-stack mechanism. The *n*-molecular orbital (*n*-MO), which is "responsible" for the formation of a hydrogen bond in complex formation, as shown in Figure 2b, is not sensitive to the replacement of the heteroatom X in compounds **2**: it remains HOMO-2, although it has slightly different energy value, which was also shown earlier on monocyclic 5-membered heterocycles [23].

Expansion of the conjugation system of the studied compounds **1a-1c** due to anellation (**1** → **2**) leads to the appearance of a new highly positioned π-MO; therefore *n*-MO is now HOMO-2. At the same time, the addition of the pyridine acceptor cycle leads to the appearance of an additional (pyridine) *n*-MO, which is much higher in energy (HOMO-1), and the *n*-MO of the heterocycle shifts downward (HOMO-3) (Figure 2c). Annelation by a more pyrimidine acceptor cycle causes the appearance of another additional *n*-MO, which occupies the HOMO position, and a subsequent shift in energy of *n*-MO of the heterocycle makes it HOMO-4 (Figure 2c). It should be noted that the interaction of the additional *n*-MOs with each other is accompanied by their splitting, which causes a greater shift of the *n*-level to higher orbital energy. Besides, such a change in the mutual position of the π-levels and *n*-levels should affect the stability of the [*Pharm-Pept*] complex stabilized by hydrogen bonds.

Index φ_0 as a quantitative characteristic of donor-acceptor properties

It was proposed earlier [32] to estimate quantitatively the donor-acceptor properties of the conjugated molecules analyzing positions of the frontier MOs relatively to the non-bonding π-level (so-called Fermi level of π-electrons) φ_0; this parameter is calculated by equation (3):

$$\varphi_0 = (\varepsilon_{LUMO} - \alpha)/\Delta \qquad (3)$$

where $\Delta = \varepsilon_{LUMO} - \varepsilon_{HOMO}$, ε_{LUMO} is the energy of the LUMO; ε_{HOMO} is the energy of the HOMO; α = -3.56 eV is the energy of Fermi level (the middle of the HOMO-LUMO gap for the polyene with 15 double bonds) [33].

If the energy gap Δ is symmetrical relative to the virtual level α, then $\varphi_0 = 0.5$ and hence the donor and acceptor properties are mutually balanced; the shift of the energy gap up (and hence increase of the parameter $\varphi_0 > 0.5$) indicates a mainly donor nature of the conjugated molecule; on the contrary, if $\varphi_0 < 0.5$, then the frontier levels are shifted down, evidencing a predominately acceptor nature [32]. The calculated MO energies and parameter φ_0 of molecules studied **1-6** are collected in Table 2.

Table 2. MO energies and parameter φ_0 of the compounds **1-2(a-c)** and **5, 6**.

Compd	X	ε^a, eV		Δ^b	$\varphi_0{}^c$
		HOMO	LUMO		
5		-8.57	3.34	11.91	0.579
5 (cis)		-8.72	2.97	11.69	0.558
6		-8.60	2.11	10.71	0.530
6 (cis)		-8.60	2.12	10.72	0.530
1a	NH	-8.12	2.59	10.71	0.574
1b	O	-8.86	1.67	10.53	0.497
1c	S	-8.27	0.64	8.91	0.471
2a	NH	-8.05	1.34	9.39	0.522
2b	O	-8.54	0.88	9.42	0.471
2c	S	-8.42	0.79	9.21	0.472
	Polyene-15[d]	-6.21	-0.91	5.30	0.500

[a]ε is energy of orbital;
[b]$\Delta = \varepsilon(LUMO) - \varepsilon(HOMO)$;
[c]$\varphi_0 = [\varepsilon(LUMO) - \alpha]/\Delta$ [33]; α= -3.56137 eV [33];
[d]see [32].

Table 2 demonstrated that the model peptides **5** and **6** (as electron-excessive π-systems) are donor molecules, whereas compound **1** and anellated derivatives **2-4** are acceptors. Also, one can see that expansion of the π-conjugated system by anellation decreases firstly the LUMO energy, then parameter φ_0 decreases also regularly in the series of the compounds **1-2-3-4**. It can be assumed that the interaction of peptides as donors should be more efficient with heterocycles **2-4** as stronger acceptors.

[Pharm:Pept] Complex stabilized by stacking π-π-interaction

Going from heterocycles **1** to the anellated derivatives **2-4** and model peptides **5** and **6**, one can see that the formation of [*Pharm-Pept* **5**] complex by the mechanism of the π,π-stacking interactions should be more efficient for compounds **1**, and [*Pharm-Pept* **6**] is more effective for anellated derivatives **2-4**.

The peptide bond =C(O)–NH– can exist in two conformations (*cis*- and *trans*-) relative to the polypeptide chain plane [34-35]. Two possible [*Pharm-Pept* **5**] complexes with the oxazole **1b** were calculated. For other molecules (**1a** and **1c**), the complex was calculated with peptide **5** in the *trans*-configuration. The binding energies calculated for different complexes [*Pharm-Pept* **5**] of compounds **1** with the model peptide **5** are presented in Table 3.

Stabilization energies of [**1b**-*Pept* **5** (*cis*-)] and [**1b**-*Pept* **5** (*trans*-)] complexes differ considerably: ≈ 3 kcal/mol; then the complex with the *cis*-isomer is more stable. Also, our modeling shows that the binding energy of the complex [*Pharm-Pept*] is sensitive to the nature of heteroatom X; going from the oxazole **1b** (X = O) to imidazole **1a** and

thiazole **1c** increases the complex stability to ≈ 2 kcal/mol and ≈ 10 kcal/mol respectively. However, there is no direct correlation between stabilization energy and parameter φ_0; it seems to be connected with the different energy gaps Δ.

Table 3. The binding energies of π-complexes of the compounds **1a-c** with model peptide **5**.

Compd	E_{mol}[a], a.u.	[Compound-Pept **5**]		
		E_{compl}[b], a.u.	E_{compl}[c], a.u.	ΔE[d], kcal/mol
1b	-245.992	-	-494.458	-9.30
1b	-245.992	-494.457	-	-12.11
1a	-226.147	-	-474.616	-11.13
1c	-568.951	-	-817.434	-19.76
5 *(trans-)*	-248.451			
5 *(cis-)*	-248.446			

[a]E_{compd} is a total energy of compounds;
[b]E_{compl} is a total energy of [*Compound-Pept* **5**]complex, where the peptide bond is in the *cis*-position;
[c]E_{compl} is a total energy of [*Compound-Pept* **5**]complex, where the peptide bond is in the *trans*-position;
[d]ΔE is a binding energy, calculated by equation (1).

Now, let us estimate the effect of expansion of the conjugated system oxazole and its derivatives during anellation. Firstly, it should be noted that bicyclic molecules **2-4** have a common plane of overlap with both peptide **5** and dipeptide **6**. For sake of illustration, Figure 3 shows the optimized geometries of the complexes of the benzoxazole **2b** with the model molecules **5** and **6**:

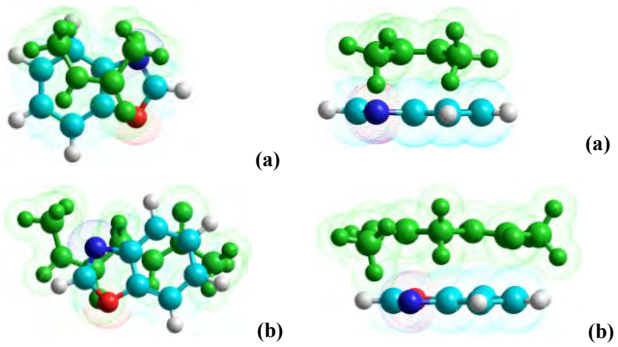

Figure 3. Mutual arrangement of both components in π-π-complex [*Pharm-Pept*]: a) compound **2b** with model peptide **5** residue in X-Y plane and X-Z plane; b) compound **2b** with model dipeptide **6** residue in X-Y plane and X-Z plane.

As indicated in Table 2 and Figure 2b, anellation is accompanied by the convergence of the frontier levels. This should increase the energy interaction between the vacant levels of the pharmacophore and occupied levels of the model peptide molecule according to equation (2). The same conclusion concerns the interaction between the occupied levels of the pharmacophore and vacant levels of the model peptide molecule. Hence, the stability of [*Pharm-Pept*] π-complex upon anellation should increases. The calculated binding energies in the complexes of the anellated molecules **2-4** with the model peptide **5** and dipeptide **6** are collected in Table 4.

Table 4. The binding energies of π-complexes of the compounds **2b, 3** and **4** with model peptides **5** and **6**.

Compd	anellation	E_{mol}[a], a.u.	[Compound-Pept **5**]		[Compound-Pept **6**]	
			E_{compl}[b], a.u.	ΔE[c], kcal/mol	E_{compl}, a.u.	ΔE, kcal/mol
2b	Benzene	-399.586298485	-648.060865334	-14.48	-856.02241454	-30.60
3	Pyridine	-415.62782517	-664.09305761	-8.63	-872.056904788	-26.19
4	Pyrimidine	-431.65161043	-680.1122263	-5.73	-888.07587177	-23.16
peptide 5		-248.451486374				
peptide 6		-456.387350963				

[a]E_{compd} is total energy of compounds;
[b]E_{compl} is total energy of [*Compound-Pept*] complex;
[c]ΔE is a binding energy, calculated by equation (1).

Comparing Tables 3 and 4 shows that anellation of the compounds **1** leads to sensible increasing of the binding energies. Going to the possible complex with the dipeptide **6** (with two parallel peptide conjugated systems) increases twofold the stabilization energy.

At the same time, the data in Table 4 point that replacing of methine groups in benzene ring by the more electronegative nitrogen atoms decreases the highest occupied level of pharmacophore and hence it holds away from the vacant level of the peptide; hence the stabilization energy decreases in the series of the compounds **2→3→4.**

Complex stabilized by hydrogen bonds

Another type of the stable [*Pharm-BioM*] complexes is formed by generation of the hydrogen bonds between the components (further: [HB]-complex). In this complex the nitrogen atoms with LEP are considered as acceptor centers of such hydrogen bonds. Also, the molecules studied can form hydrogen bonds with some amino acids in proteins containing the functional groups -NH_2, -OH, -SH. For sake of comparison, the possible complex with model amino acid residues are H_3C-Y-H, were Y = NH, O, S; the non-conjugated fragment in amino acids was modeled by methyl group. Therefore, the various conformation will not taken into consideration: we optimistically suppose that we can neglect different conformations. Besides, we will compare stabilization energies of [HB]-complexes in the series of structurally similar compounds. Before the optimization procedure, complex components were disposed at the distance of 2.1 Å; Y-H bond was in the plane, whereas the component planes in the complex were disposed perpendicularly. For molecules **3-4** containing 2 or 3 nitrogen atoms (Figure 4) all possible isomeric complexes were calculated.

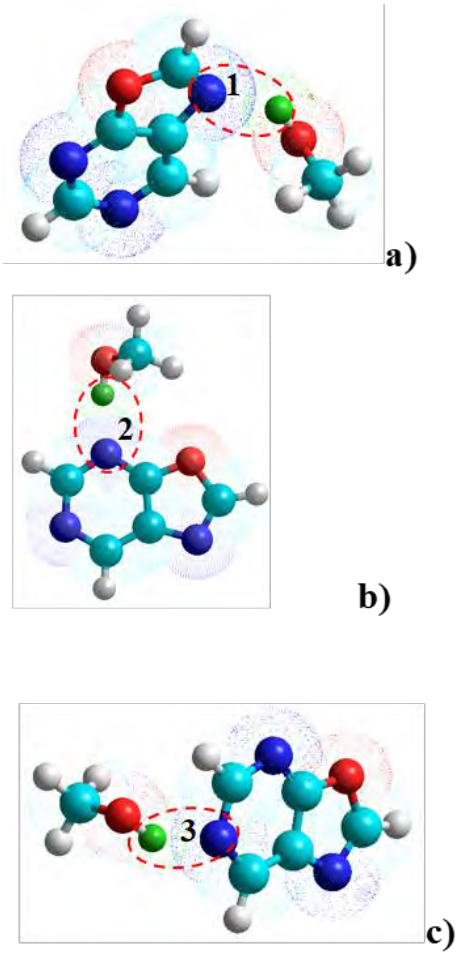

Figure 4. Possible options for creating a [HB]-complex by the mechanism of hydrogen bonding for compound **4**.

It is assumed that the energy and length of the hydrogen bond in the [HB]-complex depend on charge on the nitrogen atom; then the stability of such an isomeric [HB]-complex should be different.

First of all, the [HB]-complex of the simplest molecules **1**, **2** with model functional amino acid residues will be considered in order to study the dependence of the [HB]-complex stability on chemical composition of the model functional molecule H_3C-Y-H. The calculated binding energies are presented in Table 5.

Table 5 shows that the nitrogen atom of compounds **1-2** has a relatively large negative charge, its value depends on the nature of the heteroatom X. When compounds **1** are annelated, the charge on the nitrogen atom increases, also depending on the nature of the heteroatom X. This charge sensitivity should affect the stability of the [HB]-complex.

Variation of the functional residues in the model molecule H_3C-Y-H shows that the most stable [HB]-complex of compounds **1** is formed with OH-group; a similar tendency is observed for a number of benzoanalogues **2**, anellation of the compounds **1** increases the binding energy.

Replacing of the heteroatom also is accompanied by the [HB]-complex stability, though anellated benzothiazole **2c** (X = S) is considerably less stable, which seems to be connected with a high energy of the *n*-MO that is the LEP on the sulfur atom. Additionally, the H•••S- hydrogen bond is somewhat lengthened.

Going from the simplest oxazole **1** to its derivatives **3** and **4** anellated by the pyridine or pyrimidine, two or even three types of the [HB]-complexes could be formed by the hydrogen bond, as shown in Figure 4. The binding energies calculated for all possible [HB]-complexes with the model molecule H_3C-O-H are presented in Table 6.

Firstly, negative charge at the nitrogen atom (1) is weakly sensitive on the change of the benzene ring to pyridine and pyrimidine cycles. Going from the molecule **2b** to its nitrogen analogue **3** decreases slightly the binding energy of the [HB]-complex formed via hydrogen bonding with the nitrogen atom in 5-membered oxazole cycle. In the same time, for derivative **4**, annelated by the pyrimidine cycle, the stabilization energy ≈ 4 kcal/mol was predicted by calcularions. The analyses of both possible [HB]-complexes with molecule **3** shows that the forming of the [HB]-complex with the nitrogen atoms (2) and (3) is less stable (≈ 1.8 kcal/mol). One can also see that all three isomeric complexes with the molecule **4** are appreciably stable. Besides, the Table 5 demonstrates that these isomers differ sizeable between them, the [HB]-complex bonded by the hydrogen bond with the nitrogen atom (1) is most stable.

Finally, let us consider the [HB]-complexes of peptide molecules **5** as hydrogen-bonded complexes with the N-H proton donors. The calculated data are collected in Table 7.

Table 5. Hydrogen bond energy values for the complexes [*Compound-H-X*] involving compounds **1-2(a-c)** with H_3C-Y-H.

Complex	H-X	z[a], e.u.	*L*[b], Å	E_{compd}[c], a.u.	E_{compl}[d], a.u.	ΔE[e], kcal/mol
[compound **1b**-HX]	H_2N-CH_3	-0.430	2.434	-245.99202	-341.83384	-7.92
[compound **1b**-H-X]	H-O-CH_3	-0.430	1.949	-245.99202	-361.69005	-8.22
[compound **1b**-H-X]	H-S-CH_3	-0.430	2.283	-245.99202	-684.670094	-6.57
[compound **1a**-H-X]	H-O-CH_3	-0.449	1.922	-226.14680	-341.84861	-10.59
[compound **1c**-H-X]	H-O-CH_3	-0.359	1.973	-568.95108	-684.67167	-22.37
[compound **2b**-H-X]	H_2N-CH_3	-0.474	2.503	-399.59471	-495.43508	-7.02
[compound **2b**-H-X]	H-O-CH_3	-0.474	1.978	-399.59471	-515.295092	-9.69
[compound **2b**-H-X]	H-S-CH_3	-0.474	2.454	-399.59471	-838.275012	-7.96
[compound **2a**-H-X]	H-O-CH_3	-0.500	1.943	-379.74776	-495.45252	-12.44
[compound **2c**-H-X]	H-O-CH_3	-0.417	1.959	-722.57396	-838.27227	-8.40
		H-O-CH_3		-115.684935	-	-
		H_2N-CH_3		-95.8292016	-	-
		H-S-CH_3		-438.667606	-	-

[a]z, e.u. is the charge on the nitrogen atom, electronic units;
[b]l is the length of the hydrogen bond;
[c]E_{compd} is the energy of the compounds;
[d]E_{compl} is the energy of the [*Compound-H-X*] complex;
[e]ΔE is the stabilization energy complex, calculated by formula (1).

Table 6. Hydrogen bond energy values for the complexes [*Compound-H-X*] involving compounds **2b, 3-4** with H_3C-O-H.

Complex	N[a]	z[b], e.u.	*l*[c], Å	E_{compd}[d], a.u.	E_{compl}[e], a.u.	ΔE[f], kcal/mol
[compound **2b**-H-X]	1	-0.474	1.978	-399.59471	-515.29509	-9.69
[compound **3**-H-X]	1	-0.478	2.022	-415.62783	-531.32932	-10.39
[compound **3**-H-X]	2	-0.497	1.993	-415.62783	-531.32648	-8.61
[compound **4**-H-X]	1	-0.441	2.055	-431.65161	-547.35840	-13.71
[compound **4**-H-X]	2	0.458	2.028	-431.65161	-547.35444	-11.23
[compound **4**-H-X]	3	0.431	2.000	-431.65161	-547.35725	-12.99
		H-O-CH_3		-115.68494	-	-

[a]N - position of the nitrogen atom in the anellated cycle of a substance (according to Figure 4);
[b]z, e.u. is the charge on the nitrogen atom, electronic units;
[c]l is the length of the hydrogen bond;
[d]E_{compd} is the energy of the compounds;
[e]E_{compl} is the energy of the [*Compound-H-X*] complex;
[f]ΔE is the stabilization energy complex, calculated by formula (1).

Comparing Tables 6 and 7 shows similar tendencies obtained for the [*Compound-Pept* **5**] with both model peptide **5** and model molecule H_3C-OH. However, in contrast to H_3C-OH, the energy of hydrogen bonding with the nitrogen atom (1) for compound **4** is lower than that with the nitrogen atoms (2) and (3). It can be conclude that the [*Compound* **3**-*Pept* **5**] and [*Compound* **4**-*Pept* **5**] complexes formed with the peptide moieties of the untwisted part of the protein at the nitrogen atoms of the pyridine type are more stable.

It is to noticed that the some [*Compound-Pept* **5**] could be simultaneously formed for the molecules **3** and **4** with two or even three hydrogen bonds. This should additionally stabilize the [*Pharm-Pept*] complex.

Table 7. Stabilization energies for [*Compound-Pept* **5**] complexes of molecules **1-4** with model peptide **5**.

Complex	N[a]	E_{compd}[b], a.u.	E_{compl}[c], a.u.	ΔE[d], kcal/mol
[compound **1b**-Pept **5**]	1	-245.992	-494.46044	-10.63
[compound **2b**-Pept **5**]	1	-399.595	-648.06555	-12.14
[compound **3**-Pept **5**]	1	-415.628	-664.09780	-11.73
[compound **3**-Pept **5**]	2	-415.628	-664.09637	-10.70
[compound **4**-Pept **5**]	1	-431.652	-680.11718	-8.84
[compound **4**-Pept **5**]	2	-431.652	-680.11929	-10.16
[compound **4**-Pept **5**]	3	-431.652	-680.11929	-10.15
Peptide 5		-248.451		

[a]N - position of the nitrogen atom in the anellated cycle of a substance (according to Figure 4);
[b]E_{compd} is the energy of the compounds;
[c]E_{compl} is the energy of the [*Compound-Pept* **5**] complex;
[d]ΔE is the stabilization energy complex, calculated by formula (1).

Conclusions

In silico the theoretical analysis of the interaction between pharmacophore molecules based on bicyclic nitrogen heterocycles with model peptides shows that the stabilization of [*Pharm-Pept*] complexes is ensured by the π,π-stacking interactions of the pharmacophore molecule systems with the π-peptide bond system. The expansion of the conjugate heterocyclic compounds by anellation is accompanied by an increase in the acceptor properties of studied heterocycles, stabilizing the [*Pharm-Pept*] complexes formed by the π,π-stacking interaction mechanism increases. Elongation of the polypeptide chain increases significantly the stabilization energy of the [*Pharm-Pept*] complexes.

In the formation of complexes by the mechanism of hydrogen bonds between the LEP of the dicoordinated nitrogen atom and the functional groups of amino acids -OH, -NH_2, -SH the most stable [HB]-complexes was found for OH-group, the least stable [HB]-complexes was predicted for SH-group. The expansion of the conjugated anellated system is accompanied by an increase in the acceptor properties of nitrogen containing heterocycle as pharmacophores, especially during anellated with pyridine and pyrimidine, which leads to increased stability of the complexes formed by the hydrogen bonding mechanism. The transition to bicyclic conjugate systems with two or three dicoordinated nitrogen atoms provides additional stabilization of [*Pharm-BioM*] complexes due to the possible simultaneous formation of several hydrogen bonds. The stabilization energy of [HB]-complexes for compounds **2b** and **3** with a "free" peptide bond of the extended part of the protein is slightly lower compared to the functional OH-group of amino acids, and for compound **4**, on the contrary, 2 kcal/mol higher. Compound **4** is likely to show more pronounced properties in further *in vitro* studies.

Notes

The authors declare no conflict of interest.

Author contributions. **Ye. S. V.**: provision of study materials, computing resources, or other analysis tools. **N. V. O.**: formulation or evolution of overarching research goals and aims, application of statistical, mathematical, computational, or other formal techniques to analyze study data. **S. G. P.**: development and design of methodology; creation of models, provision of study materials, computing resources, or other analysis tools. **M. V. K.**: preparation, creation and presentation of the published work, specifically visualization. **O. D. K.**: ideas; formulation or evolution of overarching research goals and aims, development or design of methodology; creation of models. **V. S. B.** ideas; formulation or development of common goals and objectives of the research, verification of results, responsibility for managing and coordinating the planning and implementation of research activities.

References

1. Kakkar, S.; Narasimhan, B. A comprehensive review on biological activities of oxazole derivatives. *BMC Chem.* **2019**, *13*, 171-195.
2. Zhang, H. Z.; Zhao, Z. L.; Zhou, C. H. Recent advance in oxazole-based medicinal chemistry. *Eur. J. Med. Chem.* **2018**, *144*, 444-492.
3. Cameron, D. M.; Thompson, J.; March, P. E.; Dahlberg, A. E. Initiation factor IF2, thiostrepton and micrococci in prevent the binding of elongation factor G to the Escherichia coli ribosome. *J. Mol. Biol.* **2002**, *319*, 27-35.
4. Rodnina, M. V.; Savelsbergh, A.; Matassova, N. B.; Katunin, V. I.; Semenkov, Yu. P.; Wintermeyer, W. Thiostrepton inhibits the turnover but not the GTPase of elongation factor G on the ribosome. *Proc. Natl. Acad. Sci. U.S.A.* **1999**, *96*, 9586-9590.
5. Lawrence, D. S.; Copper, J. E.; Smith, C. D. Structure-Activity Studies of Substituted Quinoxalinones as Multiple-Drug-Resistance Antagonists. *J. Med. Chem.* **2001**, *44*, 594-601.
6. Borst, P. Multidrug resistance: A solvable problem? *Ann. Oncol.* **1999**, *10*, 162-164.
7. Nolt, M. B.; Smiley, M. A.; Varga, S. L.; McClain, R. T.; Wolkenberg, S. E.; Lindsley, C. W. Convenient preparation of substituted 5-aminooxazoles via a microwave-assisted Cornforth rearrangement. *Tetrahedron* **2006**, *62*, 4698-4704.
8. Fennell, K. A.; Miller, M. J. Syntheses of Amamistatin Fragments and Determination of Their HDAC and Antitumor Activity. *Org. Lett.* **2007**, *9*, 1683-1685.
9. Kachaeva, M. V.; Hodyna, D. M.; Obernikhina, N. V.; Pilyo, S. G.; Kovalenko, Y. S.; Prokopenko, V. M.; Kachkovsky, O. D.; Brovarets, V. S. Design, synthesis and evaluation of novel sulfonamides as potential anticancer agents. *J. Heterocycl. Chem.* **2019**, *56*, 3122-3134.
10. Liu, X.; Bai, L.; Pan, C.; Song, B.; Zhu, H. Novel 5-Methyl-2-[(un)substituted phenyl]-4-{4,5-dihydro- 3-[(un)substituted phenyl]-5-(1,2,3,4-tetrahydroisoquinoline-2-yl)pyrazol-1-yl}-oxazole Derivatives: Synthesis and Anticancer Activity. *Chin. J. Chem.* **2009**, *27*, 1957-1961.
11. Murphy, G. J.; Holder, J. C. Potential new treatments for type 2 diabetes. *Trends. Pharmacol. Sci.* **2000**, *21*, 259-265.
12. Marquez, B. L.; Watts, K. S.; Yokochi, A.; Roberts, M. A.;Verdier-Pinard, P.; Jimenez, J. I.; Hamel, E.; Scheuer, P. J.; Gerwick, W.H. Structure and Absolute Stereochemistry of Hectochlorin, a Potent Stimulator of Actin Assembly. *J. Nat. Prod.* **2002**, *65*, 866-871.
13. Kachaeva, M. V.; Hodyna, D. M.; Semenyuta, I. V.; Pilyo, S. G.; Prokopenko, V. M.; Kovalishyn, V. V.; Metelytsia, L. O.; Brovarets, V. S. Design, synthesis and evaluation of novel sulfonamides as potential anticancer agents. *Comput. Biol. Chem.* **2018**, *74*, 294-303.
14. Dahlqvist, A.; Leffler, H.; Nilsson, U. J. C1-Galactopyranosyl Heterocycle Structure Guides Selectivity: Triazoles Prefer Galectin-1 and Oxazoles Prefer Galectin-3. *ACS Omega* **2019**, *4*, 7047-7053.
15. Youjun, Xu.; Shiwei, W.; Qiwan, Hu; Shuaishi, G.; Xiaomin, Ma; Weilin, Z.; Yihang, S.; Fangjin, Ch.; Luhua, L.; Jianfeng, P.

CavityPlus: a web server for protein cavity detection with pharmacophore modelling, allosteric site identification and covalent ligand binding ability prediction. *Nucleic Acids Res.* **2018**, 46, 374-379.
16. Nisius, B.; Sha, F.; Gohlke, H. Structure-based computational analysis of protein binding sites for function and druggability prediction. *J. Biotechnol.* **2012**, *159*, 123-134.
17. Kasper, J.R.; Park, C. Ligand Binding to a High-Energy Partially Unfolded Protein. *Protein Sci.* **2015**, *24*, 129-137.
18. Celej, M.S.; Guillermo, G.; Montich, G.G.; Fidelio, G.D. Protein stability induced by ligand binding correlates with changes in protein flexibility. *Protein Sci.* **2003**, *12*, 1496-1506.
19. Mortenson, P. N.; Erlanson, D. A.; Esch, I. J. P.; Jahnke, W.; Johnson, C. N.; Fragment-to-Lead Medicinal Chemistry Publications in 2018. *J. Med. Chem.* **2018**, *62*, 3857-3872.
20. Neto, L. R.S.; Moreira-Filho, J. T.; Neves, B. J.; Maidana, R. L. B. R.; Guimarães, A. C. R.; Furnham, N.; Andrade, C. H.; Silva, F. P. In silico Strategies to Support Fragment-to-Lead Optimization in Drug Discovery. *Front. Chem.* **2020**, *8*, 93-102.
21. Obernikhina, N.; Zhuravlova, M.; Kachkovsky, O.; Kobzar, O.; Brovarets, V.; Pavlenko, O.; Kulish, M.; Dmytrenko, O. Stability of fullerene complexes with oxazoles as biologically active compounds. *Appl. Nanosci.* **2020**, *10*, 1345-1353.
22. Zhuravlova, M.Yu.; Obernikhina, N.V.; Pilyo, S.G.; Kachaeva, M.V.; Kachkovsky, O.D.; Brovarets, V.S. In silico binding affinity studies of phenyl-substituted 1,3-oxazoles with protein molecules. *Ukr. Bioorg. Acta* **2020**, *15*, 12-19.
23. Velihina, Ye.S.; Obernikhina, N.V.; Pilyo, S.G.; Kachaeva, M.V.; Kachkovsky, O.D.; Brovarets, V.S. In silico study of biological affinity of nitrogenous bicyclic heterocycles: fragment-to-fragment approach. *Ukr. Bioorg. Acta* **2020**, *15*, 48-58.
24. Kachaeva, M. V.; Pilyo, S. G.; Zhirnov, V. V.; Brovarets, V. S. Synthesis, characterization, and in vitro anticancer evaluation of 2-substituted 5-arylsulfonyl-1,3-oxazole-4-carbonitriles. *Med. Chem. Res.* **2019**, *28*, 71-80.
25. Kachaeva, M. V.; Obernikhina, N. V.; Veligina, E. S.; Zhuravlova, M. Yu.; Prostota, Ya. O.; Kachkovsky, O. D.; Brovarets, V. S. Estimation of biological affinity of nitrogen-containing conjugated heterocyclic pharmacophores. *Chem. Heterocycl. Compd.* **2019**, *55*, 448-454.
26. Kachaeva, M. V.; Hodyna, D. M.; Obernikhina, N. V.; Pilyo, S. G.; Kovalenko, Y. S.; Prokopenko, V. M.; Kachkovsky, O. D.; Brovarets, V. S. Dependence of the anticancer activity of 1,3-oxazole derivatives on the donor/acceptor nature of his substitues, *J. Heterocyclic Chem.* **2019**, *56*, 3122-3134.
27. Frisch, M.; Trucks, G.; Schlegel, H.; Scuseria, G.; Robb, M.; Cheeseman, J.; Montgomery, Jr. J.; Vreven, T.; Kudin, K.; Burant, J.; Millam, J. *Gaussian 03, Revision B. 05*. Gaussian Inc.: Pittsburgh, PA, Ringraziamenti, 2003.
28. Jordan, M. The meaning of affinity and the importance of identity in the designed world. *Interactions* **2010**, *17*, 6-11.
29. Obernikhina, N.V.; Nikolaev, R.O.; Kachkovsky, O.D.; Tkachuk, Z. Yu. π-electron affinity of the nitrogenous bases of nucleic acids. *Dopov. Nac. akad. nauk Ukr.* **2019**, *6*, 75-81.
30. Bissantz, C.; Kuhn, B.;Stahl, M. A. Medicinal Chemist's Guide to Molecular Interactions, *J. Med. Chem.* **2010**, *53*, 5061-5084.
31. Dewar, M. J. S. *The molecular orbital theory of organic chemistry*, New York: McGraw Hill, **1969**, 484 P.
32. Obernikhina, N.; Kachaeva, M.; Shchodryi, V.; Prostota, Ya.; Kachkovsky, O.; Brovarets, V.; Tkachuk, Z. Topological Index of Conjugated Heterocyclic Compounds as Their Donor/Acceptor Parameter. *Polycycl. Aromat. Comp.* **2019**, *40*, 1196-1209.
33. Obernikhina, N.; Pavlenko, O.; Kachkovsky, A.; Brovarets, V. Quantum-Chemical and Experimental Estimation of Non-Bonding Level (Fermi Level) and π-Electron Affinity of Conjugated Systems. *Polycycl. Aromat. Comp.* **2020**, *2020*, 1-10.
34. Palmer, T.; Bonner, P. L. The Biosynthesis and Properties of Proteins. *Enzymes* **2011**, *7*, 44-66.
35. Craveur, P.; Joseph, A.P.; Poulain, P. et al. Cis-trans isomerization of omega dihedrals in proteins. *Amino Acids* **2013**, *45*, 279-289.

In silico дослідження взаємодії гетероциклічних основ з пептидними групами білків: пофрагментний підхід

Є. С. Велігіна[1], Н. В. Оберніхіна[2]*, С. Г. Пільо[2], М. В. Качаєва[2], О. Д. Качковський[2]

[1]*Інститут біоорганічної хімії та нафтохімії ім. В. П. Кухаря НАН України, вул. Мурманська, 1, Київ, 02094, Україна.*
[2]*Національний медичний університет імені О. О. Богомольця, бульв. Т. Шевченка, 13, Київ, 01601, Україна.*

Резюме: В рамках підходу «фрагмент до фрагменту» представлені *in silico* результати біологічної спорідненості модельних пептидів (*Пепт*) та гетероциклічних основ, конденсованих з піридином та піримідином, як фармакофорів (*Фарм*). Аналіз даних показує, що розширення кон'югованих гетероциклічних сполук за допомогою анелювання супроводжується збільшенням акцепторних властивостей досліджуваних гетероциклів, в результаті чого стабільність комплексів [*Фарм-Пепт*], утворених за механізмом π,π-стекінгової взаємодії збільшується. При подовженні поліпептидного ланцюга спостерігається вдвічі збільшення енергії стабілізації комплексів [*Фарм-Пепт*]. При утворенні комплексів [*Фармакофор-Біомолекула*] між спряженими гетероциклічними основами з двома-трьома дикоординованими атомами азоту та функціональними групами амінокислот (-OH, -NH_2, -SH) за механізмом водневих зв'язків виявились найбільш стабільними комплекси з OH-групою. Розширення спряженої системи досліджуваних гетероциклів шляхом анелювання з піридином та піримідином призводить до підвищеної стабільності комплексів. Енергія комплексоутворення для сполук **2b** та **3** із «вільним» пептидним зв'язком розгорнутої частини білка дещо нижча порівняно з енергією комплексів досліджуваних сполук з OH-групою амінокислот, а для сполуки **4**, навпаки, енергія на 2 ккал/моль вище. Сполука **4**, ймовірно, проявлятиме більш виражені властивості в подальших дослідженнях *in vitro*.

Ключові слова: підхід «фрагмент до фрагмента»; пептидні зв'язки; афінність зв'язування; комплекс [*Фармакофор-Біомолекула*]; π,π-стекінгова взаємодія; водневі зв'язки.